# Numerical Methods for Hyperbolic Equations: Generalized Definition of Local Conservation and Discontinuous Galerkin Methods for Maxwell's equations in Drude Metamaterials

by

Cengke Shi

B.Sc., University of Science and Technology of China, Hefei, P. R. China, 2013

A dissertation submitted in partial fulfillment of the

requirements for the degree of Doctor of Philosophy

in the Division of Applied Mathematics at Brown University

PROVIDENCE, RHODE ISLAND

May 2018

This dissertation by Cengke Shi is accepted in its present form
by the Division of Applied Mathematics as satisfying the
dissertation requirement for the degree of Doctor of Philosophy.

Date________________ ________________________________

Chi-Wang Shu, Ph.D., Advisor

Recommended to the Graduate Council

Date________________ ________________________________

Johnny Guzmán, Ph.D., Reader

Date________________ ________________________________

Jérôme Darbon, Ph.D., Reader

Approved by the Graduate Council

Date________________ ________________________________

Andrew G. Campbell, Dean of the Graduate School

## Curriculum Vitae of Cengke Shi

### Education

- Brown University, Ph.D. in Applied Mathematics, May 2018 (expected)
- Brown University, M.S. in Computer Science, May 2018 (expected)
- University of Science and Technology of China, B.S. in Mathematics, May 2013

### Publication

- Jichun Li, Cengke Shi, Chi-Wang Shu, Optimal non-dissipative discontinuous Galerkin methods for Maxwell's equations in Drude metamaterials, Computers and Mathematics with Applications, v73 (2017), pp.1760–1780.
- Cengke Shi, Chi-Wang Shu, On local conservation of numerical methods for conservation laws, Computers and Fluids, to appear.
- Cengke Shi, Jichun Li, Chi-Wang Shu, Discontinuous Galerkin methods for Maxwell's equations in Drude metamaterials on unstructured meshes, Journal of Computational and Applied Mathematics, to appear.

### Experience

- Teaching Assistant, Brown University, Fall 2014 – Spring 2015
- Software Engineering Intern, Dassault Systèmes, Summer 2016
- Quantitative Trading Intern, Virtu Financial, Summer 2017

## Acknowledgments

I would like to express my deepest gratitude to my advisor, Professor Chi-Wang Shu, for his guidance and inspiration. Professor Shu provides me the opportunity to come to Brown University and conduct the research for this dissertation. During my five years here, he is always available for discussions, which deepen my understanding of the field and help me to think more critically. He also encourages me to pursue my interest in computer science, which helps with the computer simulation part of this dissertation and broadens my career horizons.

I am honored to have worked with Professor Jichun Li. I want to thank Professor Li for introducing me to the field of electromagnetics in metamaterials, and for providing many advices and insights during our collaborations.

I want to thank Professor Johnny Guzmán and Professor Jérôme Darbon for their time serving as my dissertation committee members and their invaluable feedback.

I feel very lucky to meet many good friends and colleagues during my graduate study at Brown. Dr. Tong Qin helps me a lot with coding scientific computing systems, especially in the debugging process. Dr. Zheng Sun and Dr. Guosheng Fu also provides many insights to my work. I also want thank Ryan Ngoy for helping me improve my English.

I would like to thank my wife, Dr. Yan Zhao, for supporting me in all my pursuits. I feel blessed that we both get our doctorate degrees and have our first son, Charles Shi, this year. I'm grateful to my parents, Chunbin Shi and Hongxia Zhang, for their teaching and unconditional love. This dissertation would not have been possible without the love and support of my family.

# Contents

# List of Tables

# List of Figures

# Chapter One

# Introduction

Conservation laws describe the phenomena that for a conserved quantity to change in any volume there must be a flux of the quantity in or out of that volume. In differential equation form, the conservation law can be described by hyperbolic equations, see, e.g., [19]. In this dissertation, we present two topics concerning numerical methods solving hyperbolic equations from both theoretical and practical points of view.

The first topic is about convergence to weak solutions for numerical methods solving hyperbolic equations. The well-known Lax-Wendroff theorem [32] states that the finite volume method (in 1D) in conservation form would converge to a weak solution of the underlying conservation law, if the numerical solutions actually converge. It is easy to give counterexamples, e.g. in LeVeque [33], that finite volume methods not in conservation form could converge to non-weak-solutions with wrong shock speed. Kröner et al. [29, 30] have extended the Lax-Wendroff theorem to finite volume methods on unstructured meshes for 2D conservation laws. We briefly review these important results in Chapter 2.

There have been discussions [28, 45, 1] about local conservation property for numerical methods other than the finite volume methods covered in the classic Law-Wendroff theorem. However, the absence of a rigorous definition makes it arguable as to whether a numerical method is locally conservative or not. In Chapter 3, we give a formal definition of the local conservation property for numerical methods in one and two space dimensions. We will prove that locally conservative numerical methods per our definition would converge to weak solutions if they do converge.

The second topic is about numerically solving an example of hyperbolic systems, the Maxwell's equations in Drude metamaterials, by discontinuous Galerkin (DG) methods. The Maxwell's equations can be viewed as conserving the energy of the electromagnetic field, see, e.g., [41]. The recently developed metamaterials also promoted some study of DG methods for solving Maxwell's equations in metamaterials (e.g., [6, 34, 35, 37]). Among these methods, there are non-dissipative ones,e.g. [35], and optimal ones, e.g. [37].

In Chapter 4, we propose a DG method on rectangular mesh, that attains both optimal convergence rate and non-dissipation. Recently Xing et al [49, 5] and Chung et al [8, 9] proposed optimal and non-dissipative discontinuous Galerkin methods for wave equations. Our approach is similar to the LDG method of Xing et al [49, 5] in terms of the choices of the numerical fluxes in the scheme and the projection in the error estimate proof. We also implement the our method on triangular meshes in Chapter 5 and find that the optimal convergence exists only for DG methods rectangular meshes with specific solution space choices.

# Chapter Two

# Local Conservation for Finite Volume Methods

## 2.1 Local Conservation in One Space Dimension

We consider numerical methods solving the following conservation law in one space dimension:

$$\begin{aligned} u_t + f(u)_x &= 0 \text{ in } \mathbb{R}^+ \times \mathbb{R}, \\ u(\cdot, 0) &= u_0 \text{ in } \mathbb{R}, \end{aligned} \tag{2.1}$$

where the flux $f$ is a Lipschitz continuous function. It is clear from the integral form of (2.1) why it is called the conservation law: Integrating over the space interval $[x_1, x_2]$, we get:

$$\frac{\mathrm{d}}{\mathrm{d}t}\int_{x_1}^{x_2} u(x,t)\,\mathrm{d}x \; + f(u(x_2,t)) - f(u(x_2,t)) = 0. \tag{2.2}$$

If we interpret $u$ as the density of gas and $f$ as the rate of flow, or flux of the gas, (2.2) means the rate of the of the volume in an interval equals to the rate of flow into it minus the rate of flow out of it. In another word, the volume of the gas is conserved.

### 2.1.1 Local Conservation for Finite Volume Methods

A finite volume method in an evenly spaced time-space mesh is locally conservative if it takes the following conservation form:

$$\frac{v_j^{n+1} - v_j^n}{\Delta t} + \frac{g(v_{j-p}^n, v_{j-p+1}^n, \ldots, v_{j+q}^n) - g(v_{j-p-1}^n, v_{j-p}^n, \ldots, v_{j+q-1}^n)}{\Delta x} = 0 \tag{2.3}$$

where $v_k^n$ is the value of the numerical solution $v$ on time level $n$ ($t = n\Delta t$) and space lattice point $j$ ($x = j\Delta x$). $g$ is Lipschitz continuous w.r.t each argument and consistent with $f$ in the following sense:

$$g(v, \dots, v) = f(v) \tag{2.4}$$

The scheme (2.3) can determine the numerical solution of all time level using the given initial value in (2.1).

A counterexample in Chapter 12 of [33] illustrate the importance of local conservation for numerical methods. The following consistent yet non-conservative method:

$$\frac{v_j^{n+1} - v_j^n}{\Delta t} = \frac{1}{\Delta x} v_j^n (v_j^n - v_{j-1}^n), \tag{2.5}$$

solving Burgers' equation with discrete initial condition:

$$u_t + u\, u_x = 0 \tag{2.6}$$

$$u(x, 0) = 1_{(\infty,0)}(x) \tag{2.7}$$

yields a non-weak-solution with a wrong shock speed. The result in the next section shows that locally conservative numerical methods never converge to non-weak-solutions.

### 2.1.2 Classic Lax-Wendroff Theorem

The following theorem guarantees that converging to the wrong solution would not happen to locally conservative finite volume schemes.

**Theorem 2.1.1** (Lax and Wendroff [32])**.** *Assume that the numerical solution $v(x, t)$ in (2.3) converges boundedly almost everywhere to some function $u(x, t)$, as $\Delta t$ and*

*$\Delta x$ go to zero. Then $u(x,t)$ is a weak solution of (2.1).*

A simplified proof is given in Chapter 12.4 of [33] by assuming $L^1$ convergence with uniformly bounded total variation as opposed to the almost-everywhere convergence with bound in Theorem 2.1.1.

As we will see the next chapter, this simplified proof is more easily generalizable to the proof of convergence to weak solutions for our generalized local conservation definition.

## 2.2 Local Conservation in Two Space Dimension

In this section, we are concerned with the conservation law in two space dimension:

$$\begin{aligned} u_t + \nabla \cdot \boldsymbol{f}(u)_x &= 0 \text{ in } \mathbb{R}^+ \times \mathbb{R}^2, \\ u(\cdot, 0) &= u_0 \text{ in } \mathbb{R}^2, \end{aligned} \tag{2.8}$$

which has a similar interpretation of conserving the amount of gas in a volume if we integrate (2.8) over this volume.

### 2.2.1 Local Conservation for Finite Volume Methods

To formulate finite volume methods, we need a partition of space into cells, $\mathbb{R}^2 = \cup_{j \in J} T_j$, satisfying the following regularity [29, 30]:

- cells are all $k$–sided polygons

- $|T_j| > c_0 h^2$, where $|T_j|$ is the area of the cell, and the mesh size $h = \max_{j\in J} \mathrm{diam}\,(T_j)$.

- $0 < c_1 \leq \frac{\Delta t}{h} \leq c_2$, where $\Delta t$ is the time step size introduced below

- for each $1 \leq l \leq k$, and any bounded domain $\Omega$:

$$\sum_{T_j\cap\Omega\neq\emptyset} \big|\, |T_j| - |T_{jl}| \,\big| = o(1)$$

  as $h \to 0$. $\{T_{jl},\ l = 1, 2 \ldots k\}$ denotes the neighboring cells of $T_j$

- for each $1 \leq l \leq k$, the mapping of $T_j \mapsto T_{jl}$ is one-to-one and

$$\cup_{j\in J} T_j = \cup_{j\in J} T_{jl} = \mathbb{R}^2$$

The definition of finite volume methods in conservation form for solving (2.8) is as follows:

$$u_j^0 = u_0(x_j),\ x_j \in T_j$$
$$u_j^{n+1} = u_j^n - \frac{\Delta t}{|T_j|} \sum_{l\in N_j} g_{jl}(u_j^n, u_l^n)$$

where $N_j$ denotes the indices of all neighboring cells of cell $j$, and the numerical flux $g_{jl}$ satisfies the following properties:

- Lipschitz continuity: $|g_{jl}(u,v) - g_{jl}(u'v')| \leq c\,h(|u-v| + |u'-v'|)$

- conservation: $g_{jl}(u,v) + g_{lj}(v,u) = 0$

- consistency: $g_{jl}(u,u) = \boldsymbol{\nu}_{jl} \cdot \boldsymbol{f}(u)$, where $\boldsymbol{\nu}_{jl}$ is the normal vector on the interface pointing from cell $j$ to $l$ with a magnitude the length of that interface

### 2.2.2 Two Dimensional Lax-Wendroff Theorem

The following is the Lax–Wendroff theorem for two dimensional finite volume methods in conservation form [29, 30].

**Theorem 2.2.1.** *Assume the $u_h$ is the solution of a finite volume method in conservation form on the regular space discretization with mesh size $h$ introduced in the previous section. Furthermore, we assume:*

$$\sup_h \sup_{x,y,t} |u_h(x,y,t)| \leq c$$

$$\|u - u_h\|_{L^2_{loc}(\mathbb{R}^2 \times \mathbb{R}^+)} \to 0, \;\; as \; \Delta t, h \to 0$$

*Then $u$ is a weak solution of the conservation law (2.8).*

# Chapter Three

# Local Conservation for Generic Numerical Methods

## 3.1 Introduction

The finite volume methods and discontinuous Galerkin (DG) methods, see, e.g., [11], are by design locally conservative numerical schemes. We present in the previous chapter the Lax–Wendroff theorem for finite volume methods in one and two space dimension. We could easily extend the Lax-Wendroff theorem to DG methods by setting the test function to value 1 in one cell and 0 in all other cells. Continuous Galerkin (CG) methods are considered only globally conservative until Hughes et al. [28] showed that it is actually locally conservative. But their definition of flux is not consistent with ours in this chapter, because in their definition at least one of the two neighboring subdomains has to be global to get the uniqueness of the flux across the boundary between these two subdomains. Perot [45] showed the local conservation of the CG methods with a different flux definition that is consistent with our definition in this chapter. See also Abgrall [1] for the discussion of local conservation of CG methods.

## 3.2 Local Conservation in One Space Dimension

### 3.2.1 Numerical Schemes

To discuss the local conservation of numerical methods, we first give the generic definition of a numerical scheme solving the conservation law (2.1):

$$\frac{u_h(\cdot, t_{n+1}) - u_h(\cdot, t_n)}{\Delta t_n} = L\left(u_h(\cdot, t_n)\right). \tag{3.1}$$

The discretization over the time domain is $0 = t_0 < t_1 < t_2 \ldots$ with $t_n \to \infty$ as $n \to \infty$. Time steps are denoted as $\Delta t_n = t_{n+1} - t_n$, and the time step size is the maximum over all time steps $\Delta t = \max_{n\geq 0} \Delta t_n$. The numerical solution $u_h$ is a (possibly discrete) function over the time-space domain $\mathbb{R}^+ \times \mathbb{R}$.

In order to define the numerical solution on the whole time domain $\mathbb{R}^+$, we expand $u_h$ to be a constant over each time interval, i.e. $u_h(x,t) \equiv u_h(x,t_n),\ \forall t \in [t_n, t_{n+1})$. Therefore, we can denote functions over the space domain $u_h^n = u_h(\cdot, t),\ \forall t \in [t_n, t_{n+1})$. For example, $u_h^n$ is a piecewise constant function for finite difference and finite volume methods, and a piecewise polynomial for Galerkin methods.

To define the local conservation property, we need (i) a partition of the spatial domain into intervals $\mathbb{R} = \cup_{j\in\mathbb{Z}} I_j$, (ii) a locally conserved quantity on each cell, and (iii) a flux on each interval endpoint. The intervals $I_j = [x_{j-\frac{1}{2}}, x_{j+\frac{1}{2}}]$, and they satisfy the regularity condition: $|I_j| > c_0\, h$, where $|I_j|$ is the length of the interval, mesh size $h = \max_{j\in\mathbb{Z}} |I_j|$, and $c_0 > 0$ is independent of the mesh size. For simplicity, we now denote $\sum_{n=0}^{+\infty}$ as $\sum_n$, and $\sum_{j\in\mathbb{Z}}$ as $\sum_j$.

### 3.2.2 Definition of local conservation

We define a numerical scheme to be locally conservative if its solution satisfies the following conservation form (cf. [32]):

$$\frac{\bar{u}_j^{n+1} - \bar{u}_j^n}{\Delta t_n} + \frac{1}{|I_j|}\left(g_{j+\frac{1}{2}}(u_h^n) - g_{j-\frac{1}{2}}(u_h^n)\right) = 0. \tag{3.2}$$

Here $\bar{u}_j^n$ (generalized locally conserved quantity) and $g_{j+\frac{1}{2}}$ (generalized flux) both depend on the numerical solution locally. More precisely, they depend on $u_h^n\,(B_j)$. $B_j = \{\, x \in \mathbb{R} : |x - w_j| < c\,h\}$, where $w_j$ is the midpoint of the interval $I_j$, and $c > 1$ is independent of the mesh size. Note that $\bar{u}_j^n$ here is not necessarily the cell average ($\frac{1}{|I_j|}\int_{I_j} u_h^n$) even though we use the traditional notation for cell averages. The conserved quantity and flux also need to be consistent and bounded in the following sense:

- *consistency*: if $u_h^n(x) \equiv u$, a constant, $\forall x \in B_j$, we have:

$$\bar{u}_j^n = u, \tag{3.3}$$

$$g_{j+\frac{1}{2}}(u_h^n) = f(u), \tag{3.4}$$

- *boundedness*: they are both bounded with respect to the $L^\infty$-norm of the solution:

$$\left|\bar{u}_j^n - \bar{v}_j^n\right| \le C\,\|u_h^n - v_h^n\|_{L^\infty(B_j)}, \tag{3.5}$$

$$\left|g_{j+\frac{1}{2}}(u_h^n) - g_{j+\frac{1}{2}}(v_h^n)\right| \le C\,\|u_h^n - v_h^n\|_{L^\infty(B_j)} \tag{3.6}$$

  for two functions ($u_h$ and $v_h$) in the numerical solution space.

To get global conservation from our definition, we also require the summation of the local conservation quantities being exactly the global conservation quantity:

$$\sum_j |I_j|\,\bar{u}_j^n = \int_{\mathbb{R}} u_h(x, t_n)\,dx,\ \forall n \ge 0. \tag{3.7}$$

It is easy to see that (3.7) together with (3.2) implies the following global conservation:

$$\int_{\mathbb{R}} u_h(x,t)\,dx = \int_{\mathbb{R}} u_h(x,0)\,dx, \ \ \forall t > 0. \tag{3.8}$$

We now have gathered all parts, and give the formal definition of local conservation.

**Definition 3.2.1.** *A numerical scheme of the form (3.1) is locally conservative if there are conserved quantities and fluxes, both of which locally depend on the numerical solution and satisfy (3.2)–(3.7).*

### 3.2.3 Lax-Wendroff type theorem

In this section, we prove a Lax-Wendroff type theorem for locally conservative numerical schemes in the sense of Definition 3.2.1. We first assume that the initial condition is weakly enforced in the numerical solution as follows:

$$\int_{\mathbb{R}} \left(u_0 - u_h^0\right) \phi \to 0, \text{ as } h \to 0, \ \forall \phi \in C_0^\infty\left(\mathbb{R}\right). \tag{3.9}$$

To get the convergence result, we also need an assumption similar to the bounded total variation of the numerical solution:

$$h \sum_j \max_{x \in B_j} \left|u_h^n(x) - u_h^n(w_j)\right| \to 0, \text{ as } h \to 0, \ \ \forall n \geq 0 \tag{3.10}$$

The assumption (3.10) on the numerical solution may seem odd at first glance, but it is actually implied by boundedness of total variation as Proposition 3.2.1 shows. Recall the definition of total variation:

$$\mathrm{TV}(u_h^n) = \sup_{\mathcal{P}} \sum_{i=-\infty}^{+\infty} \left|u_h^n(x_{i+1}) - u_h^n(x_i)\right|, \tag{3.11}$$

where $\mathcal{P}$ denotes the set of all partitions of the real line $\mathbb{R}$.

**Proposition 3.2.1.** *If the numerical solution $u_h^n$ has uniformly bounded total varia-*

*tion, i.e.*

$$TV(u_h^n) < C, \quad \forall n \geq 0, \tag{3.12}$$

*$u_h^n$ satisfies the assumption (3.10).*

*Proof.* We can deduce that there are a finite number of, say no more than $p$ (independent of mesh size), intervals in each neighborhood $B_j$ from the regularity of the mesh and the definition of $B_j$. We define the point that attains the maximal value of $|u_h^n(x) - u_h^n(w_j)|$ in $B_j$ as $m_j$, which is in some interval $I_k$ with $|j-k| < p$.

We can therefore define a series of intervals $(I_{j_1}, I_{j_2} \dots I_{j_p})$ such that $m_j \in I_{j_p}$, where $j_1 = j$, and $|j_s - j_{s+1}| \leq 1$ $(\forall 1 \leq s < p)$. The summation in (3.10) can be estimated as follows:

$$\begin{aligned}
&h \sum_j \max_{x \in B_j} |u_h^n(x) - u_h^n(w_j)| = h \sum_j |u_h^n(m_j) - u_h^n(w_j)| \\
\leq& h \sum_j \left( \left|u_h^n(m_j) - u_h^n(w_{j_p})\right| + \sum_{s=1}^{p-1} \left|u_h^n(w_{j_s}) - u_h^n(w_{j_{s+1}})\right| \right) \\
\leq& h \sum_j \sup_{x \in I_{j_p}} \left|u_h^n(x) - u_h^n(w_{j_p})\right| + 2p\, h \sum_j |u_h^n(w_{j+1}) - u_h^n(w_j)| \\
\leq& 4p\, h\, TV(u_h^n) \ \to 0, \ \text{as } h \to 0.
\end{aligned}$$

In the above calculation, we used two obvious inequalities:

$$\sum_j \sup_{x \in I_j} |u_h^n(x) - u_h^n(w_j)| \leq TV(u_h^n) \tag{3.13}$$

$$\sum_j |u_h^n(w_{j+1}) - u_h^n(w_j)| \leq TV(u_h^n) \tag{3.14}$$

$\square$

We now state and prove a Lax-Wendroff type theorem for our definition of local conservation. The proof is quite similar to the simplified proof of the Lax-Wendroff theorem in [33].

**Theorem 3.2.1.** *Assume the solution to a locally conservative numerical scheme, with initial condition imposed as (3.9), satisfies the assumption (3.10). If $u_h$ converges boundedly almost everywhere to some function $u$ as $\Delta t, h \to 0$, then $u$ is a weak solution to the conservation law (2.1), i.e.*

$$\int_{\mathbb{R}} u_0 \, \phi \; + \int_{\mathbb{R}^+ \times \mathbb{R}} u \, \phi_t \; + \int_{\mathbb{R}^+ \times \mathbb{R}} f(u) \cdot \phi_x = 0, \; \forall \phi \in C_0^\infty \left( \mathbb{R}^+ \times \mathbb{R} \right). \tag{3.15}$$

*Proof.* Multiplying $\Delta t_n \, |I_j| \, \phi(w_j, t_n)$ on both sides of (3.2) and summing it over all $n, j$, we have the following equality:

$$\sum_n \sum_j |I_j| \left( \bar{u}_j^{n+1} - \bar{u}_j^n \right) \phi_j^n + \sum_n \sum_j \Delta t_n \left( g_{j+\frac{1}{2}}(u_h^n) - g_{j-\frac{1}{2}}(u_h^n) \right) \phi_j^n = 0 \tag{3.16}$$

where we denote $\phi(w_j, t_n)$ as $\phi_j^n$, and $\phi(x, t_n)$ as $\phi^n(x)$. We can apply summation by parts on the first term and get:

$$\sum_n \sum_j |I_j| \left( \bar{u}_j^{n+1} - \bar{u}_j^n \right) \phi_j^n = - \sum_j |I_j| \, \bar{u}_j^0 \, \phi_j^0 \; - \sum_n \sum_j |I_j| \left( \phi_j^{n+1} - \phi_j^n \right) \bar{u}_j^{n+1} = -\mathrm{I} - \mathrm{II} \tag{3.17}$$

By using assumptions (3.3), (3.5), (3.9), (3.10), the fact that $\phi$ is compactly supported, and the bounded convergence theorem, we get the convergence of term I to the first integration in (3.15) as follows:

$$\begin{aligned} \sum_j |I_j| \, \bar{u}_j^0 \, \phi_j^0 &= \int_{\mathbb{R}} u_h^0(x) \, \phi^0(x) \, dx + \sum_j \int_{I_j} \left( \bar{u}_j^0 - u_h^0(x) \right) \phi^0(x) \, dx + O(h) \\ &= \int_{\mathbb{R}} u_0(x) \phi^0(x) \, dx + o(1) \end{aligned}$$

where $o(1)$ denotes a quantity which goes to zero when the mesh sizes go to zero. We similarly deduce the convergence of term II to the second integration in (3.15):

$$\begin{aligned}
&\sum_n \sum_j |I_j| \left(\phi_j^{n+1} - \phi_j^n\right) \bar{u}_j^{n+1} \\
=&\sum_{n=1}^{+\infty} \sum_j \int_{t_n}^{t_{n+1}} \int_{I_j} \phi_t(x,t)\, u_h(x,t)\, dx\, dt \\
&+ \sum_{n=1}^{+\infty} \sum_j \int_{t_n}^{t_{n+1}} \int_{I_j} \phi_t(x,t)\, \left(\bar{u}_j^n - u_h^n(x)\right)\, dx\, dt + O(h) \\
=&\int_{\mathbb{R}^+ \times \mathbb{R}} \phi_t(x,t)\, u(x,t)\, dx\, dt + o(1)
\end{aligned}$$

Lastly, we prove the convergence of the second summation in (3.16) to the third integration in (3.15):

$$\begin{aligned}
&\sum_n \sum_j \Delta t_n \left( g_{j+\frac{1}{2}}(u_h^n)\, \phi_j^n - g_{j-\frac{1}{2}}(u_h^n)\, \phi_j^n \right) \\
=&\sum_n \sum_j \Delta t_n \left( f(u_h^n(w_j)) \left(\phi_j^n - \phi_{j+\frac{1}{2}}^n\right) - f(u_h^n(w_j)) \left(\phi_j^n - \phi_{j-\frac{1}{2}}^n\right)\right) + \\
&\sum_n \sum_j \Delta t_n \Bigg( \left(g_{j+\frac{1}{2}}(u_h^n) - f(u_h^n(w_j))\right) \left(\phi_j^n - \phi_{j+\frac{1}{2}}^n\right) \\
&\qquad - \left(g_{j-\frac{1}{2}}(u_h^n) - f(u_h^n(w_j))\right) \left(\phi_j^n - \phi_{j-\frac{1}{2}}^n\right) \Bigg) \\
=&\mathrm{III} + \mathrm{IV},
\end{aligned}$$

where $\phi^n(x_{j+\frac{1}{2}})$ is denoted as $\phi_{j+\frac{1}{2}}^n$.

By using the definition (3.3)-(3.6) and the assumption (3.10), we have that term IV vanishes as the mesh size goes to zero. The convergence of term III to the last integration of (3.15) can be deduced by using the local conservation definition and the assumption

(3.10) as follows:

$$\begin{aligned}
\mathrm{III} &= -\sum_n \sum_j \Delta t_n f(u_h^n(w_j)) \left(\phi^n_{j+\frac{1}{2}} - \phi^n_{j-\frac{1}{2}}\right) \\
&= -\sum_n \sum_j \int_{t_n}^{t_{n+1}} \int_{I_j} f(u_h^n(x))\, \partial_x \phi(x, t_n)\, dx\, dt + o(1) \\
&= -\int_{\mathbb{R}^+ \times \mathbb{R}} f(u) \phi_x + o(1)
\end{aligned}$$

The proof is concluded by combining the convergence of terms I–IV. □

### 3.2.4 Examples of locally conservative numerical methods

We first point out that the DG methods (see, e.g., [11]), as well as standard finite difference and finite volume methods taking conservation form obviously have the local conservation property. In the next few subsections, we show some other examples of locally conservative numerical methods.

#### 3.2.4.1 Compact (finite difference) schemes

Compact schemes are non-standard finite difference methods, for which the numerical solution usually is defined on the grid points of a uniform mesh. We can extend the definition of the numerical solution to be a piecewise constant function defined over the whole real line. A compact scheme for the conservation law (2.1) can be written as (Cockburn and Shu [15]):

$$\frac{u_h^{n+1}(w_j) - u_j^n(w_j)}{\Delta t_n} + \frac{1}{\Delta x} \left(A^{-1}\, B\, f(u_h^n)\right)_j = 0 \tag{3.18}$$

where $A$ and $B$ are local linear operators. We can define the conserved quantity $\bar{u}_j^n = (A\, u_h^n)_j$ and the flux $g_{j+\frac{1}{2}}(u_h^n)$ satisfying

$$(B\, f(u_h^n))_j = g_{j+\frac{1}{2}}(u_h^n) - g_{j-\frac{1}{2}}(u_h^n). \tag{3.19}$$

It is not hard to check that the compact scheme is locally conservative with the conserved quantity and flux we just defined.

#### 3.2.4.2 Non-standard finite volume methods

Zhang et al. [52] have proposed a non-standard finite volume scheme, in order to design high order maximum-principle-satisfying schemes for solving convection-diffusion equations. The degrees of freedom for this method are the so called "double cell averages" as opposed to the usual cell averages for standard finite volume methods. Suppose the real line is uniformly decomposed into intervals $\mathbb{R} = \cup_{j\in\mathbb{Z}} I_j$. The cells $I_j = [x_{j-\frac{1}{2}}, x_{j+\frac{1}{2}}]$ whose midpoints are denoted as $x_j$. The scheme applied on conservation law (2.1) can be written as (see (3.19) in [52]):

$$\frac{\bar{\bar{u}}_j^{n+1} - \bar{\bar{u}}_j^n}{\Delta t} + \frac{1}{\Delta x}\sum_{\alpha=1}^{3} w_\alpha \left(\hat{f}^\alpha_{j+\frac{1}{2}} - \hat{f}^\alpha_{j-\frac{1}{2}}\right) = 0 \tag{3.20}$$

where $w_\alpha$ are quadrature weights and $\hat{f}^\alpha_{j+\frac{1}{2}}$ are numerical fluxes (clearly satisfying (3.4) and (3.6)) on the quadrature points. The double cell averages are defined as:

$$\bar{\bar{u}}_j^n = \frac{1}{\Delta x^2}\int_{I_j}\int_{x-\frac{\Delta x}{2}}^{x+\frac{\Delta x}{2}} u_h^n(\xi)\, d\xi\, dx, \tag{3.21}$$

where $u_h^n$ is the underlying numerical solution. By using the following equality

$$\bar{\bar{u}}_j^n = \frac{1}{\Delta x^2}\int_{x_{j-1}}^{x_j} u_h^n(x)(x - x_{j-1})\,dx + \frac{1}{\Delta x^2}\int_{x_j}^{x_{j+1}} u_h^n(x)(x_{j+1} - x)\,dx, \tag{3.22}$$

we can easily show that the double cell averages satisfy conditions (3.3), (3.5), and (3.7). Therefore the scheme (3.20) is locally conservative.

#### 3.2.4.3 Continuous Galerkin method

Let $U_h^k = \{v \in H^1(\mathbb{R}) : v \in P_k(e_j), \forall j \in \mathbb{Z}\}$, where the set of intervals$\{e_j = [y_j, y_{j+1}] : j \in \mathbb{Z}\}$ is a partition of the real line and $P_k(e_j)$ denotes the set of polynomials over the cell $e_j$. The CG method reads: find $u_h(\cdot, t_n) \in U_h^k$, such that for all test function $v_h \in U_h^k$

$$\int_{\mathbb{R}} \frac{u_h^{n+1} - u_h^n}{\Delta t_n} v_h - \int_{\mathbb{R}} f(u_h^n) v_h' = 0. \tag{3.23}$$

To define local conservation, we need a different partition of the domain $\mathbb{R} = \cup_{j\in\mathbb{Z}} I_j = \cup_{j\in\mathbb{Z}}[x_{j-\frac{1}{2}}, x_{j+\frac{1}{2}}]$, where $x_{j+\frac{1}{2}} = H_z(y_j + y_{j+1})$. We take the test function $v_h$ as the shape function $v_j$, which is a piecewise linear function satisfying $v_j(y_j) = \frac{1}{|I_j|}$, $v_j(y_l) = 0,\ \forall l \neq j$. The generalized conserved quantity is defined as: $\bar{u}_j^n = \int_{\mathbb{R}} u_h^n v_j$, and the generalized flux is defined as $g_{j+\frac{1}{2}}(u_h^n) = \frac{1}{|e_j|}\int_{e_j} f(u_h^n)$. It is easy to check that the above definitions satisfy the conditions (3.2)–(3.7), and thus the CG method is locally conservative. The result in this section can be generalized to CG methods with local basis satisfying the partition of unity property by a similar argument to that in section 3.3.4.3. The B-spline finite element methods (see, e.g., [23]) is one example.

## 3.3 Local Conservation in Two Space Dimension

We study numerical methods for two-dimensional scalar conservation laws of the form:

$$\begin{aligned} u_t + \nabla \cdot \boldsymbol{f}(u) = 0 \text{ in } \mathbb{R}^+ \times \mathbb{R}^2 \\ u(\cdot, 0) = u_0 \text{ in } \mathbb{R}^2, \end{aligned} \tag{3.24}$$

where the flux function $\boldsymbol{f} = (f_1,\ f_2)$, and both of its components are at least Lipschitz continuous. We similarly define the local conservation property and prove a Lax-Wendroff type theorem here.

### 3.3.1 Numerical schemes

We again consider in our presentation only schemes with Euler forward time stepping since the spatial discretization is our primary concern, and thus the schemes read:

$$\frac{u_h(\cdot, t_{n+1}) - u_h(\cdot, t_n)}{\Delta t_n} = L\left(u_h(\cdot, t_n)\right), \tag{3.25}$$

where the time domain is discretized as in 1D case. The numerical solution is a constant over each time interval, i.e. $u_h(\cdot, t) = u_h(\cdot, t_n),\ \forall t \in [t_n, t_{n+1})$, and thus we can denote $u_h^n = u_h(\cdot, t_n)$.

To define the local conservation property, we need (i) a partition of the spatial domain into cells $\mathbb{R}^2 = \cup_{j \in J} T_j$, (ii) a locally conserved quantity on each cell, and (iii) a flux on each cell interface. The cells are polygons with at most $p$ edges, and satisfy the regularity condition: $|T_j| > c_0\, h^2$, where $|T_j|$ is the area of the cell, and the mesh size $h = \max_{j\in J} \operatorname{diam}(T_j)$. For simplicity, we again denote $\sum_{n=0}^{\infty}$ as $\sum_n$, and $\sum_{j\in J}$ as $\sum_j$.

### 3.3.2 Definition of local conservation

We say a numerical scheme is locally conservative if its solution satisfies the following conservation form equality (cf. [29, 30, 2]):

$$\frac{\bar{u}_j^{n+1} - \bar{u}_j^n}{\Delta t_n} + \frac{1}{|T_j|} \sum_{l\in N_j} \sum_{s=1}^{c_{jl}} g_{jl}^{(s)}(u_h^n) = 0. \tag{3.26}$$

Here, $N_j$ denotes the set of cell indices of all cells adjacent to $T_j$, i.e. $N_j = \{l \in J : T_j \cap T_l \neq \varnothing\}$. The cell interface between $T_j$ and $T_l$ has $c_{jl}$ line segments. If $\{T_j : j \in J\}$ is a triangulation, $c_{jl}$ is always 1. If $\{T_j : j \in J\}$ is the dual mesh (see, e.g., Bush and Ginting [4]) of a triangulation, $c_{jl}$ equals to two for all the boundaries. $\bar{u}_j^n$ (generalized conserved quantity) and $g_{jl}$ (generalized flux) both depend on the numerical solution locally. More precisely, they depend on $u_h^n(B_j)$. $B_j = \left\{\boldsymbol{x} \in \mathbb{R}^2 : |\boldsymbol{x} - w_j| < c\,h\right\}$, where the center of a cell $w_j = \frac{1}{|T_j|}\int_{T_j} \boldsymbol{x}\,d\boldsymbol{x}$, and $c\,(> 1)$ is independent of the mesh size. The conserved quantity and flux also need to be consistent and bounded in the following sense:

- *consistency*: if $u_h^n(\boldsymbol{x}) \equiv u$, a constant, $\forall \boldsymbol{x} \in B_j$, we have:

$$\bar{u}_j^n = u, \tag{3.27}$$

$$g_{jl}^{(s)}(u_h^n) = \boldsymbol{\nu}_{jl}^{(s)} \cdot \boldsymbol{f}(u), \tag{3.28}$$

where $\boldsymbol{\nu}_{jl}^{(s)} = \left|S_{jl}^{(s)}\right| \boldsymbol{n}_{jl}^{(s)}$, and $S_{jl}^{(s)}$ is the $s$-th line segment on the boundary between elements $T_j$ and $T_l$. $\boldsymbol{n}_{jl}^{(s)}$ is the normal vector on $S_{jl}^{(s)}$ pointing toward

$T_l$.

- *boundedness*: they are both bounded in terms of the $L^\infty$-norm of the numerical solution:

$$\left|\bar{u}_j^n - \bar{v}_j^n\right| \leq C\,\|u_h^n - v_h^n\|_{L^\infty(B_j)}, \tag{3.29}$$

$$|g_{jl}(u_h^n) - g_{jl}(v_h^n)| \leq C\,h\,\|u_h^n - v_h^n\|_{L^\infty(B_j)}. \tag{3.30}$$

As a flux, $g_{jl}$ must be unique on cell interfaces, i.e.

$$g_{jl}(u_h^n) + g_{lj}(u_h^n) = 0, \quad \forall j \in J,\, l \in N_j. \tag{3.31}$$

To get global conservation from our definition, we also require the summation of the local conservation quantities being exactly the global conservation quantity:

$$\sum_j |T_j|\,\bar{u}_j^n = \int_{\mathbb{R}^2} u_h^n,\ \forall n \geq 0. \tag{3.32}$$

It is easy to see that (3.32) together with (3.26) and (3.31) implies the following global conservation:

$$\int_{\mathbb{R}^2} u_h(\cdot, t) = \int_{\mathbb{R}^2} u_h(\cdot, 0), \quad \forall t > 0. \tag{3.33}$$

We now have all the parts and give the formal definition of local conservation.

**Definition 3.3.1.** *A numerical scheme of the form (3.25) is locally conservative if there exist conserved quantities and fluxes, both of which locally depend on the numerical solution and satisfy (3.26)–(3.32).*

### 3.3.3 Lax-Wendroff type theorem

In this section, we prove a Lax-Wendroff type theorem for numerical schemes satisfying Definition 3.3.1. The technique of the proof is similar to that in Kröner and Rokyta [29] and Kröner et al. [30]. We first need to weakly enforce the initial condition as follows:

$$\int_{\mathbb{R}^2} \left(u_0 - u_h^0\right) \phi \to 0, \text{ as } h \to 0, \ \forall \phi \in C_0^\infty \left(\mathbb{R}^2\right). \tag{3.34}$$

To get the convergence result, we also need an assumption similar to the bounded total variation of the numerical solution:

$$h^2 \sum_j \max_{x \in B_j} |u_h^n(x) - u_h^n(w_j)| \to 0, \text{ as } h \to 0, \ \ \forall n \geq 0, \tag{3.35}$$

which is a 2D generalization of (3.10). This assumption clearly holds for piecewise smooth functions with smooth regions divided by curves.

**Theorem 3.3.1.** *Assume the solution to a locally conservative numerical scheme with initial condition imposed as (3.34) satisfies the assumption (3.35). If $u_h$ converges boundedly almost everywhere to some function $u$ as $\Delta t, h \to 0$, then $u$ is a weak solution to the conservation law (2.8), i.e.*

$$\int_{\mathbb{R}^2} u_0 \, \phi \ + \int_{\mathbb{R}^+ \times \mathbb{R}^2} u \, \phi_t \ + \int_{\mathbb{R}^+ \times \mathbb{R}^2} \boldsymbol{f}(u) \cdot \nabla \phi = 0, \ \forall \phi \in C_0^\infty \left(\mathbb{R}^+ \times \mathbb{R}^2\right). \tag{3.36}$$

*Proof.* Multiplying $\Delta t_n \, |T_j| \, \phi(w_j, t_n)$ on both sides of (3.26) and summing it over all $n, j$, we have the following equality:

$$\sum_n \sum_j |T_j| \left(\bar{u}_j^{n+1} - \bar{u}_j^n\right) \phi_j^n \ + \Delta t_n \sum_n \sum_j \sum_{l \in N_j} \sum_{s=1}^{c_{jl}} g_{jl}^{(s)}(u_h^n) \phi_j^n = 0, \tag{3.37}$$

where we denote $\phi(w_j, t_n)$ as $\phi_j^n$, and $\phi(x, t_n)$ as $\phi^n(x)$. The convergence of the first summation in (3.37) to the first two integrations in (3.36) can be proved exactly the same as in Theorem 3.2.1.

We now prove the convergence of the second summation in (3.37) to the third integration in (3.36) by using definition (3.27)–(3.31) together with the assumption (3.35):

$$
\begin{aligned}
&\sum_n \sum_j \sum_{l\in N_j} \sum_{s=1}^{c_{jl}} \Delta t_n \, g_{jl}^{(s)}(u_h^n)\, \phi_j^n \\
=&\sum_n \sum_j \sum_{l\in N_j} \sum_{s=1}^{c_{jl}} \Delta t_n \, g_{jl}^{(s)}(u_h^n) \left(\phi_j^n - \phi^n(z_{jl}^{(s)})\right) \\
=&-\sum_n \sum_j \sum_{l\in N_j} \sum_{s=1}^{c_{jl}} \Delta t_n \, \boldsymbol{\nu}_{jl}^{(s)} \cdot \boldsymbol{f}(u_h^n(w_j))\, \phi^n(z_{jl}^{(s)}) \\
&+\sum_n \sum_j \sum_{l\in N_j} \sum_{s=1}^{c_{jl}} \Delta t_n \left(g_{jl}^{(s)}(u_h^n) - g_{jl}^{(s)}(u_h^n(w_j))\right) \left(\phi_j^n - \phi^n(z_{jl}^{(s)})\right) \\
=&-\sum_n \sum_j \Delta t_n \, |T_j| \, \boldsymbol{f}(u_h^n(w_j)) \cdot \nabla\phi^n(w_j) \; + o(1) \\
=&-\int_{\mathbb{R}^+\times\mathbb{R}^2} \boldsymbol{f}(u) \cdot \nabla\phi \; + o(1)
\end{aligned}
$$

where $z_{jl}^{(s)}$ is the midpoint of $S_{jl}^{(s)}$. In the above calculation, we used the fact that

$$
\sum_{l\in N_j} \sum_{s=1}^{c_{jl}} \boldsymbol{\nu}_{jl}^{(s)} = 0, \tag{3.38}
$$

$$
\sum_j \sum_{l\in N_j} \sum_{s=1}^{c_{jl}} g_{jl}(u_h^n)\, \phi^n(z_{jl}^{(s)}) = 0, \tag{3.39}
$$

and Lemma 3.3.1 from [30]. □

**Lemma 3.3.1.** *If $\phi \in C_0^\infty\left(\mathbb{R}^2\right)$, we have the approximate integration by parts formula:*

$$
|T_j| \, \nabla\phi(w_j) = \sum_{l\in N_j} \sum_{s=1}^{c_{jl}} \phi(z_{jl}^{(s)}) \boldsymbol{\nu}_{jl}^{(s)} + O(h^3) \tag{3.40}
$$

### 3.3.4 Examples of locally conservative numerical methods

As in the one dimensional case, the DG methods (see, e.g., [11]), standard finite volume and finite element methods taking conservation form are obviously locally conservative per Definition 3.3.1. We show in this section that the two dimensional counterpart of numerical methods in section 3.2.4 are also locally conservative.

#### 3.3.4.1 Compact (finite difference) schemes

The compact schemes in the two space dimensions has their solutions defined on a 2D uniform structured grid with size $\Delta x,\ \Delta y$. We can extend the solution by making it a constant on a rectangular centered at each grid point. The size of each rectangle is $\Delta x \times \Delta y$. We denote the grid points as $\{w_{ij} \in \mathbb{R}^2 : i, j \in \mathbb{Z}\}$, and the schemes read:

$$\frac{u_h^{n+1}(w_{ij}) - u_h^n(w_{ij})}{\Delta t} + \frac{1}{\Delta x}(A_x^{-1}\, B_x\, f_1(u))_{ij} + \frac{1}{\Delta y}(A_y^{-1} B_y f_2(u))_{ij} = 0 \tag{3.41}$$

where the operator $A_x$ is the operator for the 1D compact scheme applied in the $x$ direction, and the same for other three operators. We can rewrite the scheme (3.41) into a conservation form as in Cockburn and Shu [15]:

$$\frac{\bar{u}_{ij}^{n+1} - \bar{u}_{ij}^n}{\Delta t_n} + \frac{1}{\Delta x}\left(\hat{f}_{i+H_z,j}^n - \hat{f}_{i-H_z,j}^n\right) + \frac{1}{\Delta y}\left(\hat{g}_{i,j+\frac{1}{2}}^n - \hat{g}_{i,j-\frac{1}{2}}^n\right) = 0, \tag{3.42}$$

where $\bar{u}_{ij}^n = A_y A_x u$, and flux are similarly defined as in 1D case. For example,

$$\hat{f}_{i+H_z,j}^n = H_z A_y \left(f(u_h^n(w_{i+1,j})) + f(u_h^n(w_{ij}))\right),$$

$$\hat{g}_{i,j+\frac{1}{2}}^n = H_z A_x \left(g(u_h^n(w_{i,j+1})) + g(u_h^n(w_{ij}))\right),$$

if $(Bu)_i = H_z(u_{i+1} - u_{i-1})$. We could easily check that the compact scheme in 2D is locally conservative with the form (3.42).

#### 3.3.4.2 Non-standard finite volume methods

A straightforward generalization of the non-standard finite volume methods (3.20) on 2D uniform rectangular meshes are given in [52] (see (4.3)):

$$\frac{\bar{\bar{u}}_{ij}^{n+1} - \bar{\bar{u}}_{ij}^{n}}{\Delta t} + \frac{1}{\Delta x}\left(\hat{f}_{i+H_z,j} - \hat{f}_{i-H_z,j}\right) + \frac{1}{\Delta y}\left(\hat{g}_{i,j+\frac{1}{2}} - \hat{g}_{i,j-\frac{1}{2}}\right) = 0 \tag{3.43}$$

where $\bar{\bar{u}}_{ij}^{n}$ is the 2D version of double cell average:

$$\bar{\bar{u}}_{ij}^{n} = \frac{1}{\Delta x^2}\frac{1}{\Delta y^2} = \int_{y_{j-\frac{1}{2}}}^{y_{j+\frac{1}{2}}} \int_{y-\frac{\Delta y}{2}}^{y+\frac{\Delta y}{2}} \int_{x_{i-\frac{1}{2}}}^{x_{i+\frac{1}{2}}} \int_{x-\frac{\Delta x}{2}}^{x+\frac{\Delta x}{2}} u(\xi,\eta)\, d\xi\, dx\, d\eta\, dy. \tag{3.44}$$

The 2D uniform rectangular mesh is denoted as: $\mathbb{R}^2 = \cup_{i,j\in\mathbb{Z}}[x_{i-\frac{1}{2}}, x_{i+\frac{1}{2}}]\times[y_{j-\frac{1}{2}}, y_{j+\frac{1}{2}}]$. We can similarly get the local conservation property for this scheme by using the following equality on double cell averages:

$$\begin{aligned}
\bar{\bar{u}}_{ij}^{n} =& \frac{1}{\Delta x^2}\frac{1}{\Delta y^2}\int_{x_{i-1}}^{x_i}\int_{y_{j-1}}^{y_j} u_h^n(x,y)(x - x_{i-1})(y - y_{j-1})\, dx\, dy\, + \\
& \frac{1}{\Delta x^2}\frac{1}{\Delta y^2}\int_{x_{i-1}}^{x_i}\int_{y_j}^{y_{j+1}} u_h^n(x,y)(x - x_{i-1})(y_{j+1} - y)\, dx\, dy\, + \\
& \frac{1}{\Delta x^2}\frac{1}{\Delta y^2}\int_{x_i}^{x_{i+1}}\int_{y_{j-1}}^{y_j} u_h^n(x,y)(x_{i+1} - x)(y - y_{j-1})\, dx\, dy\, + \\
& \frac{1}{\Delta x^2}\frac{1}{\Delta y^2}\int_{x_i}^{x_{i+1}}\int_{y_j}^{y_{j+1}} u_h^n(x,y)(x_{i+1} - x)(y_{j+1} - y)\, dx\, dy,
\end{aligned}$$

where $x_i$ and $y_j$ are midpoints of the the intervals in each dimension.

#### 3.3.4.3 Continuous Galerkin method

Let $U_h^k = \{v \in H^1(\mathbb{R}^2) : v \in P_k(e_i), \forall i \in \mathbb{Z}\}$, where $\{e_i,\, i \in \mathbb{Z}\}$ is a triangulation of the whole space. The CG method reads: find $u_h(\cdot, t_n) \in U_h^k$, such that for all test function $v_h \in U_h^k$

$$\int_{\mathbb{R}^2} \frac{u_h^{n+1} - u_h^n}{\Delta t_n} v_h - \int_{\mathbb{R}^2} \boldsymbol{f}(u_h^n) \cdot \nabla v_h = 0. \tag{3.45}$$

The flux defined in Hughes et al. [28] does not fall in our definition since it needs at least one of the two regions to be global to get the uniqueness of flux between the two regions. The flux and conserved quantity in Perot [45] does satisfy the requirement of Definition 3.3.1, and we briefly reproduce his formulation here.

For the purpose of defining local conservation, we use a different partition $\mathbb{R} = \cup_{j\in J} T_j$, where $\{T_j : j \in J\}$ is the dual mesh of the original triangulation $\{e_i,\, i \in \mathbb{Z}\}$. The dual mesh, see, e.g., Bush and Ginting [4], is constructed by connecting the midpoint of edges and centroids of cells in the original triangulation. Since every cell in the dual mesh corresponds to a vertex in the original triangulation, we denote $\{n_j : j \in J\}$ as the set of vertices. The shape functions are defined as $\{v_j \in U_h^1 : v_j(n_j) = 1, v_j(n_l) = 0,\, \forall l \neq j\}$. Because the partition of unity property, $\sum_{j\in J} v_j \equiv 1$ on $\mathbb{R}^2$, we have the following equality:

$$\nabla v_j = \sum_{l\in N_k} v_l \nabla v_j - v_j \nabla v_l\,, \text{ in } \mathbb{R}^2, \tag{3.46}$$

which leads to a rewriting of the scheme (3.45) if we take the test function as the shape function:

$$\begin{aligned} &\frac{1}{\Delta t_n}\left(\frac{1}{|T_j|}\int_{\mathbb{R}^2} u_h^{n+1}\, v_j - \frac{1}{|T_j|}\int_{\mathbb{R}^2} u_h^n\, v_j\right) \\ -&\sum_{l\in N_j} \frac{1}{|T_j|}\int_{\mathbb{R}^2} v_l\, \boldsymbol{f}(u_h^n)\cdot\nabla v_j - v_j\, \boldsymbol{f}(u_h^n)\cdot \nabla v_l = 0. \end{aligned} \tag{3.47}$$

We can check, with routine algebraic calculation, that the 2D CG method (3.45) is locally conservative in the sense of Definition 3.3.1 if we define the conserved quantity and flux as follows:

$$\bar{u}_j^n = \frac{1}{|T_j|} \int_{\mathbb{R}^2} u_h^n \, v_j, \tag{3.48}$$

$$g_{jl}^{(s)}(u_h^n) = \left( \frac{\left| S_{jl}^{(s)} \right|}{\left| S_{jl}^{(1)} \right| + \left| S_{jl}^{(2)} \right|} \right) \sum_{l \in N_j} \frac{1}{|T_j|} \int_{\mathbb{R}^2} v_j \, \boldsymbol{f}(u_h^n) \cdot \nabla v_l - v_l \, \boldsymbol{f}(u_h^n) \cdot \nabla v_j. \tag{3.49}$$

Note that $c_{jl}$ is always 2 here because $\{T_j,\, j \in J\}$ is the dual mesh of a triangulation. According to the above argument, all CG methods with local basis satisfying partition of unity are locally conservative. The 2D B-spline finite element methods (see, e.g., [27]) with tensor product B-spline basis is one example.

# Chapter Four

# Discontinuous Galerkin Methods for Maxwell's Equations in Drude Metamaterials on Rectangular Meshes

## 4.1 Introduction

Since the first successful construction of metamaterials with both negative permittivity and negative permeability in 2000, there has been a growing interest in the study of metamaterials and its applications in invisibility cloak design and sub-wavelength imaging. Numerical simulation of wave propagation in metamaterials plays a very important role in these investigations. Description of electromagnetic wave propagation in metamaterials leads to more complicated time domain Maxwell's equations than the standard Maxwell's equations in free space. Compared to many excellent works obtained for solving Maxwell's equations in the free space (see [20, 26, 43] and references therein), developing efficient and rigorous numerical methods for metamaterial Maxwell's equations needs much more efforts. The most recent progress in this direction can be found in the monograph by Hao and Mittra [25] on the finite-difference time-domain (FDTD) methods for modeling metamaterials, and in the monograph by Li and Huang [36] on the finite-element time-domain (FETD) methods for metamaterials.

The discontinuous Galerkin (DG) method was initially introduced in 1973 by Reed and Hill [47] for solving a neutron transport equation. Because of a few nice features of the DG methods (such as local solvability, flexibility in $h$-$p$ adaptivity, and efficiency in parallel implementation), various DG methods have been proposed for solving different partial differential equations since then. The work of Cockburn and Shu [14, 17] on Runge-Kutta DG (RKDG) methods for solving linear and nonlinear time dependent hyperbolic partial differential equations (PDEs), in which the spatial discretization is by DG and the time discretization is by Runge-Kutta methods (other time discretization methods are of course also possible, such as the leap frog method adopted in this paper), has facilitated the rapid advance and application of DG methods. Also relevant to our schemes studied in this paper, especially the choice of the alternating fluxes, we should mention the so-called local discontinuous Galerkin (LDG) method, which was introduced by Cockburn and Shu [16] for solving time-dependent convection-diffusion systems and was used in [49] for solving second-order hyperbolic equations. For more details on the algorithm design, analysis, implementation and application of DG and LDG schemes for solving time-dependent PDEs, readers can consult the review articles [18, 50] and the references therein.

Maxwell's equations play a very important role in describing wave propagation phenomena in various media. It is no surprise that many DG methods have already been developed for time-harmonic Maxwell's equations in free space (e.g., [3, 24, 44, 46]), time-dependent Maxwell's equations in both free space (e.g., [7, 13, 22, 26]) and dispersive media (e.g., [31, 40, 48]). The recently developed metamaterials also promoted some study of DG methods for solving Maxwells equations in metamaterials (e.g., [6, 34, 35, 37]). Among these methods, there are non-dissipative ones, e.g. [35], and optimal ones, e.g. [37]. However, our new method in this paper appears to be the only one to attain both optimal convergence rate and non-dissipation. Recently Xing et al [49, 5] and Chung et al [8, 9] proposed optimal and non-dissipative discontinuous Galerkin methods for wave equations. Our approach is similar to the LDG method of Xing et al [49, 5] in terms of the choices of the numerical fluxes in the scheme and the projection in the error estimate proof.

## 4.2 The governing equations

Consider the metamaterial Drude model [36] in the domain $\Omega$:

$$\epsilon_0 \frac{\partial \boldsymbol{E}}{\partial t} = \nabla \times \boldsymbol{H} - \boldsymbol{J} \tag{4.1}$$

$$\mu_0 \frac{\partial \boldsymbol{H}}{\partial t} = -\nabla \times \boldsymbol{E} - \boldsymbol{K} \tag{4.2}$$

$$\frac{1}{\epsilon_0 \omega_{pe}^2} \frac{\partial \boldsymbol{J}}{\partial t} + \frac{\Gamma_e}{\epsilon_0 \omega_{pe}^2} \boldsymbol{J} = \boldsymbol{E} \tag{4.3}$$

$$\frac{1}{\mu_0 \omega_{pm}^2} \frac{\partial \boldsymbol{K}}{\partial t} + \frac{\Gamma_m}{\mu_0 \omega_{pm}^2} \boldsymbol{K} = \boldsymbol{H} \tag{4.4}$$

supplemented with the perfect conduct (PEC) boundary condition

$$\boldsymbol{n} \times \boldsymbol{E} = \boldsymbol{0} \quad \text{on } \partial\Omega, \tag{4.5}$$

and the initial conditions

$$\boldsymbol{E}(\boldsymbol{x}, 0) = \boldsymbol{E}_0(\boldsymbol{x}), \quad \boldsymbol{H}(\boldsymbol{x}, 0) = \boldsymbol{H}_0(\boldsymbol{x}), \quad \boldsymbol{J}(\boldsymbol{x}, 0) = \boldsymbol{J}_0(\boldsymbol{x}), \quad \boldsymbol{K}(\boldsymbol{x}, 0) = \boldsymbol{K}_0(\boldsymbol{x}), \tag{4.6}$$

where $\boldsymbol{n}$ denotes the outward unit normal vector of $\partial\Omega$, $\boldsymbol{E}_0(\boldsymbol{x}), \boldsymbol{H}_0(\boldsymbol{x}), \boldsymbol{J}_0(\boldsymbol{x})$ and $\boldsymbol{K}_0(\boldsymbol{x})$ are some given proper functions. Here $\epsilon_0$ is the vacuum permittivity, $\mu_0$ is the vacuum permeability, $\omega_{pe} \geq 0$ and $\omega_{pm} \geq 0$ are the electric and magnetic plasma frequencies respectively, $\Gamma_e$ and $\Gamma_m$ are the electric and magnetic damping frequencies respectively, $\boldsymbol{E}(\boldsymbol{x}, t)$ and $\boldsymbol{H}(\boldsymbol{x}, t)$ are the electric and magnetic fields respectively, and $\boldsymbol{J}(\boldsymbol{x}, t)$ and $\boldsymbol{K}(\boldsymbol{x}, t)$ are the induced electric and magnetic currents respectively.

To avoid the technicality of the proof for 3D problem, below we only consider the transverse-electric mode with respect to $z$ in two dimensions (2-D), i.e., the so-called $TE_z$ mode, which involves only fields $\boldsymbol{E} = (E_x, E_y), \boldsymbol{H} = H_z := H, \boldsymbol{J} = (J_x, J_y), \boldsymbol{K} = K_z$, and the curls $\nabla \times \boldsymbol{E} = \frac{\partial E_y}{\partial x} - \frac{\partial E_x}{\partial y}$ and $\nabla \times \boldsymbol{H} = (\frac{\partial H}{\partial y}, -\frac{\partial H}{\partial x})'$. Here the subindices

$x, y$ and $z$ denote the components in the $x, y$ and $z$ directions, respectively. More specifically, the governing equations of the $TE_z$ Drude model can be written as:

$$\epsilon_0 \frac{\partial E_x}{\partial t} = \frac{\partial H_z}{\partial y} - J_x, \tag{4.7}$$

$$\epsilon_0 \frac{\partial E_y}{\partial t} = -\frac{\partial H_z}{\partial x} - J_y, \tag{4.8}$$

$$\mu_0 \frac{\partial H_z}{\partial t} = -\frac{\partial E_y}{\partial x} + \frac{\partial E_x}{\partial y} - K_z, \tag{4.9}$$

$$\frac{1}{\epsilon_0 \omega_{pe}^2} \frac{\partial J_x}{\partial t} + \frac{\Gamma_e}{\epsilon_0 \omega_{pe}^2} J_x = E_x, \tag{4.10}$$

$$\frac{1}{\epsilon_0 \omega_{pe}^2} \frac{\partial J_y}{\partial t} + \frac{\Gamma_e}{\epsilon_0 \omega_{pe}^2} J_y = E_y, \tag{4.11}$$

$$\frac{1}{\mu_0 \omega_{pm}^2} \frac{\partial K_z}{\partial t} + \frac{\Gamma_m}{\mu_0 \omega_{pm}^2} K_z = H_z. \tag{4.12}$$

For simplicity, we consider solving (4.7)-(4.12) on a rectangular type physical domain $\Omega = [a, b] \times [c, d]$, which is discretized by a non-uniform grid

$$a = x_{\frac{1}{2}} < x_{\frac{3}{2}} < \cdots < x_{N_x+\frac{1}{2}} = b, \quad c = y_{\frac{1}{2}} < y_{\frac{3}{2}} < \cdots < y_{N_y+\frac{1}{2}} = d.$$

The time domain $[0, T]$ is discretized into $N_t + 1$ uniform intervals by discrete times $0 = t_0 < t_1 < \cdots < t_{N_t+1} = T$, where $t_n = n \cdot \tau$, and the time step size $\tau = \frac{T}{N_t+1}$. For simplicity, we define the rectangular cells $K_{i,j} = I_i \times J_j$, where $I_i = [x_{i-\frac{1}{2}}, x_{i+\frac{1}{2}}]$, $i = 1, \cdots, N_x$, and $J_j = [y_{j-\frac{1}{2}}, y_{j+\frac{1}{2}}]$, $j = 1, \cdots, N_y$. The mesh sizes are denoted by $h_i^x = x_{i+\frac{1}{2}} - x_{i-\frac{1}{2}}$, $h_j^y = y_{j+\frac{1}{2}} - y_{j-\frac{1}{2}}$, with $h^x = \max_{1 \le i \le N_x} h_i^x, h^y = \max_{1 \le j \le N_y} h_j^y$, and $h = \max(h^x, h^y)$ the maximal mesh size. We also assume that the mesh is regular, i.e. $h_i^x \ge C \cdot h$ and $h_j^y \ge C \cdot h \ \ \forall i, j$, for some $C$ independent of $i, j$.

The finite element space $V_h^k$ is chosen as the space of tensor products of piecewise polynomials of degree at most $k$ in each variable on every element $K_{i,j}$, i.e.,

$$V_h^k = \{v: \ v|_K \in Q_k(K), \quad \forall\ K \in \mathcal{T}_h\}, \tag{4.13}$$

where $\mathcal{T}_h$ denotes the Cartesian grid on $\Omega$ described above with mesh size $h$, and $Q_k$ is the space of tensor products of one-dimensional polynomials of degree up to $k$.

For the corresponding variable $u$ we denote its numerical solution $u_h$, which belongs to the finite element space $V_h^k$. Note that functions in $V_h^k$ are allowed to have discontinuities across element interfaces. Furthermore we denote by $u_h(x^+_{i+\frac{1}{2}}, y)$ (or $(u_h)^+_{i+\frac{1}{2},y}$, $u_h^+(x_{i+\frac{1}{2}}, y)$) and $u_h(x^-_{i+\frac{1}{2}}, y)$ (or $(u_h)^-_{i+\frac{1}{2},y}$, $u_h^-(x_{i+\frac{1}{2}}, y)$) the limit values of $u_h$ at $x_{i+\frac{1}{2}}$ from the right cell $K_{i+1,j}$ and from the left cell $K_{i,j}$, respectively. $u_h(x, y^+_{j+\frac{1}{2}})$ (or $(u_h)^+_{x,j+\frac{1}{2}}$, $u_h^+(x, y_{j+\frac{1}{2}})$) and $u_h(x, y^-_{j+\frac{1}{2}})$ (or $(u_h)^-_{x,j+\frac{1}{2}}$, $u_h^-(x, y_{j+\frac{1}{2}})$) are defined similarly. We denote by $||\cdot||$ the $L^2$ norm over the domain $\Omega$.

Finally, we would like to remark that the corresponding PEC boundary condition (4.5) in 2-D becomes:

$$E_x(x, y, t)|_{y=c,d} = 0, \quad E_y(x, y, t)|_{x=a,b} = 0. \tag{4.14}$$

## 4.3 The semi-discrete DG method

The DG method for (4.7)-(4.12) can be formulated as follows: find

$$E_{xh}, E_{yh}, H_{zh}, J_{xh}, J_{yh}, K_{zh} \in C^1([0,T]; V_h^k)$$

such that

$$\begin{aligned}
&\epsilon_0 \int_{K_{i,j}} \frac{\partial E_{xh}}{\partial t}\phi - \int_{I_i} \Big( (\hat{H}_{zh}\phi^-)_{x,j+\frac{1}{2}} - (\hat{H}_{zh}\phi^+)_{x,j-\frac{1}{2}} \Big)\, dx \\
&\quad + \int_{K_{i,j}} H_{zh}\frac{\partial \phi}{\partial y} + \int_{K_{i,j}} J_{xh}\phi = 0,
\end{aligned} \tag{4.15}$$

$$\begin{aligned}
&\epsilon_0 \int_{K_{i,j}} \frac{\partial E_{yh}}{\partial t}\psi + \int_{J_j} \Big( (\hat{H}_{zh}\psi^-)_{i+\frac{1}{2},y} - (\hat{H}_{zh}\psi^+)_{i-\frac{1}{2},y} \Big)\, dy \\
&\quad - \int_{K_{i,j}} H_{zh}\frac{\partial \psi}{\partial x} + \int_{K_{i,j}} J_{yh}\psi = 0,
\end{aligned} \tag{4.16}$$

$$\begin{aligned}
&\mu_0 \int_{K_{i,j}} \frac{\partial H_{zh}}{\partial t}\chi + \int_{J_j} \Big( (\hat{E}_{yh}\chi^-)_{i+\frac{1}{2},y} - (\hat{E}_{yh}\chi^+)_{i-\frac{1}{2},y} \Big)\, dy - \int_{K_{i,j}} E_{yh}\frac{\partial \chi}{\partial x} \\
&\quad - \int_{I_i} \Big( (\hat{E}_{xh}\chi^-)_{x,j+\frac{1}{2}} - (\hat{E}_{xh}\chi^+)_{x,j-\frac{1}{2}} \Big)\, dx + \int_{K_{i,j}} E_{xh}\frac{\partial \chi}{\partial y} + \int_{K_{i,j}} K_{zh}\chi = 0,
\end{aligned} \tag{4.17}$$

$$\frac{1}{\epsilon_0\omega_{pe}^2}\int_{K_{i,j}} \frac{\partial J_{xh}}{\partial t}u_1 + \frac{\Gamma_e}{\epsilon_0\omega_{pe}^2}\int_{K_{i,j}} J_{xh}u_1 - \int_{K_{i,j}} E_{xh}u_1 = 0, \tag{4.18}$$

$$\frac{1}{\epsilon_0\omega_{pe}^2}\int_{K_{i,j}} \frac{\partial J_{yh}}{\partial t}u_2 + \frac{\Gamma_e}{\epsilon_0\omega_{pe}^2}\int_{K_{i,j}} J_{yh}u_2 - \int_{K_{i,j}} E_{yh}u_2 = 0, \tag{4.19}$$

$$\frac{1}{\mu_0\omega_{pm}^2}\int_{K_{i,j}} \frac{\partial K_{zh}}{\partial t}v + \frac{\Gamma_m}{\mu_0\omega_{pm}^2}\int_{K_{i,j}} K_{zh}v - \int_{K_{i,j}} H_{zh}v = 0, \tag{4.20}$$

for all test functions $\phi, \psi, \chi, u_1, u_2, v \in V_h^k$. $\hat{H}_{zh}, \hat{E}_{yh}, \hat{E}_{xh}$ are the cell boundary terms obtained from integration by parts, and they are the so-called numerical fluxes. These numerical fluxes are functions on cell boundaries and should be designed carefully to ensure numerical stability or energy conservation, and optimal rate of convergence, for different PDEs. Motivated by the LDG schemes for diffusion equations and second order wave equations [16, 49], here we choose the simple but elegant alternating fluxes:

$$\hat{E}_{xh}(x, y_{j+\frac{1}{2}}) = E_{xh}^+(x, y_{j+\frac{1}{2}}) \qquad \forall j = 1, \cdots, N_y - 1, \tag{4.21}$$

$$\hat{E}_{xh}(x, y_{\frac{1}{2}}) = \hat{E}_{xh}(x, y_{N_y+\frac{1}{2}}) = 0, \tag{4.22}$$

$$\hat{E}_{yh}(x_{i+\frac{1}{2}}, y) = E_{yh}^+(x_{i+\frac{1}{2}}, y) \qquad \forall i = 1, \cdots, N_x - 1, \tag{4.23}$$

$$\hat{E}_{yh}(x_{\frac{1}{2}}, y) = \hat{E}_{yh}(x_{N_x+\frac{1}{2}}, y) = 0, \tag{4.24}$$

$$\begin{aligned}
\hat{H}_{zh}(x, y_{j+\frac{1}{2}}) &= H^-_{zh}(x, y_{j+\frac{1}{2}}) \qquad \forall j = 1, \cdots, N_y, && (4.25)\\
\hat{H}_{zh}(x, y_{\frac{1}{2}}) &= H^+_{zh}(x, y_{\frac{1}{2}}) + c_0[[E_{xh}(x, y_{\frac{1}{2}})]], && (4.26)\\
\hat{H}_{zh}(x_{i+\frac{1}{2}}, y) &= H^-_{zh}(x_{i+\frac{1}{2}}, y) \qquad \forall i = 1, \cdots, N_x, && (4.27)\\
\hat{H}_{zh}(x_{\frac{1}{2}}, y) &= H^+_{zh}(x_{\frac{1}{2}}, y) - c_0[[E_{yh}(x_{\frac{1}{2}}, y)]], && (4.28)
\end{aligned}$$

where $c_0$ is a constant independent of mesh size $h$, and the jumps $[[E_{xh}(x, y_{\frac{1}{2}})]] = E^+_{xh}(x, y_{\frac{1}{2}}) - 0, [[E_{yh}(x_{\frac{1}{2}}, y)]] = E^+_{yh}(x_{\frac{1}{2}}, y) - 0$. Here we use the standard notation $[[\phi]] = \phi^+ - \phi^-$ for jumps on cell boundaries.

**Remark 4.3.1.** *We will see later why the jump terms in (4.26) and (4.28) are necessary at the physical boundary, in the proof of optimal error estimates (Theorem 4.3.2), see also e.g. [39]. Note also that when $c_0 = \frac{1}{2}$, (4.26) and (4.28) coincide with the standard upwind fluxes, which are:*

$$\hat{H}_{zh}(x, y_{\frac{1}{2}}) = \frac{1}{2}(H^+_{zh}(x, y_{\frac{1}{2}}) + H^-_{zh}(x, y_{\frac{1}{2}})) + \frac{1}{2}[[E_{xh}(x, y_{\frac{1}{2}})]]$$
$$\hat{H}_{zh}(x_{\frac{1}{2}}, y) = \frac{1}{2}(H^+_{zh}(x_{\frac{1}{2}}, y) + H^-_{zh}(x_{\frac{1}{2}}, y)) - \frac{1}{2}[[E_{yh}(x_{\frac{1}{2}}, y)]]$$

*where the undefined $H^-_{zh}(x, y_{\frac{1}{2}})$ and $H^-_{zh}(x_{\frac{1}{2}}, y)$ are replaced by $H^+_{zh}(x, y_{\frac{1}{2}})$ and $H^+_{zh}(x_{\frac{1}{2}}, y)$.*

### 4.3.1 The stability analysis

In this subsection, we present the stability analysis for our scheme.

First, let us look at the stability for the governing equations. Multiplying the governing equations (4.7)–(4.12) by $E_x, E_y, H_z, J_x, J_y, K_z$ , respectively, then integrating over domain $\Omega$, summing up the resultants, and using the 2D PEC boundary condition (4.14), we can easily obtain (cf. [38])

$$
\begin{aligned}
&\frac{1}{2}\frac{d}{dt}\left[\epsilon_0(||E_x||^2+||E_y||^2)+\mu_0||H_z||^2+\frac{1}{\epsilon_0\omega_{pe}^2}(||J_x||^2+||J_y||^2)+\frac{1}{\mu_0\omega_{pm}^2}||K_z||_0^2\right] \\
&+\frac{\Gamma_e}{\epsilon_0\omega_{pe}^2}(||J_x||^2+||J_y||^2)+\frac{\Gamma_m}{\mu_0\omega_{pm}^2}||K_z||^2=0. \qquad (4.29)
\end{aligned}
$$

Integrating (4.29) with respect to time from 0 to $t$, we have the energy identity in the continuous case: For any $t \geq 0$,

$$
\begin{aligned}
&\left[\epsilon_0(||E_x||^2+||E_y||^2)+\mu_0||H_z||^2+\frac{1}{\epsilon_0\omega_{pe}^2}(||J_x||^2+||J_y||^2)+\frac{1}{\mu_0\omega_{pm}^2}||K_z||^2\right](t) \\
&+\int_0^t\left[\frac{2\Gamma_e}{\epsilon_0\omega_{pe}^2}(||J_x||^2+||J_y||^2)+\frac{2\Gamma_m}{\mu_0\omega_{pm}^2}||K_z||^2\right](s)ds \\
=&\left[\epsilon_0(||E_x||^2+||E_y||^2)+\mu_0||H_z||^2+\frac{1}{\epsilon_0\omega_{pe}^2}(||J_x||^2+||J_y||^2)+\frac{1}{\mu_0\omega_{pm}^2}||K_z||^2\right](0). \qquad (4.30)
\end{aligned}
$$

Below we will show that our proposed semi-discrete DG method satisfies a similar energy identity as that given in the continuous level (4.30).

**Theorem 4.3.1.** *The semi-discrete DG method* (4.15)-(4.20) *with alternating fluxes* (4.21)-(4.28) *satisfies the following energy identity: For any $t \geq 0$,*

$$
\begin{aligned}
&\left[\epsilon_0(||E_{xh}||^2+||E_{yh}||^2)+\mu_0||H_{zh}||^2+\frac{1}{\epsilon_0\omega_{pe}^2}(||J_{xh}||^2+||J_{yh}||^2)+\frac{1}{\mu_0\omega_{pm}^2}||K_{zh}||^2\right](t) \\
&+\int_0^t\left[\frac{2\Gamma_e}{\epsilon_0\omega_{pe}^2}(||J_{xh}||^2+||J_{yh}||^2)+\frac{2\Gamma_m}{\mu_0\omega_{pm}^2}||K_{zh}||^2\right](s)ds \\
&+\int_0^t\left[c_0\int_a^b(E_{xh}^+)^2_{x,\frac{1}{2}}\,dx+c_0\int_c^d(E_{yh}^+)^2_{\frac{1}{2},y}\,dy\right](s)\,ds \\
=&\left[\epsilon_0(||E_{xh}||^2+||E_{yh}||^2)+\mu_0||H_{zh}||^2+\frac{1}{\epsilon_0\omega_{pe}^2}(||J_{xh}||^2+||J_{yh}||^2)+\frac{1}{\mu_0\omega_{pm}^2}||K_{zh}||^2\right](0). \qquad (4.31)
\end{aligned}
$$

*Proof.* Taking $\phi = E_{xh}, \psi = E_{yh}, \chi = H_{zh}, u_1 = J_{xh}, u_2 = J_{yh}, v = K_{zh}$ in (4.15)-(4.20), respectively, adding the resultants together, we have

$$\begin{aligned}
&\frac{1}{2}\frac{d}{dt}\int_{K_{i,j}}\left[\epsilon_0(|E_{xh}|^2+|E_{yh}|^2)+\mu_0|H_{zh}|^2+\frac{1}{\epsilon_0\omega_{pe}^2}(|J_{xh}|^2+|J_{yh}|^2)+\frac{1}{\mu_0\omega_{pm}^2}|K_{zh}|^2\right]\\
&\quad+\int_{K_{i,j}}\left[\frac{\Gamma_e}{\epsilon_0\omega_{pe}^2}(|J_{xh}|^2+|J_{yh}|^2)+\frac{\Gamma_m}{\mu_0\omega_{pm}^2}|K_{zh}|^2\right]+sum_I+sum_J\\
&\quad+\int_{K_{i,j}}(H_{zh}\frac{\partial E_{xh}}{\partial y}+E_{xh}\frac{\partial H_{zh}}{\partial y})-\int_{K_{i,j}}(H_{zh}\frac{\partial E_{yh}}{\partial x}+E_{yh}\frac{\partial H_{zh}}{\partial x})=0,
\end{aligned} \tag{4.32}$$

where we denote the boundary integral terms

$$\begin{aligned}
sum_I=&-\int_{I_i}\left((\hat{H}_{zh}E_{xh}^-)_{x,j+\frac{1}{2}}-(\hat{H}_{zh}E_{xh}^+)_{x,j-\frac{1}{2}}\right)dx\\
&-\int_{I_i}\left((\hat{E}_{xh}H_{zh}^-)_{x,j+\frac{1}{2}}-(\hat{E}_{xh}H_{zh}^+)_{x,j-\frac{1}{2}}\right)dx,
\end{aligned}$$

and

$$\begin{aligned}
sum_J=&\int_{J_j}\left((\hat{H}_{zh}E_{yh}^-)_{i+\frac{1}{2},y}-(\hat{H}_{zh}E_{yh}^+)_{i-\frac{1}{2},y}\right)dy\\
&+\int_{J_j}\left((\hat{E}_{yh}H_{zh}^-)_{i+\frac{1}{2},y}-(\hat{E}_{yh}H_{zh}^+)_{i-\frac{1}{2},y}\right)dy.
\end{aligned}$$

From the choice of fluxes given above, we can simplify $sum_I$ as follows:

$$\begin{aligned}
&\sum_{1\le j\le N_y}\left(sum_I + \int_{K_{i,j}} (H_{zh}\frac{\partial E_{xh}}{\partial y} + E_{xh}\frac{\partial H_{zh}}{\partial y})\right)\\
=&\sum_{1\le j\le N_y} -\int_{I_i} (H_{zh}^{-}E_{xh}^{-})_{x,j+\frac{1}{2}}\,dx + \sum_{1\le j\le N_y-1}\int_{I_i}(H_{zh}^{-}E_{xh}^{+})_{x,j+\frac{1}{2}}\,dx\\
&+\int_{I_i}(H_{zh}^{+}E_{xh}^{+})_{x,\frac{1}{2}}\,dx + c_0\int_{I_i}(E_{xh}^{+})^2_{x,\frac{1}{2}}\,dx\\
&-\sum_{1\le j\le N_y-1}\int_{I_i}(E_{xh}^{+}H_{zh}^{-})_{x,j+\frac{1}{2}}\,dx + \sum_{1\le j\le N_y-1}\int_{I_i}(E_{xh}^{+}H_{zh}^{+})_{x,j+\frac{1}{2}}\,dx\\
&+\sum_{1\le j\le N_y}\int_{I_i}(H_{zh}^{-}E_{xh}^{-})_{x,j+\frac{1}{2}}\,dx - \sum_{0\le j\le N_y-1}\int_{I_i}(H_{zh}^{+}E_{xh}^{+})_{x,j+\frac{1}{2}}\,dx\\
=&c_0\int_{I_i}(E_{xh}^{+})^2_{x,\frac{1}{2}}\,dx
\end{aligned} \tag{4.33}$$

By the similar technique, we can have

$$\begin{aligned}
&\sum_{1\le i\le N_x}\left(sum_J - \int_{K_{i,j}} (H_{zh}\frac{\partial E_{yh}}{\partial x} + E_{yh}\frac{\partial H_{zh}}{\partial x})\right)\\
=&c_0\int_{J_j}(E_{yh}^{+})^2_{\frac{1}{2},y}\,dy
\end{aligned} \tag{4.34}$$

Hence, summing up (4.32) with respect to both $1 \le i \le N_x$ and $1 \le j \le N_y$, and using (4.33) and (4.34), we conclude the proof. □

**Remark 4.3.2.** *We can see from the above theorem that our method is non-dissipative since we use the alternating flux rather than upwind flux as in e.g. [37] . Note that if we do not add the jump term in the flux definition* (4.26) *and* (4.28)*, i.e.* $c_0 = 0$*, then the numerical solutions of our semi-discrete scheme satisfy the same energy equality as the exact solutions.*

### 4.3.2 The error analysis

We denote the errors between the exact solutions $(E_x, E_y, H_z, J_x, J_y, K_z)$ of (4.7)-(4.12) and the corresponding numerical solutions $(E_{xh}, E_{yh}, H_{zh}, J_{xh}, J_{yh}, K_{zh})$ of the semi-discrete scheme (4.15)-(4.20) by

$$\begin{aligned}\mathcal{E}_x = E_x - E_{xh}, \mathcal{E}_y = E_y - E_{yh}, \mathcal{H}_z = H_z - H_{zh},\\ \mathcal{J}_x = J_x - J_{xh}, \mathcal{J}_y = J_y - J_{yh}, \mathcal{K}_z = K_z - K_{zh}.\end{aligned} \tag{4.35}$$

Subtracting (4.15)-(4.20) from the weak formulation of (4.7)-(4.12) and assuming that the exact solutions are continuous in the domain $\Omega$, we can obtain the error equations:

$$\epsilon_0 \int_{K_{i,j}} \frac{\partial \mathcal{E}_x}{\partial t}\phi - \int_{I_i} \left( (\hat{\mathcal{H}}_z \phi^-)_{x,j+\frac{1}{2}} - (\hat{\mathcal{H}}_z \phi^+)_{x,j-\frac{1}{2}} \right) dx + \int_{K_{i,j}} \mathcal{H}_z \frac{\partial \phi}{\partial y} + \int_{K_{i,j}} \mathcal{J}_x \phi = 0, \tag{4.36}$$

$$\epsilon_0 \int_{K_{i,j}} \frac{\partial \mathcal{E}_y}{\partial t}\psi + \int_{J_j} \left( (\hat{\mathcal{H}}_z \psi^-)_{i+\frac{1}{2},y} - (\hat{\mathcal{H}}_z \psi^+)_{i-\frac{1}{2},y} \right) dy - \int_{K_{i,j}} \mathcal{H}_z \frac{\partial \psi}{\partial x} + \int_{K_{i,j}} \mathcal{J}_y \psi = 0, \tag{4.37}$$

$$\begin{aligned}&\mu_0 \int_{K_{i,j}} \frac{\partial \mathcal{H}_z}{\partial t}\chi + \int_{J_j} \left( (\hat{\mathcal{E}}_y \chi^-)_{i+\frac{1}{2},y} - (\hat{\mathcal{E}}_y \chi^+)_{i-\frac{1}{2},y} \right) dy - \int_{K_{i,j}} \mathcal{E}_y \frac{\partial \chi}{\partial x}\\ &\quad - \int_{I_i} \left( (\hat{\mathcal{E}}_x \chi^-)_{x,j+\frac{1}{2}} - (\hat{\mathcal{E}}_x \chi^+)_{x,j-\frac{1}{2}} \right) dx + \int_{K_{i,j}} \mathcal{E}_x \frac{\partial \chi}{\partial y} + \int_{K_{i,j}} \mathcal{K}_z \chi = 0, \end{aligned} \tag{4.38}$$

$$\frac{1}{\epsilon_0 \omega_{pe}^2} \int_{K_{i,j}} \frac{\partial \mathcal{J}_x}{\partial t} u_1 + \frac{\Gamma_e}{\epsilon_0 \omega_{pe}^2} \int_{K_{i,j}} \mathcal{J}_x u_1 - \int_{K_{i,j}} \mathcal{E}_x u_1 = 0, \tag{4.39}$$

$$\frac{1}{\epsilon_0 \omega_{pe}^2} \int_{K_{i,j}} \frac{\partial \mathcal{J}_y}{\partial t} u_2 + \frac{\Gamma_e}{\epsilon_0 \omega_{pe}^2} \int_{K_{i,j}} \mathcal{J}_y u_2 - \int_{K_{i,j}} \mathcal{E}_y u_2 = 0, \tag{4.40}$$

$$\frac{1}{\mu_0 \omega_{pm}^2} \int_{K_{i,j}} \frac{\partial \mathcal{K}_z}{\partial t} v + \frac{\Gamma_m}{\mu_0 \omega_{pm}^2} \int_{K_{i,j}} \mathcal{K}_z v - \int_{K_{i,j}} \mathcal{H}_z v = 0, \tag{4.41}$$

for all test functions $\phi, \psi, \chi, u_1, u_2, v \in V_h^k$.

To estimate those errors in (4.35), we need some projection operators often used in DG and LDG methods (e.g., [12, 21]). Given a function $u \in H^1(I_i)$, the 1-D projections

$$P_x^{\pm}: \quad H^1(I_i) \to \mathcal{P}_k(I_i)$$

are defined as the elements of the $k$-th polynomial space $\mathcal{P}_k(I_i)$ that satisfy

$$\int_{I_i} (P_x^+ u - u) w \; dx = 0 \quad \forall\, w \in \mathcal{P}_{k-1}(I_i), \text{ and } P_x^+ u(x_{i-\frac{1}{2}}^+) = u(x_{i-\frac{1}{2}}^+), \tag{4.42}$$

$$\int_{I_i} (P_x^- u - u) w \; dx = 0 \quad \forall\, w \in \mathcal{P}_{k-1}(I_i), \text{ and } P_x^- u(x_{i+\frac{1}{2}}^-) = u(x_{i+\frac{1}{2}}^-). \tag{4.43}$$

The 1-D projections $P_x^{\pm}$ in the $y$-direction can be defined similarly. It is easy to check that these 1-D projections are well-defined.

Furthermore, we denote the standard 1-D $L^2$ projections

$$P_x: \quad H^1(I_i) \to \mathcal{P}_k(I_i), \quad P_y: \quad H^1(J_j) \to \mathcal{P}_k(J_j),$$

that satisfy

$$\int_{I_i} (P_x u - u) w \; dx = 0 \quad \forall\, w \in \mathcal{P}_k(I_i), \tag{4.44}$$

$$\int_{J_j} (P_y u - u) w \; dy = 0 \quad \forall\, w \in \mathcal{P}_k(J_j), \tag{4.45}$$

respectively.

For a 2-D rectangular element $K_{i,j} = I_i \times J_j$, we use projections that are tensor products of the 1-D projections. More specifically, we adopt the projection

$$\Pi_1 = P_x \otimes P_y^+ : H^2(K_{i,j}) \to Q_k(K_{i,j}),$$

which satisfies that [42]: For any $w \in H^2(K_{i,j})$ and any $v_h \in Q_k(K_{i,j})$,

$$\int_{K_{i,j}} \Pi_1 w(x,y) \frac{\partial v_h(x,y)}{\partial y}\, dxdy = \int_{K_{i,j}} w(x,y) \frac{\partial v_h(x,y)}{\partial y}\, dxdy, \tag{4.46}$$

$$\int_{I_i} \Pi_1 w(x, y^+_{j-\frac{1}{2}}) v_h(x, y^+_{j-\frac{1}{2}})\, dx = \int_{I_i} w(x, y^+_{j-\frac{1}{2}}) v_h(x, y^+_{j-\frac{1}{2}})\, dx; \tag{4.47}$$

the projection

$$\Pi_2 = P_x^+ \otimes P_y : H^2(K_{i,j}) \to Q_k(K_{i,j}),$$

which satisfies that: For any $w \in H^2(K_{i,j})$ and any $v_h \in Q_k(K_{i,j})$,

$$\int_{K_{i,j}} \Pi_2 w(x,y) \frac{\partial v_h(x,y)}{\partial x}\, dxdy = \int_{K_{i,j}} w(x,y) \frac{\partial v_h(x,y)}{\partial x}\, dxdy \tag{4.48}$$

$$\int_{J_j} \Pi_2 w(x^+_{i-\frac{1}{2}}, y) v_h(x^+_{i-\frac{1}{2}}, y)\, dy = \int_{J_j} w(x^+_{i-\frac{1}{2}}, y) v_h(x^+_{i-\frac{1}{2}}, y)\, dy; \tag{4.49}$$

the projection

$$\Pi_3 = P_x^- \otimes P_y^- : H^2(K_{i,j}) \to Q_k(K_{i,j}),$$

which satisfies that: For any $w \in H^2(K_{i,j})$ and any $v_h \in Q_{k-1}(K_{i,j})$,

$$\int_{K_{i,j}} \Pi_3 w(x,y) v_h(x,y)\, dxdy = \int_{K_{i,j}} w(x,y) v_h(x,y)\, dxdy, \tag{4.50}$$

$$\int_{I_i} \Pi_3 w(x, y^-_{j+\frac{1}{2}}) v_h(x, y^-_{j+\frac{1}{2}})\, dx = \int_{I_i} w(x, y^-_{j+\frac{1}{2}}) v_h(x, y^-_{j+\frac{1}{2}})\, dx, \tag{4.51}$$

$$\int_{I_i} \Pi_3 w(x^-_{i+\frac{1}{2}}, y) v_h(x^-_{i+\frac{1}{2}}, y)\, dy = \int_{I_i} w(x^-_{i+\frac{1}{2}}, y) v_h(x^-_{i+\frac{1}{2}}, y)\, dy, \tag{4.52}$$

$$\Pi_3 w(x^-_{i+\frac{1}{2}}, y^-_{j+\frac{1}{2}}) = w(x^-_{i+\frac{1}{2}}, y^-_{j+\frac{1}{2}}). \tag{4.53}$$

Note that we use $H^2$ for the point values to make sense by the Sobolev embedding $H^2 \subset C^0$ in two dimensional spaces. The usual $L^2$ projection is denoted:

$$\Pi_4 = P_x \otimes P_y : L^2(K_{i,j}) \to Q_k(K_{i,j}),$$

which satisfies that: For any $w \in L^2(K_{i,j})$ and any $v_h \in Q_k(K_{i,j})$,

$$\int_{K_{i,j}} \Pi_4 w(x,y) v_h(x,y)\, dxdy \;= \int_{K_{i,j}} w(x,y) v_h(x,y)\, dxdy. \tag{4.54}$$

It is easy to see that

**Lemma 4.3.1.** *There exists a unique polynomial $\Pi_1 w \in Q_k(K_{i,j})$ as defined above. The same applies to $\Pi_2 w$ , $\Pi_3 w$ and $\Pi_4 w$.*

**Lemma 4.3.2.** *If $w(x,y)$ is a product of 1-D functions, i.e. $w(x,y) = f(x)g(y)$ where $f \in H^1(I_i)$, $g \in H^1(J_j)$, then we have:*

$$\begin{aligned}
\Pi_1 w(x,y) &= P_x f(x) P_y^+ g(y), \\
\Pi_2 w(x,y) &= P_x^+ f(x) P_y g(y), \\
\Pi_3 w(x,y) &= P_x^- f(x) P_y^- g(y). \\
\Pi_4 w(x,y) &= P_x f(x) P_y g(y).
\end{aligned}$$

This lemma explains why we write the 2-D projections as the tensor products of 1-D projections.

Moreover, it is known that these projections have the following property (e.g., [12, 21]).

**Lemma 4.3.3.** *Let $\Pi_i$ $(i = 1,2,3,4)$ be the projections defined above. Then for any $u \in H^{k+1}(\Omega)$ $(k \geq 1)$,*

$$||\Pi_i u - u|| \leq C h^{k+1} ||u||_{H^{k+1}(\Omega)}, \quad \forall\ i = 1,2,3,4,$$

*where the constant $C > 0$ is independent of $h$, the mesh size introduced in Section 4.2.*

With the above preparation, we can prove the following optimal error estimate.

**Theorem 4.3.2.** *Let $(E_x, E_y, H_z, J_x, J_y, K_z)$ and $(E_{xh}, E_{yh}, H_{zh}, J_{xh}, J_{yh}, K_{zh})$ be the solutions of (4.7)-(4.12) and (4.15)-(4.20), respectively. The following optimal error estimate holds true:*

$$
\begin{aligned}
& \left(\epsilon_0(||E_x - E_{xh}||^2 + ||E_y - E_{yh}||^2) + \mu_0||H_z - H_{zh}||^2\right)(t) \\
& + \left(\frac{1}{\epsilon_0\omega_{pe}^2}(||J_x - J_{xh}||^2 + ||J_y - J_{yh}||^2) + \frac{1}{\mu_0\omega_{pm}^2}||K_z - K_{zh}||^2\right)(t) \\
\leq\ & Ch^{2(k+1)} + \left(\epsilon_0(||E_x - E_{xh}||^2 + ||E_y - E_{yh}||^2) + \mu_0||H_z - H_{zh}||^2\right)(0) \\
& + \left(\frac{1}{\epsilon_0\omega_{pe}^2}(||J_x - J_{xh}||^2 + ||J_y - J_{yh}||^2) + \frac{1}{\mu_0\omega_{pm}^2}||K_z - K_{zh}||^2\right)(0),
\end{aligned}
$$

*where the constant $C > 0$ is independent of $h$, and $k \geq 1$ is the order of the basis function in $V_h^k$.*

*Proof.* Using the projections defined above, we can decompose the errors given in (4.35) as follows:

$$
\begin{aligned}
\mathcal{E}_x &= E_x - E_{xh} = (\Pi_1 E_x - E_{xh}) - (\Pi_1 E_x - E_x) := E_{x\xi} - E_{x\eta}, \\
\mathcal{E}_y &= E_y - E_{yh} = (\Pi_2 E_y - E_{yh}) - (\Pi_2 E_y - E_y) := E_{y\xi} - E_{y\eta}, \\
\mathcal{H}_z &= H_z - H_{zh} = (\Pi_3 H_z - H_{zh}) - (\Pi_3 H_z - H_z) := H_{z\xi} - H_{z\eta}, \\
\mathcal{J}_x &= J_x - J_{xh} = (\Pi_4 J_x - J_{xh}) - (\Pi_4 J_x - J_x) := J_{x\xi} - J_{x\eta}, \\
\mathcal{J}_y &= J_y - J_{yh} = (\Pi_4 J_y - J_{yh}) - (\Pi_4 J_y - J_y) := J_{y\xi} - J_{y\eta}, \\
\mathcal{K}_z &= K_z - K_{zh} = (\Pi_4 K_z - K_{zh}) - (\Pi_4 K_z - K_z) := K_{z\xi} - K_{z\eta}.
\end{aligned}
$$

Substituting the above error decompositions into (4.36) – (4.41), and choosing the test functions $\phi = E_{x\xi}, \psi = E_{y\xi}, \chi = H_{z\xi},\ u_1 = J_{x\xi}, u_2 = J_{y\xi}, v = K_{z\xi}$, we obtain

$$
\begin{aligned}
(i)\epsilon_0 \int_{K_{i,j}} \frac{\partial E_{x\xi}}{\partial t} E_{x\xi} &- \int_{I_i} \Big( (\hat{H}_{z\xi} E_{x\xi}^-)(x, y_{j+\frac{1}{2}}) - (\hat{H}_{z\xi} E_{x\xi}^+)(x, y_{j-\frac{1}{2}}) \Big) \\
&+ \int_{K_{i,j}} H_{z\xi} \frac{\partial E_{x\xi}}{\partial y} + \int_{K_{i,j}} J_{x\xi} E_{x\xi} \\
=\epsilon_0 \int_{K_{i,j}} \frac{\partial E_{x\eta}}{\partial t} E_{x\xi} &- \int_{I_i} \Big( (\hat{H}_{z\eta} E_{x\xi}^-)(x, y_{j+\frac{1}{2}}) - (\hat{H}_{z\eta} E_{x\xi}^+)(x, y_{j-\frac{1}{2}}) \Big) \\
&+ \int_{K_{i,j}} H_{z\eta} \frac{\partial E_{x\xi}}{\partial y} + \int_{K_{i,j}} J_{x\eta} E_{x\xi},
\end{aligned}
\tag{4.55}
$$

$$
\begin{aligned}
(ii)\epsilon_0 \int_{K_{i,j}} \frac{\partial E_{y\xi}}{\partial t} E_{y\xi} &+ \int_{J_j} \Big( (\hat{H}_{z\xi} E_{y\xi}^-)(x_{i+\frac{1}{2}}, y) - (\hat{H}_{z\xi} E_{y\xi}^+)(x_{i-\frac{1}{2}}, y) \Big) \\
&- \int_{K_{i,j}} H_{z\xi} \frac{\partial E_{y\xi}}{\partial y} + \int_{K_{i,j}} J_{y\xi} E_{y\xi} \\
=\epsilon_0 \int_{K_{i,j}} \frac{\partial E_{y\eta}}{\partial t} E_{y\xi} &+ \int_{J_j} \Big( (\hat{H}_{z\eta} E_{y\xi}^-)(x_{i+\frac{1}{2}}, y) - (\hat{H}_{z\eta} E_{y\xi}^+)(x_{i-\frac{1}{2}}, y) \Big) \\
&- \int_{K_{i,j}} H_{z\eta} \frac{\partial E_{y\xi}}{\partial y} + \int_{K_{i,j}} J_{y\eta} E_{y\xi},
\end{aligned}
\tag{4.56}
$$

$$
\begin{aligned}
(iii)\mu_0 \int_{K_{i,j}} \frac{\partial H_{z\xi}}{\partial t} H_{z\xi} &+ \int_{J_j} \Big( (\hat{E}_{y\xi} H_{z\xi}^-)(x_{i+\frac{1}{2}}, y) - (\hat{E}_{y\xi} H_{z\xi}^+)(x_{i-\frac{1}{2}}, y) \Big) - \int_{K_{i,j}} E_{y\xi} \frac{\partial H_{z\xi}}{\partial x} \\
&- \int_{I_i} \Big( (\hat{E}_{x\xi} H_{z\xi}^-)(x, y_{j+\frac{1}{2}}) - (\hat{E}_{x\xi} H_{z\xi}^+)(x, y_{j-\frac{1}{2}}) \Big) + \int_{K_{i,j}} E_{x\xi} \frac{\partial H_{z\xi}}{\partial y} + \int_{K_{i,j}} K_{z\xi} H_{z\xi} \\
=\mu_0 \int_{K_{i,j}} \frac{\partial H_{z\eta}}{\partial t} H_{z\xi} &+ \int_{J_j} \Big( (\hat{E}_{y\eta} H_{z\xi}^-)(x_{i+\frac{1}{2}}, y) - (\hat{E}_{y\eta} H_{z\xi}^+)(x_{i-\frac{1}{2}}, y) \Big) - \int_{K_{i,j}} E_{y\eta} \frac{\partial H_{z\xi}}{\partial x} \\
&- \int_{I_i} \Big( (\hat{E}_{x\eta} H_{z\xi}^-)(x, y_{j+\frac{1}{2}}) - (\hat{E}_{x\eta} H_{z\xi}^+)(x, y_{j-\frac{1}{2}}) \Big) + \int_{K_{i,j}} E_{x\eta} \frac{\partial H_{z\xi}}{\partial y} + \int_{K_{i,j}} K_{z\eta} H_{z\xi},
\end{aligned}
\tag{4.57}
$$

$$
\begin{aligned}
(iv)\frac{1}{\epsilon_0 \omega_{pe}^2} \int_{K_{i,j}} \frac{\partial J_{x\xi}}{\partial t} J_{x\xi} + \frac{\Gamma_e}{\epsilon_0 \omega_{pe}^2} \int_{K_{i,j}} J_{x\xi} J_{x\xi} - \int_{K_{i,j}} E_{x\xi} J_{x\xi} \\
=\frac{1}{\epsilon_0 \omega_{pe}^2} \int_{K_{i,j}} \frac{\partial J_{x\eta}}{\partial t} J_{x\xi} + \frac{\Gamma_e}{\epsilon_0 \omega_{pe}^2} \int_{K_{i,j}} J_{x\eta} J_{x\xi} - \int_{K_{i,j}} E_{x\eta} J_{x\xi},
\end{aligned}
\tag{4.58}
$$

$$
\begin{aligned}
(v)\frac{1}{\epsilon_0 \omega_{pe}^2} \int_{K_{i,j}} \frac{\partial J_{y\xi}}{\partial t} J_{y\xi} + \frac{\Gamma_e}{\epsilon_0 \omega_{pe}^2} \int_{K_{i,j}} J_{y\xi} J_{y\xi} - \int_{K_{i,j}} E_{y\xi} J_{y\xi} \\
=\frac{1}{\epsilon_0 \omega_{pe}^2} \int_{K_{i,j}} \frac{\partial J_{y\eta}}{\partial t} J_{y\xi} + \frac{\Gamma_e}{\epsilon_0 \omega_{pe}^2} \int_{K_{i,j}} J_{y\eta} J_{y\xi} - \int_{K_{i,j}} E_{y\eta} J_{y\xi},
\end{aligned}
\tag{4.59}
$$

$$
\begin{aligned}
(vi)\frac{1}{\mu_0 \omega_{pm}^2} \int_{K_{i,j}} \frac{\partial K_{z\xi}}{\partial t} K_{z\xi} + \frac{\Gamma_m}{\mu_0 \omega_{pm}^2} \int_{K_{i,j}} K_{z\xi} K_{z\xi} - \int_{K_{i,j}} H_{z\xi} K_{z\xi} \\
=\frac{1}{\mu_0 \omega_{pm}^2} \int_{K_{i,j}} \frac{\partial K_{z\eta}}{\partial t} K_{z\xi} + \frac{\Gamma_m}{\mu_0 \omega_{pm}^2} \int_{K_{i,j}} K_{z\eta} K_{z\xi} - \int_{K_{i,j}} H_{z\eta} K_{z\xi}.
\end{aligned}
\tag{4.60}
$$

If we sum (4.55)-(4.60) together over $i = 1 \dots N_x, j = 1 \dots N_y$ and look at the left hand side (LHS), we could observe that it is exactly the same thing as in the stability proof. Hence we have:

$$
\begin{aligned}
\text{LHS} =& \frac{1}{2}\frac{d}{dt}\Bigg( \epsilon_0 \|E_{x\xi}\|^2 + \epsilon_0 \|E_{y\xi}\|^2 + \mu_0 \|H_{z\xi}\|^2 \\
&\quad + \frac{1}{\epsilon_0 \omega_{pe}^2} \left( \|J_{x\xi}\|^2 + \|J_{y\xi}\|^2 \right) + \frac{1}{\mu_0 \omega_{pm}^2} \|K_{z\xi}\|^2 \Bigg) \\
&+ \frac{\Gamma_e}{\epsilon_0 \omega_{pe}^2} \left( \|J_{x\xi}\|^2 + \|J_{y\xi}\|^2 \right) + \frac{\Gamma_m}{\mu_0 \omega_{pm}^2} \|K_{z\xi}\|^2 \\
&+ \sum_{i=1}^{N_x} \int_{I_i} \left( (\hat{H}_{z\xi} - H_{z\xi}^+) E_{x\xi}^+ \right) (x, y_{\frac{1}{2}}) + \sum_{j=1}^{N_y} \int_{J_j} \left( H_{z\xi}^+ - \hat{H}_{z\xi}) E_{y\xi}^+ \right) (x_{\frac{1}{2}}, y) \\
=& \text{GT} + \sum_{i=1}^{N_x} c_0 \int_{I_i} \left( E_{x\xi}^+ (x, y_{\frac{1}{2}}) \right)^2 + \sum_{j=1}^{N_y} c_0 \int_{J_j} \left( E_{y\xi}^+ (x_{\frac{1}{2}}, y) \right)^2
\end{aligned}
$$

Note that those terms in the first two lines in the above equation are referred as GT (good terms) and the third line is computed using the boundary fluxes (4.26) and (4.28).

Let us now consider the terms on the right hand side (RHS). By the definition of $\Pi_4$ in (4.54), and the fact that $\Pi_l u_t = (\Pi_l u)_t, l \in \{1, 2, 3, 4\}$, we can have: $\forall\ i \in \{1, \cdots, N_x\}, \forall\, j \in \{1, \cdots, N_y\}$ :

$$\tfrac{1}{\epsilon_0 \omega_{pe}^2} \int_{K_{i,j}} \tfrac{\partial J_{x\eta}}{\partial t} J_{x\xi} + \tfrac{\Gamma_e}{\epsilon_0 \omega_{pe}^2} \int_{K_{i,j}} J_{x\eta} J_{x\xi} = 0, \tag{4.61}$$

$$\tfrac{1}{\epsilon_0 \omega_{pe}^2} \int_{K_{i,j}} \tfrac{\partial J_{x\eta}}{\partial t} J_{x\xi} + \tfrac{\Gamma_e}{\epsilon_0 \omega_{pe}^2} \int_{K_{i,j}} J_{x\eta} J_{x\xi} = 0, \tag{4.62}$$

$$\tfrac{1}{\mu_0 \omega_{pm}^2} \int_{K_{i,j}} \tfrac{\partial K_{z\eta}}{\partial t} K_{z\xi} + \tfrac{\Gamma_m}{\mu_0 \omega_{pm}^2} \int_{K_{i,j}} K_{z\eta} K_{z\xi} = 0, \tag{4.63}$$

$$\int_{K_{i,j}} J_{x\eta} E_{x\xi} = \int_{K_{i,j}} J_{y\eta} E_{y\xi} = \int_{K_{i,j}} K_{z\eta} H_{z\xi} = 0. \tag{4.64}$$

By the definition of $\Pi_1$ in (4.46)-(4.47), and the fluxes of $E_x$ in (4.21)-(4.22), we have that: $\forall\, i = 1, \cdots, N_x$,

$$\int_{K_{i,j}} E_{x\eta} \frac{\partial H_{z\xi}}{\partial y} = 0, \quad \forall j = 1, \cdots, N_y, \tag{4.65}$$

$$\int_{I_i} (\hat{E}_{x\eta} H_{z\xi}^-)(x, y_{j+\frac{1}{2}}) = \int_{I_i} (E_{x\eta}^+ H_{z\xi}^-)(x, y_{j+\frac{1}{2}}) = 0, \quad \forall j = 1, \cdots, N_y - 1, \tag{4.66}$$

$$\int_{I_i} (\hat{E}_{x\eta} H_{z\xi}^-)(x, y_{N_y+\frac{1}{2}}) = 0, \tag{4.67}$$

$$\int_{I_i} (\hat{E}_{x\eta} H_{z\xi}^+)(x, y_{j-\frac{1}{2}}) = \int_{J_j} (E_{x\eta}^+ H_{z\xi}^+)(x, y_{j-\frac{1}{2}}) = 0, \quad \forall j = 2, \cdots, N_y, \tag{4.68}$$

$$\int_{I_i} (\hat{E}_{x\eta} H_{z\xi}^+)(x, y_{\frac{1}{2}}) = 0. \tag{4.69}$$

By the definition of $\Pi_2$ in (4.48)-(4.49), and the fluxes of $E_y$ in (4.23)-(4.24), we have that: $\forall\, j = 1, \cdots, N_y$,

$$\int_{K_{i,j}} E_{y\eta} \frac{\partial H_{z\xi}}{\partial x} = 0, \quad \forall i = 1, \cdots, N_x, \tag{4.70}$$

$$\int_{I_i} (\hat{E}_{y\eta} H_{z\xi}^-)(x_{i+\frac{1}{2}}, y) = \int_{I_i} (E_{y\eta}^+ H_{z\xi}^-)(x_{i+\frac{1}{2}}, y) = 0, \quad \forall i = 1, \cdots, N_x - 1, \tag{4.71}$$

$$\int_{I_i} (\hat{E}_{y\eta} H_{z\xi}^-)(x_{N+\frac{1}{2}}, y) = 0, \tag{4.72}$$

$$\int_{I_i} (\hat{E}_{y\eta} H_{z\xi}^+)(x_{i-\frac{1}{2}}, y) = \int_{I_i} (E_{y\eta}^+ H_{z\xi}^+)(x_{i-\frac{1}{2}}, y) = 0, \quad \forall i = 2, \cdots, N_x, \tag{4.73}$$

$$\int_{I_i} (\hat{E}_{y\eta} H_{z\xi}^+)(x_{\frac{1}{2}}, y) = 0. \tag{4.74}$$

Using the above equalities (4.61)-(4.74), we can simplify the right hand side of the summation of (4.55)-(4.60) over $i = 1, \cdots, N_x$ and $j = 1, \cdots, N_y$ :

$$\begin{aligned} \text{RHS} = \int_\Omega \left( \epsilon_0 \frac{\partial E_{x\eta}}{\partial t} E_{x\xi} + \epsilon_0 \frac{\partial E_{y\eta}}{\partial t} E_{y\xi} + \mu_0 \frac{\partial H_{z\eta}}{\partial t} H_{z\xi} - E_{x\eta} J_{x\xi} - E_{y\eta} J_{y\xi} - H_{z\eta} K_{z\xi} \right) \\ + \sum_{j=1}^{N_y} \text{TEX}_j + \sum_{i=1}^{N_x} \text{TEY}_i, \end{aligned}$$

where we denote

$$\text{TEX}_j = \sum_{i=1}^{N_x} \left( -\int_{I_i} \left( (\hat{H}_{z\eta} E_{x\xi}^{-})(x, y_{j+\frac{1}{2}}) - (\hat{H}_{z\eta} E_{x\xi}^{+})(x, y_{j-\frac{1}{2}}) \right) + \int_{K_{i,j}} H_{z\eta} \frac{\partial E_{x\xi}}{\partial y} \right), \tag{4.75}$$

$$\text{TEY}_i = \sum_{j=1}^{N_y} \left( \int_{J_j} \left( (\hat{H}_{z\eta} E_{y\xi}^{-})(x_{i+\frac{1}{2}}, y) - (\hat{H}_{z\eta} E_{y\xi}^{+})(x_{i-\frac{1}{2}}, y) \right) - \int_{K_{i,j}} H_{z\eta} \frac{\partial E_{y\xi}}{\partial y} \right). \tag{4.76}$$

Using the super-convergence results given in Lemmas 4.3.4 and 4.3.5 below (similar to [12] and proved at the end of this section) to estimate TEX (terms of $E_x$) and TEY (terms of $E_y$), we obtain:

$$\begin{aligned} \text{GT} \leq & Ch^{2k+2} + C\|E_{x\xi}\|^2 + C\|E_{y\xi}\|^2 \\ & + \int_\Omega \left( \epsilon_0 \frac{\partial E_{x\eta}}{\partial t} E_{x\xi} + \epsilon_0 \frac{\partial E_{y\eta}}{\partial t} E_{y\xi} + \mu_0 \frac{\partial H_{z\eta}}{\partial t} H_{z\xi} - E_{x\eta} J_{x\xi} - E_{y\eta} J_{y\xi} - H_{z\eta} K_{z\xi} \right). \end{aligned} \tag{4.77}$$

We can first bound all the right hand side terms of (4.77) using the Cauchy-Schwarz inequality and Lemma 4.3.3, then use the Gronwall inequality and the triangle inequality to conclude the proof. □

**Remark 4.3.3.** *We would like to remark that the optimal error estimate $O(h^{k+1})$ in the $L^2$ norm*

$$\begin{aligned} & \left( \epsilon_0 (||E_x - E_{xh}||^2 + ||E_y - E_{yh}||^2) + \mu_0 ||H_z - H_{zh}||^2 \right)(t) \\ & + \left( \frac{1}{\epsilon_0 \omega_{pe}^2} (||J_x - J_{xh}||^2 + ||J_y - J_{yh}||^2) + \frac{1}{\mu_0 \omega_{pm}^2} ||K_z - K_{zh}||^2 \right)(t) \leq Ch^{2(k+1)} \end{aligned}$$

*can be simply achieved if we choose $O(h^{k+1})$ initial approximations:*

$$E_{xh}(0) = \Pi_1 E_x(0), \quad E_{yh}(0) = \Pi_2 E_y(0), \quad H_{zh}(0) = \Pi_3 H_z(0),$$
$$J_{xh}(0) = \Pi_4 J_x(0), \quad J_{yh}(0) = \Pi_4 J_y(0), \quad K_{zh}(0) = \Pi_4 J_z(0).$$

*It is also worth mentioning that we cannot choose all the initial values as the standard $L^2$ projections ($\Pi_4$) of exact solutions, which are easier to implement. The numerical order of convergence would fluctuate if we use $\Pi_4$ for all the six initial values. The reason may be that no numerical dissipation is included to dissipate the initial error, see also [5].*

In the rest of this section, we will prove the superconvergence results used above.

**Lemma 4.3.4.** *Let $TEX_i$ and $TEY_j$ be defined by (4.75)-(4.76). Then we have:*

$$\sum_{j=2}^{N_y} TEX_j \leq Ch^{2k+2} + \|E_{x\xi}\|^2, \tag{4.78}$$
$$\sum_{i=2}^{N_x} TEY_i \leq Ch^{2k+2} + \|E_{y\xi}\|^2, \tag{4.79}$$

*where the positive constant $C$ is independent of the mesh size $h$.*

*Proof.* First we define the individual summands in $\mathrm{TEX}_j$ $(j \geq 2)$ as $L_i(H_z, E_{x\xi})$ :

$$\begin{aligned} L_i(H_z, E_{x\xi}) = &\int_{K_{i,j}} (\Pi_3 - I) H_z \frac{\partial E_{x\xi}}{\partial y} - \int_{I_i} (((\Pi_3 - I)H_z)^- E_{x\xi}^-)(x, y_{j+\frac{1}{2}}) \\ &+ \int_{I_i} (((\Pi_3 - I)H_z)^- E_{x\xi}^+)(x, y_{j-\frac{1}{2}}). \end{aligned} \tag{4.80}$$

Note that on $y = y_{j+\frac{1}{2}}$ $(j \geq 1)$, the flux $\hat{H}_{z\eta} = H_{z\eta}^-$. By comparing (4.52) and (4.53) in the definition of $\Pi_3$ and the definition of $P_x^-$, we easily have

$$(\Pi_3 H_z)(x, y^-_{j-\frac{1}{2}}) = P_x^- \left( H_z(x, y_{j-\frac{1}{2}}) \right). \tag{4.81}$$

Therefore, $L_i(H_z, E_{x\xi})$ becomes:

$$\begin{aligned} L_i(H_z, E_{x\xi}) = &\int_{K_{i,j}} (\Pi_3 - I) H_z \frac{\partial E_{x\xi}}{\partial y} \\ &- \int_{I_i} \left( P_x^- \left( H_z(x, y_{j+\frac{1}{2}}) \right) - H_z(x, y_{j+\frac{1}{2}}) \right) E^-_{x\xi}(x, y_{j+\frac{1}{2}}) \\ &+ \int_{I_i} \left( P_x^- \left( H_z(x, y_{j-\frac{1}{2}}) \right) - H_z(x, y_{j-\frac{1}{2}}) \right) E^+_{x\xi}(x, y_{j-\frac{1}{2}}). \end{aligned} \tag{4.82}$$

Next we want to show that:

$$L_i(H_z, E_{x\xi}) = 0, \ \forall H_z \in \mathcal{P}_{k+1}(K_{i,j}), \ i = 1, \cdots, N_x, \ j = 2, \cdots, N_y. \tag{4.83}$$

where $\mathcal{P}_{k+1}$ is the standard notation for polynomials of degree not greater than $k+1$, i.e. $\mathcal{P}_{k+1} = \{x^i \cdot y^j | i \geq 0, j \geq 0, i + j \leq k+1\}$.

Since $\Pi_3$ is a $k$-th polynomial preserving projection, (4.83) is trivially true for $H_z \in Q_k(K_{i,j})$. Therefore, we only need to prove (4.83) for $H_z = x^{k+1}$ and $y^{k+1}$.

When $H_z = y^{k+1}$, by Theorem 4.3.2 we have $\Pi_3 H_z = P_y^- H_z$ since $H_z$ is only a function of $y$. Hence (4.83) is true by the definition of $P_y^-$.

When $H_z = x^{k+1}$, we have that

$$\begin{aligned} H_{z\eta}(x, y) &= (\Pi_3 - I) H_z(x, y) \\ &= (P_x^- - I) H_z(x, y) \end{aligned}$$

$$= P_x^-(x^{k+1}) - x^{k+1}$$

is a function of variable $x$ only. Therefore $H_{z\eta}(x, y^+_{j-\frac{1}{2}}) = H_{z\eta}(x, y^-_{j-\frac{1}{2}})$

Using this equality, we can simplify $L_i(H_z, E_{x\xi})$:

$$\begin{aligned}
L_i(H_z, E_{x\xi}) &= \int_{K_{i,j}} H_{z\eta}\frac{\partial E_{x\xi}}{\partial y} - \int_{I_i}\Big((H^-_{z\eta}E^-_{x\xi})(x, y_{j+\frac{1}{2}}) - (H^-_{z\eta}E^+_{x\xi})(x, y_{j-\frac{1}{2}})\Big)\\
&= \int_{K_{i,j}} H_{z\eta}\frac{\partial E_{x\xi}}{\partial y} - \int_{I_i}\Big((H^-_{z\eta}E^-_{x\xi})(x, y_{j+\frac{1}{2}}) - (H^+_{z\eta}E^+_{x\xi})(x, y_{j-\frac{1}{2}})\Big)\\
&= -\int_{K_{i,j}} \frac{\partial H_{z\eta}}{\partial y}E_{x\xi} \quad \text{(by integration by parts)}\\
&= 0 \quad (H_{z\eta} \text{ only depends on } x)\,.
\end{aligned}$$

Therefore, we have shown that (4.83) is true.

Using the standard scaling argument [10] to map a function $v(x, y)$ defined on $K_{i,j}$ between a function $\tilde{v}(\tilde{x}, \tilde{y})$ on the reference cell $\tilde{K} = [-\frac{1}{2}, \frac{1}{2}]^2 = \tilde{I} \times \tilde{J}$ (through mapping $(x, y) = (h\tilde{x} + x_i, h\tilde{y} + y_j)$), we have:

$$\begin{aligned}
L_i(H_z, E_{x\xi}) =& \int_{K_{i,j}} (\Pi_3 - I)H_z\frac{\partial E_{x\xi}}{\partial y}\\
&- \int_{I_i}\left(P_x^-\left(H_z(x, y_{j+\frac{1}{2}})\right) - H_z(x, y_{j+\frac{1}{2}})\right)E^-_{x\xi}(x, y_{j+\frac{1}{2}})\\
&+ \int_{I_i}\left(P_x^-\left(H_z(x, y_{j-\frac{1}{2}})\right) - H_z(x, y_{j-\frac{1}{2}})\right)E^+_{x\xi}(x, y_{j-\frac{1}{2}})\\
=& h\int_{\tilde{K}} (\tilde{\Pi}_3 - I)\tilde{H}_z\frac{\partial \tilde{E}_{x\xi}}{\partial y}\\
&- h\int_{\tilde{I}}\left(\tilde{P}_x^-\left(\tilde{H}_z(x, \frac{1}{2})\right) - \tilde{H}_z(x, \frac{1}{2})\right)\tilde{E}^-_{x\xi}(x, \frac{1}{2})\\
&+ h\int_{\tilde{I}}\left(\tilde{P}_x^-\left(\tilde{H}_z(x, -\frac{1}{2})\right) - \tilde{H}_z(x, -\frac{1}{2})\right)\tilde{E}^+_{x\xi}(x, -\frac{1}{2})\\
\leq& Ch\|\tilde{H}_z\|_{H^{k+2}(\tilde{K})}\|\tilde{E}_{x\xi}\|_{L^2(\tilde{K})},
\end{aligned}$$

where in the last step we used norm equivalence in finite dimensional spaces, and Sobolev embedding $H^{k+2} \subset L^\infty$.

Using the fact that $L_i(p, E_{x\xi}) = 0$ ,$\forall\, p \in \mathcal{P}_{k+1}(K_{i,j})$, we get:

$$\begin{aligned}
L_i(H_z, E_{x\xi}) =& \inf_{p \in P^{k+1}(K_{i,j})} L_i(H_z + p, E_{x\xi}) \\
\leq& \inf_{\tilde{p} \in P^{k+1}(\tilde{K})} Ch\|\tilde{H}_z + \tilde{p}\|_{H^{k+2}(\tilde{K})}\|\tilde{E}_{x\xi}\|_{L^2(\tilde{K})} \\
\leq& Ch|\tilde{H}_z|_{H^{k+2}(\tilde{K})}\|\tilde{E}_{x\xi}\|_{L^2(\tilde{K})} \text{ (by [10, Theorem 3.1.1])} \\
\leq& Ch^{k+1}|H_z|_{H^{k+2}(K_{i,j})}\|E_{x\xi}\|_{L^2(K_{i,j})} \text{ (by [10, Theorem 3.1.2])} \\
\leq& Ch^{2k+2}|H_z|^2_{H^{k+2}(K_{i,j})} + \|E_{x\xi}\|^2_{L^2(K_{i,j})}.
\end{aligned}$$

where $|\cdot|_{H^{k+2}}$ denotes the standard Sobolev semi-norm. We can now proceed to the proof of (4.78) from the above estimate

$$\begin{aligned}
\sum_{j=2}^{N_y} \text{TEX}_j =& \sum_{j=2}^{N_y}\sum_{i=1}^{N_x} L_i(H_z, E_{x\xi}) \\
\leq& \sum_{j=2}^{N_y}\sum_{i=1}^{N_x} \left( Ch^{2k+2}|H_z|^2_{H^{k+2}(K_{i,j})} + \|E_{x\xi}\|^2_{L^2(K_{i,j})} \right) \\
\leq& Ch^{2k+2}|H_z|^2_{H^{k+2}(\Omega)} + \|E_{x\xi}\|^2_{L^2(\Omega)}.
\end{aligned}$$

The proof of TEY is exactly the same as that of TEX by exchanging the role of $x$ and $y$. □

**Remark 4.3.4.** *Most part of the proof of Lemma 4.3.4 follows closely the proof of Lemma 3.6 in [12].*

**Lemma 4.3.5.** *Let $TEX_i$ and $TEY_j$ be defined by (4.75)-(4.76), and $c_0$ independent of mesh size $h$. Then we have:*

$$TEX_1 - \sum_{i=1}^{N_x} c_0 \int_{I_i} \left( E^+_{x\xi}(x, y_{\frac{1}{2}}) \right)^2 \leq Ch^{2k+2} + \|E_{x\xi}\|^2, \tag{4.84}$$

$$TEY_1 - \sum_{j=1}^{N_y} c_0 \int_{J_j} \left(E^+_{y\xi}(x_{\frac{1}{2}}, y)\right)^2 \leq Ch^{2k+2} + \|E_{y\xi}\|^2, \tag{4.85}$$

*where the positive constant $C$ is independent of the mesh size $h$.*

*Proof.* Since $y_{\frac{1}{2}} = c$, we have:

$$\begin{aligned}
&\mathrm{TEX}_1 - \sum_{i=1}^{N_x} c_0 \int_{I_i} \left(E^+_{x\xi}(x, y_{\frac{1}{2}})\right)^2 \\
=&\sum_{i=1}^{N_x} \int_{K_{i,1}} H_{z\eta} \frac{\partial E_{x\xi}}{\partial y} - \int_{I_i} (H^-_{z\eta} E^-_{x\xi})(x, y_{\frac{3}{2}}) + \int_{I_i} (P^-_x\,(H_z(x,c)) - H_z(x,c)) E^+_{x\xi}(x,c) \\
&- \int_{I_i} (P^-_x\,(H_z(x,c)) - H_z(x,c)) E^+_{x\xi}(x,c) + \int_{I_i} (H^+_{z\eta} E^+_{x\xi})(x,c) \\
&+ c_0 \int_{I_i} (E^+_{x\eta} E^+_{x\xi})(x,c) - c_0 \int_{I_i} \left(E^+_{x\xi}(x,c)\right)^2.
\end{aligned}$$

If we define

$$\begin{aligned}
L_A(H_z, E_{x\xi}) = \int_{K_{i,1}} H_{z\eta} \frac{\partial E_{x\xi}}{\partial y} - \int_{I_i} (H^-_{z\eta} E^-_{x\xi})(x, y_{\frac{3}{2}}) \\
+ \int_{I_i} (P^-_x\,(H_z(x,c)) - H_z(x,c)) E^+_{x\xi}(x,c),
\end{aligned} \tag{4.86}$$

and compare (4.86) with (4.82), we see that $L_A$ satisfies the same polynomial preserving properties. Hence we have

$$\sum_{i=1}^{N_x} L_A(H_z, E_{x\xi}) \leq Ch^{2k+2} |H_z|^2_{H^{k+2}(\Omega)} + \|E_{x\xi}\|^2, \tag{4.87}$$

which leads to:

$$
\begin{aligned}
&\mathrm{TEX}_1 - \sum_{i=1}^{N_x} c_0 \int_{I_i} \left(E^+_{x\xi}(x, y_{\frac{1}{2}})\right)^2 \\
\leq & Ch^{2k+2}|H_z|^2_{H^{k+2}(\Omega)} + \|E_{x\xi}\|^2 \\
& + \sum_{i=1}^{N_x} \left( -\int_{I_i} (P_x^- (H_z(x,c)) - H_z(x,c)) E^+_{x\xi}(x,c) + \int_{I_i} (H^+_{z\eta} E^+_{x\xi})(x,c) \right) \\
& + c_0 \int_a^b (E^+_{x\eta} E^+_{x\xi})(x,c) - c_0 \int_a^b \left(E^+_{x\xi}(x,c)\right)^2 \\
\leq & Ch^{2k+2}|H_z|^2_{H^{k+2}(\Omega)} + \|E_{x\xi}\|^2 \\
& + C \int_a^b (P_x^- (H_z(x,c)) - H_z(x,c))^2 + \int_a^b H^+_{z\eta}(x,c)^2 \\
\leq & Ch^{2k+2}|H_z|^2_{H^{k+2}(\Omega)} + \|E_{x\xi}\|^2 + Ch^{2k+2}|H_z|^2_{H^{k+1}(\Gamma)}
\end{aligned}
$$

where we denote $\Gamma = \{(x,c) : x \in (a,b)\}$. In deriving the second inequality, we used the definition of $\Pi_1$ to obtain

$$\int_{I_i} (E^+_{x\eta} E^+_{x\xi})(x,c)\, dx = 0.$$

In the last step we used the approximation properties of the projections.

The proof of (4.85) follows the same line as (4.84). □

**Remark 4.3.5.** *If $c_0 = 0$, we get a straightforward PEC boundary condition without the jump terms in (4.26) and (4.28). In this case, we can only control the term $\sum_{i=1}^{N_x} \int_{I_i} (H^+_{z\eta} E^+_{x\xi})(x,c)$ as follows:*

$$
\begin{aligned}
\sum_{i=1}^{N_x} \int_{I_i} (H^+_{z\eta} E^+_{x\xi})(x,c) &\leq h^{-1} \int_a^b (H^+_{z\eta})^2(x,c) + h \int_a^b (E^+_{x\xi})^2(x,c) \\
&\leq C \cdot h^{2k+1} + \|E_{x\xi}\|^2 \ \textit{(by inverse inequality)}
\end{aligned}
$$

*Therefore, we lose half an order. It is verified numerically that for basis function of odd orders of polynomial degree, like $Q_1$ and $Q_3$, we do observe this sub-optimal* *order of convergence. See Table 4.3 and Table 4.5.*

## 4.4 The fully-discrete DG method

We consider the following leap-frog LDG scheme: For any $n \geq 0$, find $E_{xh}^{n+1}, E_{yh}^{n+1}, H_{zh}^{n+\frac{3}{2}}, J_{xh}^{n+\frac{3}{2}}, J_{yh}^{n+\frac{3}{2}}, K_{zh}^{n+2} \in V_h^k$ such that

$$\begin{aligned}\epsilon_0 \int_{K_{i,j}} \frac{E_{xh}^{n+1} - E_{xh}^{n}}{\tau}\phi - \int_{I_i} \left( (\hat{H}_{zh}^{n+\frac{1}{2}}\phi^-)_{x,j+\frac{1}{2}} - (\hat{H}_{zh}^{n+\frac{1}{2}}\phi^+)_{x,j-\frac{1}{2}} \right) dx \\ + \int_{K_{i,j}} H_{zh}^{n+\frac{1}{2}} \frac{\partial \phi}{\partial y} + \int_{K_{i,j}} J_{xh}^{n+\frac{1}{2}} \phi = 0,\end{aligned} \tag{4.88}$$

$$\begin{aligned}\epsilon_0 \int_{K_{i,j}} \frac{E_{yh}^{n+1} - E_{yh}^{n}}{\tau}\psi + \int_{J_j} \left( (\hat{H}_{zh}^{n+\frac{1}{2}}\psi^-)_{i+\frac{1}{2},y} - (\hat{H}_{zh}^{n+\frac{1}{2}}\psi^+)_{i-\frac{1}{2},y} \right) dy \\ - \int_{K_{i,j}} H_{zh}^{n+\frac{1}{2}} \frac{\partial \psi}{\partial x} + \int_{K_{i,j}} J_{yh}^{n+\frac{1}{2}} \psi = 0,\end{aligned} \tag{4.89}$$

$$\begin{aligned}\mu_0 \int_{K_{i,j}} \frac{H_{zh}^{n+\frac{3}{2}} - H_{zh}^{n+\frac{1}{2}}}{\tau}\chi + \int_{J_j} \left( (\hat{E}_{yh}^{n+1}\chi^-)_{i+\frac{1}{2},y} - (\hat{E}_{yh}^{n+1}\chi^+)_{i-\frac{1}{2},y} \right) dy - \int_{K_{i,j}} E_{yh}^{n+1} \frac{\partial \chi}{\partial x} \\ - \int_{I_i} \left( (\hat{E}_{xh}^{n+1}\chi^-)_{x,j+\frac{1}{2}} - (\hat{E}_{xh}^{n+1}\chi^+)_{x,j-\frac{1}{2}} \right) dx + \int_{K_{i,j}} E_{xh}^{n+1} \frac{\partial \chi}{\partial y} + \int_{K_{i,j}} K_{zh}^{n+1} \chi = 0,\end{aligned} \tag{4.90}$$

$$\frac{1}{\epsilon_0 \omega_{pe}^2} \int_{K_{i,j}} \frac{J_{xh}^{n+\frac{3}{2}} - J_{xh}^{n+\frac{1}{2}}}{\tau} u_1 + \frac{\Gamma_e}{\epsilon_0 \omega_{pe}^2} \int_{K_{i,j}} \frac{J_{xh}^{n+\frac{3}{2}} + J_{xh}^{n+\frac{1}{2}}}{2} u_1 - \int_{K_{i,j}} E_{xh}^{n+1} u_1 = 0, \tag{4.91}$$

$$\frac{1}{\epsilon_0 \omega_{pe}^2} \int_{K_{i,j}} \frac{J_{yh}^{n+\frac{3}{2}} - J_{yh}^{n+\frac{1}{2}}}{\tau} u_2 + \frac{\Gamma_e}{\epsilon_0 \omega_{pe}^2} \int_{K_{i,j}} \frac{J_{yh}^{n+\frac{3}{2}} + J_{yh}^{n+\frac{1}{2}}}{2} u_2 - \int_{K_{i,j}} E_{yh}^{n+1} u_2 = 0, \tag{4.92}$$

$$\frac{1}{\mu_0 \omega_{pm}^2} \int_{K_{i,j}} \frac{K_{zh}^{n+2} - K_{zh}^{n+1}}{\tau} v + \frac{\Gamma_m}{\mu_0 \omega_{pm}^2} \int_{K_{i,j}} \frac{K_{zh}^{n+2} + K_{zh}^{n+1}}{2} v - \int_{K_{i,j}} H_{zh}^{n+\frac{3}{2}} v = 0, \tag{4.93}$$

for all test functions $\phi, \psi, \chi, u_1, u_2, v \in V_h^k$. With the following fluxes:

$$\hat{E}_{xh}^{n+1}(x, y_{j+\frac{1}{2}}) = E_{xh}^{n+1,+}(x, y_{j+\frac{1}{2}}) \qquad \forall j = 1, \cdots, N_y - 1, \tag{4.94}$$

$$\hat{E}_{xh}^{n+1}(x, y_{\frac{1}{2}}) = \hat{E}_{xh}^{n+1}(x, y_{N_y+\frac{1}{2}}) = 0, \tag{4.95}$$

$$\hat{E}_{yh}^{n+1}(x_{i+\frac{1}{2}}, y) = E_{yh}^{n+1,+}(x_{i+\frac{1}{2}}, y) \qquad \forall i = 1, \cdots, N_x - 1, \tag{4.96}$$

$$\hat{E}_{yh}^{n+1}(x_{\frac{1}{2}}, y) = \hat{E}_{yh}^{n+1}(x_{N_x+\frac{1}{2}}, y) = 0, \tag{4.97}$$

$$\hat{H}_{zh}^{n+\frac{1}{2}}(x, y_{j+\frac{1}{2}}) = H_{zh}^{n+\frac{1}{2},-}(x, y_{j+\frac{1}{2}}) \qquad \forall j = 1, \cdots, N_y, \tag{4.98}$$

$$\hat{H}_{zh}^{n+\frac{1}{2}}(x, y_{\frac{1}{2}}) = H_{zh}^{n+\frac{1}{2},+}(x, y_{\frac{1}{2}}) + \frac{c_0}{2}\left(E_{xh}^{n+1}(x, y_{\frac{1}{2}}^{+}) + E_{xh}^{n}(x, y_{\frac{1}{2}}^{+})\right), \tag{4.99}$$

$$\hat{H}_{zh}^{n+\frac{1}{2}}(x_{i+\frac{1}{2}}, y) = H_{zh}^{n+\frac{1}{2},-}(x_{i+\frac{1}{2}}, y) \qquad \forall i = 1, \cdots, N_x, \tag{4.100}$$

$$\hat{H}_{zh}^{n+\frac{1}{2}}(x_{\frac{1}{2}}, y) = H_{zh}^{n+\frac{1}{2},+}(x_{\frac{1}{2}}, y) - \frac{c_0}{2}\left(E_{yh}^{n+1}(x_{\frac{1}{2}}^{+}, y) + E_{yh}^{n}(x_{\frac{1}{2}}^{+}, y)\right), \tag{4.101}$$

Note that by PEC boundary condition $E_{xh}^{n+1}(x, y_{\frac{1}{2}}^{+}) = [[E_{xh}^{n+1}(x, y_{\frac{1}{2}})]]$ in (4.99), and the same for other artificial viscosity in (4.99) and (4.101).

To prove the stability for our fully-discrete scheme, we need some lemmas. Let us denote boundary integral terms

$$\begin{aligned} sum_{Ih} :=& -\int_{I_i}\left((\hat{H}_{zh}^{n+\frac{1}{2}}(E_{xh}^{n+1} + E_{xh}^{n})^{-})_{x,j+\frac{1}{2}} - (\hat{H}_{zh}^{n+\frac{1}{2}}(E_{xh}^{n+1} + E_{xh}^{n})^{+})_{x,j-\frac{1}{2}}\right) dx \\ & -\int_{I_i}\left((\hat{E}_{xh}^{n+1}(H_{zh}^{n+\frac{3}{2}} + H_{zh}^{n+\frac{1}{2}})^{-})_{x,j+\frac{1}{2}} - (\hat{E}_{xh}^{n+1}(H_{zh}^{n+\frac{3}{2}} + H_{zh}^{n+\frac{1}{2}})^{+})_{x,j-\frac{1}{2}}\right) dx \end{aligned} \tag{4.102}$$

and

$$\begin{aligned} sum_{Jh} :=& \int_{J_j}\left((\hat{H}_{zh}^{n+\frac{1}{2}}(E_{yh}^{n+1} + E_{yh}^{n})^{-})_{i+\frac{1}{2},y} - (\hat{H}_{zh}^{n+\frac{1}{2}}(E_{yh}^{n+1} + E_{yh}^{n})^{+})_{i-\frac{1}{2},y}\right) dy \\ & +\int_{J_j}\left((\hat{E}_{yh}^{n+1}(H_{zh}^{n+\frac{3}{2}} + H_{zh}^{n+\frac{1}{2}})^{-})_{i+\frac{1}{2},y} - (\hat{E}_{yh}^{n+1}(H_{zh}^{n+\frac{3}{2}} + H_{zh}^{n+\frac{1}{2}})^{+})_{i-\frac{1}{2},y}\right) dy. \end{aligned} \tag{4.103}$$

Furthermore, for any function $\phi \in V_h^k$ we introduce the common notation

$$||\phi||_{\Gamma_h,x} = (\sum_{1\leq i\leq N_x}\int_c^d(|\phi_{i+\frac{1}{2}}^{+}|^2 + |\phi_{i+\frac{1}{2}}^{-}|^2)dy)^{1/2},$$

$$||\phi||_{\Gamma_{h,y}} = (\sum_{1\le i\le N_y}\int_a^b (|\phi^+_{j+\frac{1}{2}}|^2 + |\phi^-_{j+\frac{1}{2}}|^2)dx)^{1/2},$$

for the $L^2$-norms on $\Gamma_{h,x}$ (union of all element interface points along the $x$-direction) and $\Gamma_{h,y}$ (union of all element interface points along the $y$-direction), respectively.

**Lemma 4.4.1.** *With the flux choices of* (4.94) – (4.101) *for any* $m \ge 1$ *we have*

$$\begin{aligned}
&\sum_{n=0}^{m}\sum_{i,j}\int_{K_{i,j}}\left\{H_{zh}^{n+\frac{1}{2}}\frac{\partial}{\partial y}(E_{xh}^{n+1}+E_{xh}^{n}) + E_{xh}^{n+1}\frac{\partial}{\partial y}(H_{zh}^{n+\frac{3}{2}}+H_{zh}^{n+\frac{1}{2}})\right\} + \sum_{n=0}^{m}\sum_{i,j} sum_{Ih}\\
&=\sum_{j=1}^{N_y-1}\left(\int_a^b (E_{xh}^{m+1,+}[[H_{zh}^{m+\frac{3}{2}}]])_{x,j+\frac{1}{2}} - \int_a^b (E_{xh}^{0,+}[[H_{zh}^{\frac{1}{2}}]])_{x,j+\frac{1}{2}}\right)\\
&\quad+\sum_{i,j}\int_{K_{i,j}}\left\{-E_{xh}^{0}\frac{\partial}{\partial y}H_{zh}^{\frac{1}{2}} + E_{xh}^{m+1}\frac{\partial}{\partial y}H_{zh}^{m+\frac{3}{2}}\right\} + \frac{c_0}{2}\sum_{n=0}^{m}\int_a^b (E_{xh}^{n+1,+}+E_{xh}^{n,+})^2_{x,\frac{1}{2}}
\end{aligned} \tag{4.104}$$

*where for simplicity we denote* $\sum_{i,j} := \sum_{1\le i\le N_x}\sum_{1\le j\le N_y}$.

*Proof.* By the definition of $sum_{Ih}$ and flux choices (4.94) − (4.101), we easily have

$$
\begin{aligned}
&\sum_{n=0}^{m}\sum_{j=1}^{N_y} sum_{Ih} \\
=&-\sum_{n=0}^{m}\sum_{j=1}^{N_y}\int_{I_i}(H_{zh}^{n+\frac{1}{2},-}E_{xh}^{n+1,-})_{x,j+\frac{1}{2}}-\sum_{n=0}^{m}\sum_{j=1}^{N_y}\int_{I_i}(H_{zh}^{n+\frac{1}{2},-}E_{xh}^{n,-})_{x,j+\frac{1}{2}} \\
&+\sum_{n=0}^{m}\sum_{j=1}^{N_y-1}\int_{I_i}(H_{zh}^{n+\frac{1}{2},-}E_{xh}^{n+1,+})_{x,j+\frac{1}{2}}+\sum_{n=0}^{m}\sum_{j=1}^{N_y-1}\int_{I_i}(H_{zh}^{n+\frac{1}{2},-}E_{xh}^{n,+})_{x,j+\frac{1}{2}} \\
&+\sum_{n=0}^{m}\int_{I_i}(H_{zh}^{n+\frac{1}{2},+}E_{xh}^{n+1,+})_{x,\frac{1}{2}}+\sum_{n=0}^{m}\int_{I_i}(H_{zh}^{n+\frac{1}{2},+}E_{xh}^{n,+})_{x,\frac{1}{2}} \\
&+\frac{c_0}{2}\sum_{n=0}^{m}\int_{I_i}(E_{xh}^{n+1,+}+E_{xh}^{n,+})^2_{x,\frac{1}{2}} \\
&-\sum_{n=0}^{m}\sum_{j=1}^{N_y-1}\int_{I_i}(E_{xh}^{n+1,+}H_{zh}^{n+\frac{3}{2},-})_{x,j+\frac{1}{2}}-\sum_{n=0}^{m}\sum_{j=1}^{N_y-1}\int_{I_i}(E_{xh}^{n+1,+}H_{zh}^{n+\frac{1}{2},-})_{x,j+\frac{1}{2}} \\
&+\sum_{n=0}^{m}\sum_{j=1}^{N_y-1}\int_{I_i}(E_{xh}^{n+1,+}H_{zh}^{n+\frac{3}{2},+})_{x,j+\frac{1}{2}}+\sum_{n=0}^{m}\sum_{j=1}^{N_y-1}\int_{I_i}(E_{xh}^{n+1,+}H_{zh}^{n+\frac{1}{2},+})_{x,j+\frac{1}{2}}
\end{aligned}
\tag{4.105}
$$

On the other hand, we see that

$$
\begin{aligned}
&\sum_{n=0}^{m}\sum_{i,j}\int_{K_{i,j}}\left\{H_{zh}^{n+\frac{1}{2}}\frac{\partial}{\partial y}(E_{xh}^{n+1}+E_{xh}^{n})+E_{xh}^{n+1}\frac{\partial}{\partial y}(H_{zh}^{n+\frac{3}{2}}+H_{zh}^{n+\frac{1}{2}})\right\}dxdy\\
=&\sum_{n=0}^{m}\sum_{i,j}\int_{K_{i,j}}\left\{\frac{\partial}{\partial y}(E_{xh}^{n+1}H_{zh}^{n+\frac{1}{2}})+\frac{\partial}{\partial y}(E_{xh}^{n}H_{zh}^{n+\frac{1}{2}})\right.\\
&\qquad\qquad\left.-E_{xh}^{n}\frac{\partial}{\partial y}H_{zh}^{n+\frac{1}{2}}+E_{xh}^{n+1}\frac{\partial}{\partial y}H_{zh}^{n+\frac{3}{2}}\right\}dxdy\\
=&\sum_{n=0}^{m}\sum_{i,j}\int_{K_{i,j}}\left\{\frac{\partial}{\partial y}(E_{xh}^{n+1}H_{zh}^{n+\frac{1}{2}})+\frac{\partial}{\partial y}(E_{xh}^{n}H_{zh}^{n+\frac{1}{2}})\right\}\\
&+\sum_{n=0}^{m}\sum_{i,j}\int_{K_{i,j}}\left\{-E_{xh}^{n}\frac{\partial}{\partial y}H_{zh}^{n+\frac{1}{2}}+E_{xh}^{n+1}\frac{\partial}{\partial y}H_{zh}^{n+\frac{3}{2}}\right\}\\
=&\sum_{n=0}^{m}\sum_{i=1}^{N_x}\sum_{j=1}^{N_y}\int_{I_i}(E_{xh}^{n+1,-}H_{zh}^{n+\frac{1}{2},-})_{x,j+\frac{1}{2}}-\sum_{n=0}^{m}\sum_{i=1}^{N_x}\sum_{j=0}^{N_y-1}\int_{I_i}(E_{xh}^{n+1,+}H_{zh}^{n+\frac{1}{2},+})_{x,j+\frac{1}{2}}\\
&+\sum_{n=0}^{m}\sum_{i=1}^{N_x}\sum_{j=1}^{N_y}\int_{I_i}(E_{xh}^{n,-}H_{zh}^{n+\frac{1}{2},-})_{x,j+\frac{1}{2}}-\sum_{n=0}^{m}\sum_{i=1}^{N_x}\sum_{j=0}^{N_y-1}\int_{I_i}(E_{xh}^{n,+}H_{zh}^{n+\frac{1}{2},+})_{x,j+\frac{1}{2}}\\
&+\sum_{i,j}\int_{K_{i,j}}\left\{-E_{xh}^{0}\frac{\partial}{\partial y}H_{zh}^{\frac{1}{2}}+E_{xh}^{m+1}\frac{\partial}{\partial y}H_{zh}^{m+\frac{3}{2}}\right\}
\end{aligned}
\tag{4.106}
$$

Combining (4.105) and (4.106), we get

$$
\begin{aligned}
&\sum_{n=0}^{m}\sum_{i,j}\int_{K_{i,j}}\left\{H_{zh}^{n+\frac{1}{2}}\frac{\partial}{\partial y}(E_{xh}^{n+1}+E_{xh}^{n})+E_{xh}^{n+1}\frac{\partial}{\partial y}(H_{zh}^{n+\frac{3}{2}}+H_{zh}^{n+\frac{1}{2}})\right\}+\sum_{n=0}^{m}\sum_{i,j}sum_{Ih}\\
=&\sum_{n=0}^{m}\sum_{i=1}^{N_x}\sum_{j=1}^{N_y-1}\left(\int_{I_i}(E_{xh}^{n+1,+}[[H_{zh}^{n+\frac{3}{2}}]])_{x,j+\frac{1}{2}}-\int_{I_i}(E_{xh}^{n,+}[[H_{zh}^{n+\frac{1}{2}}]])_{x,j+\frac{1}{2}}\right)\\
&+\sum_{i,j}\int_{K_{i,j}}\left\{-E_{xh}^{0}\frac{\partial}{\partial y}H_{zh}^{\frac{1}{2}}+E_{xh}^{m+1}\frac{\partial}{\partial y}H_{zh}^{m+\frac{3}{2}}\right\}\\
&+\frac{c_0}{2}\sum_{n=0}^{m}\int_a^b(E_{xh}^{n+1,+}+E_{xh}^{n,+})_{x,\frac{1}{2}}^2
\end{aligned}
$$

$$= \sum_{j=1}^{N_y-1} \left( \int_a^b (E_{xh}^{m+1,+}[[H_{zh}^{m+\frac{3}{2}}]])_{x,j+\frac{1}{2}} - \int_a^b (E_{xh}^{0,+}[[H_{zh}^{\frac{1}{2}}]])_{x,j+\frac{1}{2}} \right)$$
$$+ \sum_{i,j} \int_{K_{i,j}} \left\{ -E_{xh}^0 \frac{\partial}{\partial y} H_{zh}^{\frac{1}{2}} + E_{xh}^{m+1} \frac{\partial}{\partial y} H_{zh}^{m+\frac{3}{2}} \right\}$$
$$+ \frac{c_0}{2} \sum_{n=0}^{m} \int_a^b (E_{xh}^{n+1,+} + E_{xh}^{n,+})^2_{x,\frac{1}{2}}$$

□

Using the similar technique, we can also prove the following lemma.

**Lemma 4.4.2.** *With the flux choices of* (4.94) – (4.101) *for any* $m \geq 1$ *we have*

$$\sum_{n=0}^{m} \sum_{i,j} sum_{Jh} - \sum_{n=0}^{m} \sum_{i,j} \int_{K_{i,j}} \left\{ H_{zh}^{n+\frac{1}{2}} \frac{\partial}{\partial x} (E_{yh}^{n+1} + E_{yh}^{n}) \right.$$
$$\left. + E_{yh}^{n+1} \frac{\partial}{\partial x} (H_{zh}^{n+\frac{3}{2}} + H_{zh}^{n+\frac{1}{2}}) \right\}$$
$$= \sum_{i=1}^{N_x-1} \left( - \int_c^d (E_{yh}^{m+1,+}[[H_{zh}^{m+\frac{3}{2}}]])_{i+\frac{1}{2},y} + \int_c^d (E_{yh}^{0,+}[[H_{zh}^{\frac{1}{2}}]])_{i+\frac{1}{2},y} \right) \tag{4.107}$$
$$+ \sum_{i,j} \int_{K_{i,j}} \left\{ E_{yh}^0 \frac{\partial}{\partial x} H_{zh}^{\frac{1}{2}} - E_{yh}^{m+1} \frac{\partial}{\partial x} H_{zh}^{m+\frac{3}{2}} \right\}$$
$$+ \frac{c_0}{2} \sum_{n=0}^{m} \int_c^d (E_{yh}^{n+1,+} + E_{yh}^{n,+})^2_{\frac{1}{2},y}$$

With the above preparation, we can now prove the following stability. To shorten the notation, we introduce the vector $L^2$ norm $||\boldsymbol{E}_h||^2 = ||E_{xh}||^2 + ||E_{yh}||^2$ for vector $\boldsymbol{E}_h = (E_{xh}, E_{yh})$. Similar notation will be used for $||\boldsymbol{J}_h||^2$ for vector $\boldsymbol{J}_h = (J_{xh}, J_{yh})$.

**Theorem 4.4.1.** *Denote* $C_v = \frac{1}{\sqrt{\epsilon_0 \mu_0}}$ *for the speed of light, and* $C_{inv}$ *for the positive constant appearing in (4.114). Under the assumption*

$$\tau \leq \min\left(\frac{1}{2\omega_{pe}}, \frac{1}{2\omega_{pm}}, \frac{h}{2C_{inv}C_v}\right), \tag{4.108}$$

*for any $m \geq 1$ we have*

$$
\begin{aligned}
&\epsilon_0||\boldsymbol{E}_h^{m+1}||^2 + \mu_0||H_{zh}^{m+\frac{3}{2}}||^2 + \frac{1}{\epsilon_0\omega_{pe}^2}||\boldsymbol{J}_h^{m+\frac{3}{2}}||^2 + \frac{1}{\mu_0\omega_{pm}^2}||K_{zh}^{m+2}||^2 \\
\leq\ & C\left(\epsilon_0||\boldsymbol{E}_h^0||^2 + \mu_0||H_{zh}^{\frac{1}{2}}||^2 + \frac{1}{\epsilon_0\omega_{pe}^2}||\boldsymbol{J}_h^{\frac{1}{2}}||^2 + \frac{1}{\mu_0\omega_{pm}^2}||K_{zh}^1||^2\right),
\end{aligned}
\tag{4.109}
$$

*where the constant $C > 1$ is independent of the mesh size $h$ and the time step size $\tau$.*

*Proof.* Choosing $\phi = \tau(E_{xh}^{n+1} + E_{xh}^n), \psi = \tau(E_{yh}^{n+1} + E_{yh}^n), \chi = \tau(H_{zh}^{n+\frac{3}{2}} + H_{zh}^{n+\frac{1}{2}})$, $u_1 = \tau(J_{xh}^{n+\frac{3}{2}} + J_{xh}^{n+\frac{1}{2}}), u_2 = \tau(J_{yh}^{n+\frac{3}{2}} + J_{yh}^{n+\frac{1}{2}}), v = \tau(K_{zh}^{n+2} + K_{zh}^{n+1})$, we obtain

$$
\begin{aligned}
&\epsilon_0(||\boldsymbol{E}_h^{n+1}||^2_{L^2(K_{i,j})} - ||\boldsymbol{E}_h^n||^2_{L^2(K_{i,j})}) + \mu_0(||H_{zh}^{n+\frac{3}{2}}||^2_{L^2(K_{i,j})} - ||H_{zh}^{n+\frac{1}{2}}||^2_{L^2(K_{i,j})}) \\
&+ \frac{1}{\epsilon_0\omega_{pe}^2}(||\boldsymbol{J}_h^{n+\frac{3}{2}}||^2_{L^2(K_{i,j})} - ||\boldsymbol{J}_{zh}^{n+\frac{1}{2}}||^2_{L^2(K_{i,j})}) \\
&+ \frac{1}{\mu_0\omega_{pm}^2}(||K_{zh}^{n+2}||^2_{L^2(K_{i,j})} - ||K_{zh}^{n+1}||^2_{L^2(K_{i,j})}) \\
&+ \int_{K_{i,j}} H_{zh}^{n+\frac{1}{2}} \cdot \tau\frac{\partial}{\partial y}(E_{xh}^{n+1} + E_{xh}^n) + \int_{K_{i,j}} \boldsymbol{J}_h^{n+\frac{1}{2}} \cdot \tau(\boldsymbol{E}_h^{n+1} + \boldsymbol{E}_h^n) \\
&- \int_{K_{i,j}} H_{zh}^{n+\frac{1}{2}} \cdot \tau\frac{\partial}{\partial x}(E_{yh}^{n+1} + E_{yh}^n) - \int_{K_{i,j}} E_{yh}^{n+1} \cdot \tau\frac{\partial}{\partial x}(H_{zh}^{n+\frac{3}{2}} + H_{zh}^{n+\frac{1}{2}}) \\
&+ \int_{K_{i,j}} E_{xh}^{n+1} \cdot \tau\frac{\partial}{\partial y}(H_{zh}^{n+\frac{3}{2}} + H_{zh}^{n+\frac{1}{2}}) + \int_{K_{i,j}} K_{zh}^{n+1} \cdot \tau(H_{zh}^{n+\frac{3}{2}} + H_{zh}^{n+\frac{1}{2}}) \\
&+ \frac{\tau\Gamma_e}{2\epsilon_0\omega_{pe}^2}||\boldsymbol{J}_h^{n+\frac{3}{2}} + \boldsymbol{J}_{zh}^{n+\frac{1}{2}}||^2_{L^2(K_{i,j})} + \frac{\tau\Gamma_m}{2\mu_0\omega_{pm}^2}||K_{zh}^{n+2} + K_{zh}^{n+1}||^2_{L^2(K_{i,j})} \\
&- \int_{K_{i,j}} \boldsymbol{E}_h^{n+1} \cdot \tau(\boldsymbol{J}_h^{n+\frac{3}{2}} + \boldsymbol{J}_h^{n+\frac{1}{2}}) - \int_{K_{i,j}} H_{zh}^{n+\frac{3}{2}} \cdot \tau(K_{zh}^{n+2} + K_{zh}^{n+1}) \\
&+ \tau(sum_{Ih} + sum_{Jh}) = 0.
\end{aligned}
\tag{4.110}
$$

Summing up (4.110) over $1 \leq i \leq N_x, 1 \leq j \leq N_y$, and time levels $0 \leq n \leq m$ for any $m \geq 1$, dropping the non-negative terms $\frac{\tau\Gamma_e}{2\epsilon_0\omega_{pe}^2}||\boldsymbol{J}_h^{n+\frac{3}{2}} + \boldsymbol{J}_{zh}^{n+\frac{1}{2}}||^2_{L^2(K_{i,j})}$, $\frac{\tau\Gamma_m}{2\mu_0\omega_{pm}^2}||K_{zh}^{n+2} + K_{zh}^{n+1}||^2_{L^2(K_{i,j})}$, $\frac{c_0}{2}\sum_{n=0}^m \int_c^d (E_{yh}^{n+1,+} + E_{yh}^{n,+})^2_{\frac{1}{2},y}$ , and $\frac{c_0}{2}\sum_{n=0}^m \int_a^b (E_{xh}^{n+1,+} + E_{xh}^{n,+})^2_{x,\frac{1}{2}}$. Using

Lemmas 4.4.1 and 4.4.2, we have

$$
\begin{aligned}
&\epsilon_0(||\boldsymbol{E}_h^{m+1}||^2 - ||\boldsymbol{E}_h^0||^2) + \mu_0(||H_{zh}^{m+\frac{3}{2}}||^2 - ||H_{zh}^{\frac{1}{2}}||^2) \\
&+\frac{1}{\epsilon_0\omega_{pe}^2}(||\boldsymbol{J}_h^{m+\frac{3}{2}}||^2 - ||\boldsymbol{J}_{zh}^{\frac{1}{2}}||^2) + \frac{1}{\mu_0\omega_{pm}^2}(||K_{zh}^{m+2}||^2 - ||K_{zh}^1||^2) \\
\leq\ & -\sum_{0\leq n\leq m}\int_\Omega \boldsymbol{J}_h^{n+\frac{1}{2}}\cdot\tau(\boldsymbol{E}_h^{n+1}+\boldsymbol{E}_h^n) - \sum_{0\leq n\leq m}\int_\Omega K_{zh}^{n+1}\cdot\tau(H_{zh}^{n+\frac{3}{2}}+H_{zh}^{n+\frac{1}{2}}) \\
&+\sum_{0\leq n\leq m}\int_\Omega \boldsymbol{E}_h^{n+1}\cdot\tau(\boldsymbol{J}_h^{n+\frac{3}{2}}+\boldsymbol{J}_h^{n+\frac{1}{2}}) + \sum_{0\leq n\leq m}\int_\Omega H_{zh}^{n+\frac{3}{2}}\cdot\tau(K_{zh}^{n+2}+K_{zh}^{n+1}) \\
&+B^y(E_{xh}^0, H_{zh}^{\frac{1}{2}}) - B^y(E_{xh}^{m+1}, H_{zh}^{m+\frac{3}{2}}) - B^x(E_{yh}^0, H_{zh}^{\frac{1}{2}}) + B^x(E_{yh}^{m+1}, H_{zh}^{m+\frac{3}{2}}),
\end{aligned}
\tag{4.111}
$$

where we introduced the bilinear forms (cf. [51, (4.1)])

$$
\begin{aligned}
B^y(u,v) &= \tau\left(\sum_{i,j}\int_{K_{i,j}} u\partial_y v + \sum_{1\leq j\leq N_y-1}\int_a^b u_{j+\frac{1}{2}}^+[[v]]_{j+\frac{1}{2}}dx\right), \\
B^x(u,v) &= \tau\left(\sum_{i,j}\int_{K_{i,j}} u\partial_x v + \sum_{1\leq i\leq N_x-1}\int_c^d u_{i+\frac{1}{2}}^+[[v]]_{i+\frac{1}{2}}dy\right).
\end{aligned}
$$

Note that the sum of the first and third terms of (4.111) can be estimated as follows:

$$
\begin{aligned}
S_1+S_3 =& -\tau\sum_{0\leq n\leq m}\int_\Omega\left(\boldsymbol{J}_h^{n+\frac{1}{2}}\cdot\boldsymbol{E}_h^n - \boldsymbol{J}_h^{n+\frac{3}{2}}\cdot\boldsymbol{E}_h^{n+1}\right) \\
=& -\tau\int_\Omega\left(\boldsymbol{J}_h^{\frac{1}{2}}\cdot\boldsymbol{E}_h^0 - \boldsymbol{J}_h^{m+\frac{3}{2}}\cdot\boldsymbol{E}_h^{m+1}\right) \\
\leq& \frac{\tau\omega_{pe}}{2}(\frac{1}{\epsilon_0\omega_{pe}^2}||\boldsymbol{J}_h^{\frac{1}{2}}||^2 + \epsilon_0||\boldsymbol{E}_h^0||^2) \\
&+\frac{\tau\omega_{pe}}{2}(\frac{1}{\epsilon_0\omega_{pe}^2}||\boldsymbol{J}_h^{m+\frac{3}{2}}||^2 + \epsilon_0||\boldsymbol{E}_h^{m+1}||^2),
\end{aligned}
\tag{4.112}
$$

where in the last step we used the Cauchy-Schwarz inequality.

Similarly, we can bound the sum of the second and fourth terms of (4.111) as follows:

$$
\begin{aligned}
S_2+S_4 =&\tau \sum_{0\le n\le m}\int_\Omega \Big\{ -K_{zh}^{n+1}\cdot\tau(H_{zh}^{n+\frac{3}{2}}+H_{zh}^{n+\frac{1}{2}})+H_{zh}^{n+\frac{3}{2}}\cdot\tau(K_{zh}^{n+2}+K_{zh}^{n+1})\Big\}\\
=&-\tau\int_\Omega\Big(K_{zh}^1H_{zh}^{\frac{1}{2}}-K_{zh}^{m+2}H_{zh}^{m+\frac{3}{2}}\Big)\\
\le&\frac{\tau\omega_{pm}}{2}(\frac{1}{\mu_0\omega_{pm}^2}||K_{zh}^1||^2+\mu_0||H_{zh}^{\frac{1}{2}}||^2)\\
&+\frac{\tau\omega_{pm}}{2}(\frac{1}{\mu_0\omega_{pm}^2}||K_{zh}^{m+2}||^2+\mu_0||H_{zh}^{m+\frac{3}{2}}||^2).
\end{aligned}
\tag{4.113}
$$

By using the Cauchy-Schwarz inequality and the inverse estimate, we have (cf. [51, Lemma 4.1]):

$$
\begin{aligned}
B^y(E_{xh}^{m+1},H_{zh}^{m+\frac{3}{2}})\le&\tau\cdot C_{inv}h^{-1}||E_{xh}^{m+1}||\cdot||H_{zh}^{m+\frac{3}{2}}||\\
=&\tau\cdot C_{inv}C_vh^{-1}\sqrt{\epsilon_0}||E_{xh}^{m+1}||\sqrt{\mu_0}||H_{zh}^{m+\frac{3}{2}}||\\
\le&\tau\cdot\frac{C_{inv}C_v}{2h}(\epsilon_0||E_{xh}^{m+1}||^2+\mu_0||H_{zh}^{m+\frac{3}{2}}||^2),
\end{aligned}
\tag{4.114}
$$

where the positive constant $C_{inv}$ is independent of $\tau$ and $h$.

Similarly, we can obtain

$$B^y(E_{xh}^0,H_{zh}^{\frac{1}{2}})\le\tau\cdot\frac{C_{inv}C_v}{2h}(\epsilon_0||E_{xh}^0||^2+\mu_0||H_{zh}^{\frac{1}{2}}||^2), \tag{4.115}$$

$$B^x(E_{yh}^{m+1},H_{zh}^{m+\frac{3}{2}})\le\tau\cdot\frac{C_{inv}C_v}{2h}(\epsilon_0||E_{yh}^{m+1}||^2+\mu_0||H_{zh}^{m+\frac{3}{2}}||^2), \tag{4.116}$$

$$B^x(E_{yh}^0,H_{zh}^{\frac{1}{2}})\le\tau\cdot\frac{C_{inv}C_v}{2h}(\epsilon_0||E_{yh}^0||^2+\mu_0||H_{zh}^{\frac{1}{2}}||^2). \tag{4.117}$$

The proof is completed by substituting the above estimates (4.112)-(4.117) into (4.111) and using the assumptions $\frac{\tau\omega_{pm}}{2}, \frac{\tau\omega_{pe}}{2}, \frac{\tau C_{inv}C_v}{2h}\le\frac{1}{4}$. □

**Remark 4.4.1.** *We would like to remark that under the same assumption as Theo-*

*rem 4.4.1 coupled with the assumptions on the initial value:*

$$\epsilon_0||\boldsymbol{E}^0 - \boldsymbol{E}_h^0||^2 + \mu_0||H_z^{\frac{1}{2}} - H_{zh}^{\frac{1}{2}}||^2$$
$$+\frac{1}{\epsilon_0\omega_{pe}^2}||\boldsymbol{J}^{\frac{1}{2}} - \boldsymbol{J}_h^{\frac{1}{2}}||^2 + \frac{1}{\mu_0\omega_{pm}^2}||K_z^1 - K_{zh}^1||^2 \leq Ch^{2(k+1)},$$

*we can prove the following optimal error estimate: for any $m \geq 1$*

$$\epsilon_0||\boldsymbol{E}^{m+1} - \boldsymbol{E}_h^{m+1}||^2 + \mu_0||H_z^{m+\frac{3}{2}} - H_{zh}^{m+\frac{3}{2}}||^2$$
$$+\frac{1}{\epsilon_0\omega_{pe}^2}||\boldsymbol{J}^{m+\frac{3}{2}} - \boldsymbol{J}_h^{m+\frac{3}{2}}||^2 + \frac{1}{\mu_0\omega_{pm}^2}||K_z^{m+2} - K_{zh}^{m+2}||^2 \leq C\left(h^{(k+1)} + \tau^2\right)^2.$$

*where $\boldsymbol{J} = (J_x, J_y)$., and $\boldsymbol{E} = (E_x, E_y)$. The proof can be carried out by following the similar idea to the proofs of Theorem 4.3.2 and 4.4.1 coupled with time discretization estimates (cf. [36, Ch.3]). Considering that the proof is very lengthy and technical, we skip it.*

## 4.5 Numerical results

To validate our theoretical analysis, we solve the model problem (4.7)-(4.12) with imposed sources $f_x, f_y$ and $g$ on $\Omega = [0,1]^2$:

$$\frac{\partial E_x}{\partial t} = \frac{\partial H_z}{\partial y} - J_x + f_x \tag{4.118}$$
$$\frac{\partial E_y}{\partial t} = -\frac{\partial H_z}{\partial x} - J_y + f_y \tag{4.119}$$
$$\frac{\partial H_z}{\partial t} = -\frac{\partial E_y}{\partial x} + \frac{\partial E_x}{\partial y} - K_z + g \tag{4.120}$$
$$\frac{1}{\omega^2\pi^2}\frac{\partial J_x}{\partial t} = -\frac{2}{\omega\pi}J_x + E_x \tag{4.121}$$
$$\frac{1}{\omega^2\pi^2}\frac{\partial J_y}{\partial t} = -\frac{2}{\omega\pi}J_y + E_y \tag{4.122}$$
$$\frac{1}{\omega^2\pi^2}\frac{\partial K_z}{\partial t} = -\frac{2}{\omega\pi}K_z + H_z \tag{4.123}$$

which has the exact solutions:

$$
\begin{aligned}
E_x(x,y,t) &= \cos(\omega\pi x)\sin(\omega\pi y)e^{-\omega\pi t} && (4.124)\\
E_y(x,y,t) &= -\sin(\omega\pi x)\cos(\omega\pi y)e^{-\omega\pi t} && (4.125)\\
H_z(x,y,t) &= \cos(\omega\pi x)\cos(\omega\pi y)e^{-\omega\pi t} && (4.126)\\
J_x(x,y,t) &= \omega\pi E_x(x,y,t) && (4.127)\\
J_y(x,y,t) &= \omega\pi E_y(x,y,t) && (4.128)\\
K(x,y,t) &= \omega\pi H(x,y,t), && (4.129)
\end{aligned}
$$

and the source terms:

$$
f_x = J_x, \quad f_y = J_y \quad g = -2\omega\pi H. \tag{4.130}
$$

With the added source terms, we only need to modify the original scheme (4.88)-(4.93) by adding

$$
\int_{K_{i,j}} f_x^{n+\frac{1}{2}}\phi, \quad \int_{K_{i,j}} f_y^{n+\frac{1}{2}}\psi, \quad \int_{K_{i,j}} g^{n+1}\chi
$$

to the right hand sides of (4.88), (4.89) and (4.90), respectively. For the initial values at time $t=0$, we set

$$
E_{xh}(\cdot,0) = \Pi_1 E_x(\cdot,0), \quad E_{yh}(\cdot,0) = \Pi_2 E_y(\cdot,0), \quad H_{zh}(\cdot,0) = \Pi_3 H_z(\cdot,0),
$$

and

$$
J_{xh}(\cdot,0) = \Pi_4 J_x(\cdot,0), \quad J_{yh}(\cdot,0) = \Pi_4 J_y(\cdot,0), \quad K_{zh}(\cdot,0) = \Pi_4 K_z(\cdot,0).
$$

The first step values $H_{zh}^{\frac{1}{2}}, J_{xh}^{\frac{1}{2}}, J_{yh}^{\frac{1}{2}}, K_{zh}^{1}$ are calculated by using the third order Runge-Kutta scheme, see e.g. [18].

## Example 1: Periodic boundary conditions (BCs)

Since the exact solutions are all periodic, we can simply choose the periodic boundary conditions in our DG scheme. To be more precise, we define the unavailable function values periodically by:

$$E_{xh}(x, y^+_{N_y+\frac{1}{2}}) = E_{xh}(x, y^+_{\frac{1}{2}}), \quad E_{yh}(x^+_{N_x+\frac{1}{2}}, y) = E_{yh}(x^+_{\frac{1}{2}}, y), \tag{4.131}$$

$$H_{zh}(x, y^-_{\frac{1}{2}}) = H_{zh}(x, y^-_{N_y+\frac{1}{2}}), \quad H_{zh}(x^-_{\frac{1}{2}}, y) = H_{zh}(x^-_{N_x+\frac{1}{2}}, y). \tag{4.132}$$

in addition to the alternating flux:

$$\hat{E}_{xh}(x, y_{j+\frac{1}{2}}) = E_{xh}(x, y^+_{j+\frac{1}{2}}),\ j = 0 \ldots N_y$$

$$\hat{E}_{yh}(x_{i+\frac{1}{2}}, y) = E_{yh}(x^+_{i+\frac{1}{2}}, y),\ i = 0 \ldots N_x$$

$$\hat{H}_{zh}(x, y_{j+\frac{1}{2}}) = H_{zh}(x, y^-_{j+\frac{1}{2}}),\ j = 0 \ldots N_y$$

$$\hat{H}_{zh}(x_{i+\frac{1}{2}}, y) = H_{zh}(x^-_{i+\frac{1}{2}}, y),\ i = 0 \ldots N_x.$$

The purpose of this example is to convince ourselves that the algorithm is correct, before we proceed to the computation with the practical PEC boundary conditions.

We present the numerical results in Tables 4.1 and 4.2, which are obtained with bilinear (denoted as $Q_1$) and biquadratic (denoted as $Q_2$) basis functions, respectively. We calculate the $L^2$ errors on a series of uniformly refined rectangular meshes with $N$ partitions in both $x$- and $y$-directions, with the time steps ($\Delta t$) shown on the header of each table. Tables 4.1 and 4.2 clearly show that the $L^2$ errors for all variables are $O(h^{k+1})$ for $Q_k, k = 1, 2$, where the mesh size $h = \frac{1}{N}$. We take final time $T = 0.1$ for all our simulations in this section.

Table 4.1: Periodic BCs, $Q_1$ basis function, $T = 0.1$, $\Delta t = 0.2h$

| N | Error of $E_x$ | | Error of $E_y$ | | Error of $H_z$ | |
|---|---|---|---|---|---|---|
| | $L^2$ Error | Order | $L^2$ Error | Order | $L^2$ Error | Order |
| 10 | 8.51e-03 | – | 8.51e-03 | – 10 | 9.57e-03 | – |
| 20 | 2.08e-03 | 2.03 | 2.08e-03 | 2.03 | 2.40e-03 | 1.99 |
| 40 | 5.17e-04 | 2.01 | 5.17e-04 | 2.01 | 6.01e-04 | 2.00 |
| 80 | 1.29e-04 | 2.00 | 1.29e-04 | 2.00 | 1.50e-04 | 2.00 |
| 160 | 3.21e-05 | 2.01 | 3.21e-05 | 2.01 | 3.72e-05 | 2.01 |
| 320 | 7.99e-06 | 2.01 | 7.99e-06 | 2.01 | 9.26e-06 | 2.01 |
| N | Error of $J_x$ | | Error of $J_y$ | | Error of $K_z$ | |
| | $L^2$ Error | Order | $L^2$ Error | Order | $L^2$ Error | Order |
| 10 | 3.56e-02 | – | 3.56e-02 | – | 3.93e-02 | – |
| 20 | 9.10e-03 | 1.97 | 9.10e-03 | 1.97 | 1.02e-02 | 1.94 |
| 40 | 2.30e-03 | 1.98 | 2.30e-03 | 1.98 | 2.60e-03 | 1.97 |
| 80 | 5.79e-04 | 1.99 | 5.79e-04 | 1.99 | 6.57e-04 | 1.99 |
| 160 | 1.45e-04 | 2.00 | 1.45e-04 | 2.00 | 1.65e-04 | 1.99 |
| 320 | 3.64e-05 | 2.00 | 3.64e-05 | 2.00 | 4.14e-05 | 2.00 |

### Example 2: PEC BCs with pure alternating fluxes

To see the important role of those jump terms in the fluxes $\hat{H}_{zh}(x, y_{\frac{1}{2}})$ and $\hat{H}_{zh}(x_{\frac{1}{2}}, y)$ in (4.26) and (4.28), we let $c_0 = 0$ and run the numerical tests. The numerical errors obtained in this case are presented in Tables 4.3–4.6. It seems that the accuracy becomes sub-optimal for odd orders of polynomial degree, but stays optimal for even orders.

### Example 3: PEC BCs with the fluxes used in the proof

Here we solve the same problem as Example 2 using the alternating fluxes modified on the PEC boundaries as defined in (4.21)-(4.28) with $c_0 = \frac{1}{2}$. As expected in Remark 4.1, results obtained in Tables 4.7-4.10 clearly show that the optimal convergence rates are obtained for all variables.

Table 4.2: Periodic BCs, $Q_2$ basis function, $T = 0.1$, $\Delta t = 0.6h^{\frac{3}{2}}$

| N | Error of $E_x$ | | Error of $E_y$ | | Error of $H_z$ | |
|---|---|---|---|---|---|---|
| | $L^2$ Error | Order | $L^2$ Error | Order | $L^2$ Error | Order |
| 10 | 4.27e-04 | – | 4.27e-04 | – | 5.40e-04 | – |
| 20 | 5.40e-05 | 2.98 | 5.40e-05 | 2.98 | 7.66e-05 | 2.82 |
| 40 | 6.87e-06 | 2.98 | 6.87e-06 | 2.98 | 9.79e-06 | 2.97 |
| 80 | 8.54e-07 | 3.01 | 8.54e-07 | 3.01 | 1.23e-06 | 2.99 |
| 160 | 1.08e-07 | 2.99 | 1.08e-07 | 2.99 | 1.56e-07 | 2.98 |
| 320 | 1.35e-08 | 3.00 | 1.35e-08 | 3.00 | 1.95e-08 | 3.00 |
| N | Error of $J_x$ | | Error of $J_y$ | | Error of $K_z$ | |
| | $L^2$ Error | Order | $L^2$ Error | Order | $L^2$ Error | Order |
| 10 | 2.36e-03 | – | 2.36e-03 | – | 2.37e-03 | – |
| 20 | 3.41e-04 | 2.79 | 3.41e-04 | 2.79 | 3.44e-04 | 2.79 |
| 40 | 4.27e-05 | 3.00 | 4.27e-05 | 3.00 | 4.39e-05 | 2.97 |
| 80 | 5.44e-06 | 2.97 | 5.44e-06 | 2.97 | 5.60e-06 | 2.97 |
| 160 | 6.84e-07 | 2.99 | 6.84e-07 | 2.99 | 7.05e-07 | 2.99 |
| 320 | 8.56e-08 | 3.00 | 8.56e-08 | 3.00 | 8.83e-08 | 3.00 |

Table 4.3: Straightforward PEC BCs ($c_0 = 0$), $Q_1$ basis function, $T = 0.1$, $\Delta t = 0.2h$

| N | Error of $E_x$ | | Error of $E_y$ | | Error of $H_z$ | |
|---|---|---|---|---|---|---|
| | $L^2$ Error | Order | $L^2$ Error | Order | $L^2$ Error | Order |
| 10 | 2.02e-02 | – | 2.02e-02 | – | 1.21e-02 | – |
| 20 | 6.69e-03 | 1.60 | 6.69e-03 | 1.60 | 2.80e-03 | 2.12 |
| 40 | 2.30e-03 | 1.54 | 2.30e-03 | 1.54 | 6.70e-04 | 2.06 |
| 80 | 8.01e-04 | 1.52 | 8.01e-04 | 1.52 | 1.58e-04 | 2.08 |
| 160 | 2.81e-04 | 1.51 | 2.81e-04 | 1.51 | 3.83e-05 | 2.05 |
| 320 | 9.91e-05 | 1.50 | 9.91e-05 | 1.50 | 9.40e-06 | 2.03 |
| N | Error of $J_x$ | | Error of $J_y$ | | Error of $K_z$ | |
| | $L^2$ Error | Order | $L^2$ Error | Order | $L^2$ Error | Order |
| 10 | 4.80e-02 | – | 4.80e-02 | – | 3.99e-02 | – |
| 20 | 1.37e-02 | 1.81 | 1.37e-02 | 1.81 | 1.05e-02 | 1.93 |
| 40 | 4.17e-03 | 1.72 | 4.17e-03 | 1.72 | 2.64e-03 | 1.99 |
| 80 | 1.34e-03 | 1.64 | 1.34e-03 | 1.64 | 6.61e-04 | 2.00 |
| 160 | 4.47e-04 | 1.58 | 4.47e-04 | 1.58 | 1.66e-04 | 2.00 |
| 320 | 1.53e-04 | 1.54 | 1.53e-04 | 1.54 | 4.15e-05 | 2.00 |

Table 4.4: Straightforward PEC BCs ($c_0 = 0$), $Q_2$ basis function, $T = 0.1$, $\Delta t = 0.6h^{\frac{3}{2}}$

| N | Error of $E_x$ | | Error of $E_y$ | | Error of $H_z$ | |
|---|---|---|---|---|---|---|
| | $L^2$ Error | Order | $L^2$ Error | Order | $L^2$ Error | Order |
| 10 | 5.42e-04 | – | 5.42e-04 | – | 6.08e-04 | – |
| 20 | 5.94e-05 | 3.19 | 5.94e-05 | 3.19 | 7.72e-05 | 2.98 |
| 40 | 7.17e-06 | 3.05 | 7.17e-06 | 3.05 | 9.80e-06 | 2.98 |
| 80 | 8.75e-07 | 3.03 | 8.75e-07 | 3.03 | 1.23e-06 | 2.99 |
| 160 | 1.09e-07 | 3.01 | 1.09e-07 | 3.01 | 1.56e-07 | 2.98 |
| 320 | 1.35e-08 | 3.01 | 1.35e-08 | 3.01 | 1.95e-08 | 3.00 |
| N | Error of $J_x$ | | Error of $J_y$ | | Error of $K_z$ | |
| | $L^2$ Error | Order | $L^2$ Error | Order | $L^2$ Error | Order |
| 10 | 2.38e-03 | – | 2.38e-03 | – | 2.39e-03 | – |
| 20 | 3.42e-04 | 2.80 | 3.42e-04 | 2.80 | 3.44e-04 | 2.79 |
| 40 | 4.27e-05 | 3.00 | 4.27e-05 | 3.00 | 4.39e-05 | 2.97 |
| 80 | 5.44e-06 | 2.97 | 5.44e-06 | 2.97 | 5.60e-06 | 2.97 |
| 160 | 6.84e-07 | 2.99 | 6.84e-07 | 2.99 | 7.05e-07 | 2.99 |
| 320 | 8.56e-08 | 3.00 | 8.56e-08 | 3.00 | 8.83e-08 | 3.00 |

Table 4.5: Straightforward PEC BCs ($c_0 = 0$), $Q_3$ basis function, $T = 0.1$, $\Delta t = 0.6h^2$

| N | Error of $E_x$ | | Error of $E_y$ | | Error of $H_z$ | |
|---|---|---|---|---|---|---|
| | $L^2$ Error | Order | $L^2$ Error | Order | $L^2$ Error | Order |
| 10 | 7.81e-05 | - | 7.81e-05 | - | 4.18e-05 | - |
| 20 | 7.02e-06 | 3.48 | 7.02e-06 | 3.48 | 2.84e-06 | 3.88 |
| 40 | 6.10e-07 | 3.52 | 6.10e-07 | 3.52 | 1.73e-07 | 4.04 |
| 80 | 5.40e-08 | 3.50 | 5.40e-08 | 3.50 | 1.09e-08 | 3.99 |
| 160 | 4.75e-09 | 3.51 | 4.75e-09 | 3.51 | 6.76e-10 | 4.02 |
| N | Error of $J_x$ | | Error of $J_y$ | | Error of $K_z$ | |
| | $L^2$ Error | Order | $L^2$ Error | Order | $L^2$ Error | Order |
| 10 | 2.35e-04 | - | 2.35e-04 | - | 1.90e-04 | - |
| 20 | 1.68e-05 | 3.80 | 1.68e-05 | 3.80 | 1.26e-05 | 3.91 |
| 40 | 1.24e-06 | 3.76 | 1.24e-06 | 3.76 | 8.02e-07 | 3.98 |
| 80 | 9.62e-08 | 3.69 | 9.62e-08 | 3.69 | 5.03e-08 | 3.99 |
| 160 | 7.84e-09 | 3.62 | 7.84e-09 | 3.62 | 3.15e-09 | 4.00 |

Table 4.6: Straightforward PEC BCs ($c_0 = 0$), $Q_4$ basis function, $T = 0.1$, $\Delta t = 0.8h^{\frac{5}{2}}$

| N | Error of $E_x$ | | Error of $E_y$ | | Error of $H_z$ | |
|---|---|---|---|---|---|---|
| | $L^2$ Error | Order | $L^2$ Error | Order | $L^2$ Error | Order |
| 10 | 3.20e-06 | - | 3.20e-06 | - | 7.08e-06 | - |
| 20 | 1.00e-07 | 4.99 | 1.00e-07 | 4.99 | 2.28e-07 | 4.96 |
| 40 | 3.12e-09 | 5.01 | 3.12e-09 | 5.01 | 7.15e-09 | 4.99 |
| 80 | 9.71e-11 | 5.01 | 9.71e-11 | 5.01 | 2.24e-10 | 5.00 |
| N | Error of $J_x$ | | Error of $J_y$ | | Error of $K_z$ | |
| | $L^2$ Error | Order | $L^2$ Error | Order | $L^2$ Error | Order |
| 10 | 3.52e-05 | - | 3.52e-05 | - | 3.09e-05 | - |
| 20 | 1.13e-06 | 4.96 | 1.13e-06 | 4.96 | 1.00e-06 | 4.94 |
| 40 | 3.55e-08 | 4.99 | 3.55e-08 | 4.99 | 3.16e-08 | 4.99 |
| 80 | 1.11e-09 | 5.00 | 1.11e-09 | 5.00 | 9.87e-10 | 5.00 |

Table 4.7: Modified PEC BCs ($c_0 = \frac{1}{2}$), $Q_1$ basis function, $T = 0.1$, $\Delta t = 0.2h$

| N | Error of $E_x$ | | Error of $E_y$ | | Error of $H_z$ | |
|---|---|---|---|---|---|---|
| | $L^2$ Error | Order | $L^2$ Error | Order | $L^2$ Error | Order |
| 10 | 1.19e-02 | – | 1.19e-02 | – | 1.01e-02 | – |
| 20 | 2.81e-03 | 2.08 | 2.81e-03 | 2.08 | 2.54e-03 | 1.99 |
| 40 | 6.08e-04 | 2.21 | 6.08e-04 | 2.21 | 6.16e-04 | 2.04 |
| 80 | 1.40e-04 | 2.12 | 1.40e-04 | 2.12 | 1.52e-04 | 2.02 |
| 160 | 3.35e-05 | 2.06 | 3.35e-05 | 2.06 | 3.74e-05 | 2.02 |
| 320 | 8.16e-06 | 2.04 | 8.16e-06 | 2.04 | 9.29e-06 | 2.01 |
| N | Error of $J_x$ | | Error of $J_y$ | | Error of $K_z$ | |
| | $L^2$ Error | Order | $L^2$ Error | Order | $L^2$ Error | Order |
| 10 | 3.98e-02 | – | 3.98e-02 | – | 3.92e-02 | – |
| 20 | 9.93e-03 | 2.00 | 9.93e-03 | 2.00 | 1.02e-02 | 1.94 |
| 40 | 2.44e-03 | 2.03 | 2.44e-03 | 2.03 | 2.60e-03 | 1.97 |
| 80 | 5.97e-04 | 2.03 | 5.97e-04 | 2.03 | 6.57e-04 | 1.98 |
| 160 | 1.48e-04 | 2.02 | 1.48e-04 | 2.02 | 1.65e-04 | 1.99 |
| 320 | 3.67e-05 | 2.01 | 3.67e-05 | 2.01 | 4.14e-05 | 2.00 |

Table 4.8: Modified PEC BCs ($c_0 = \frac{1}{2}$), $Q_2$ basis function, $T = 0.1$, $\Delta t = 0.6h^{\frac{3}{2}}$

| N | Error of $E_x$ | | Error of $E_y$ | | Error of $H_z$ | |
|---|---|---|---|---|---|---|
| | $L^2$ Error | Order | $L^2$ Error | Order | $L^2$ Error | Order |
| 10 | 4.54e-04 | – | 4.54e-04 | – | 5.89e-04 | – |
| 20 | 5.36e-05 | 3.08 | 5.36e-05 | 3.08 | 7.68e-05 | 2.94 |
| 40 | 6.84e-06 | 2.97 | 6.84e-06 | 2.97 | 9.79e-06 | 2.97 |
| 80 | 8.54e-07 | 3.00 | 8.54e-07 | 3.00 | 1.23e-06 | 2.99 |
| 160 | 1.08e-07 | 2.99 | 1.08e-07 | 2.99 | 1.56e-07 | 2.98 |
| 320 | 1.35e-08 | 3.00 | 1.35e-08 | 3.00 | 1.95e-08 | 3.00 |
| N | Error of $J_x$ | | Error of $J_y$ | | Error of $K_z$ | |
| | $L^2$ Error | Order | $L^2$ Error | Order | $L^2$ Error | Order |
| 10 | 2.35e-03 | – | 2.35e-03 | – | 2.38e-03 | – |
| 20 | 3.41e-04 | 2.79 | 3.41e-04 | 2.79 | 3.44e-04 | 2.79 |
| 40 | 4.27e-05 | 3.00 | 4.27e-05 | 3.00 | 4.39e-05 | 2.97 |
| 80 | 5.44e-06 | 2.97 | 5.44e-06 | 2.97 | 5.60e-06 | 2.97 |
| 160 | 6.84e-07 | 2.99 | 6.84e-07 | 2.99 | 7.05e-07 | 2.99 |
| 320 | 8.56e-08 | 3.00 | 8.56e-08 | 3.00 | 8.83e-08 | 3.00 |

Table 4.9: Modified PEC BCs ($c_0 = \frac{1}{2}$), $Q_3$ basis function, $T = 0.1$, $\Delta t = 0.6h^2$

| N | Error of $E_x$ | | Error of $E_y$ | | Error of $H_z$ | |
|---|---|---|---|---|---|---|
| | $L^2$ Error | Order | $L^2$ Error | Order | $L^2$ Error | Order |
| 10 | 3.00e-05 | - | 3.00e-05 | - | 4.21e-05 | - |
| 20 | 1.70e-06 | 4.14 | 1.70e-06 | 4.14 | 2.73e-06 | 3.95 |
| 40 | 1.00e-07 | 4.09 | 1.00e-07 | 4.09 | 1.72e-07 | 3.99 |
| 80 | 6.07e-09 | 4.04 | 6.07e-09 | 4.04 | 1.08e-08 | 3.99 |
| 160 | 3.74e-10 | 4.02 | 3.74e-10 | 4.02 | 6.75e-10 | 4.00 |
| N | Error of $J_x$ | | Error of $J_y$ | | Error of $K_z$ | |
| | $L^2$ Error | Order | $L^2$ Error | Order | $L^2$ Error | Order |
| 10 | 2.08e-04 | - | 2.08e-04 | - | 1.90e-04 | - |
| 20 | 1.35e-05 | 3.95 | 1.35e-05 | 3.95 | 1.26e-05 | 3.91 |
| 40 | 8.46e-07 | 3.99 | 8.46e-07 | 3.99 | 8.03e-07 | 3.98 |
| 80 | 5.29e-08 | 4.00 | 5.29e-08 | 4.00 | 5.04e-08 | 3.99 |
| 160 | 3.30e-09 | 4.00 | 3.30e-09 | 4.00 | 3.15e-09 | 4.00 |

Table 4.10: Modified PEC BCs ($c_0 = \frac{1}{2}$), $Q_4$ basis function, $T = 0.1$, $\Delta t = 0.8h^{\frac{5}{2}}$

| N | Error of $E_x$ | | Error of $E_y$ | | Error of $H_z$ | |
|---|---|---|---|---|---|---|
| | $L^2$ Error | Order | $L^2$ Error | Order | $L^2$ Error | Order |
| 10 | 3.11e-06 | - | 3.11e-06 | - | 7.08e-06 | - |
| 20 | 9.89e-08 | 4.98 | 9.89e-08 | 4.98 | 2.28e-07 | 4.96 |
| 40 | 3.10e-09 | 5.00 | 3.10e-09 | 5.00 | 7.15e-09 | 4.99 |
| 80 | 9.68e-11 | 5.00 | 9.68e-11 | 5.00 | 2.24e-10 | 5.00 |
| N | Error of $J_x$ | | Error of $J_y$ | | Error of $K_z$ | |
| | $L^2$ Error | Order | $L^2$ Error | Order | $L^2$ Error | Order |
| 10 | 3.52e-05 | - | 3.52e-05 | - | 3.09e-05 | - |
| 20 | 1.13e-06 | 4.96 | 1.13e-06 | 4.96 | 1.00e-06 | 4.94 |
| 40 | 3.55e-08 | 4.99 | 3.55e-08 | 4.99 | 3.16e-08 | 4.99 |
| 80 | 1.11e-09 | 5.00 | 1.11e-09 | 5.00 | 9.87e-10 | 5.00 |

# Chapter Five

# Discontinuous Galerkin Methods for Maxwell's Equations in Drude Metamaterials on Triangular Meshes

## 5.1 The governing equations

We consider the same model equations (4.7)-(4.12) on a rectangular type physical domain $\Omega = [a,b]\times[c,d]$, with the same initial conditions (4.6) and boundary conditions (4.14) as in the previous chapter.

The physical domain is discretized by a triangular mesh, $\Omega = \cup_{e\in\mathcal{T}_h} e$ as opposed to the rectangular meshes in the previous chapter. $\mathcal{T}_h$ represents a triangulation on $\Omega$ with mesh size $h$ defined as the largest diameter of all triangles. The time domain $[0,T]$ is discretized into $N_t+1$ uniform intervals by discrete times $0 = t_0 < t_1 < \cdots < t_{N_t+1} = T$, where $t_n = n\cdot\tau$, and the time step size $\tau = \frac{T}{N_t+1}$.

The finite element space $V_h^k$ is chosen as piecewise polynomials of degree at most $k$ on every element $e$, i.e.,

$$V_h^k = \{v : \; v|_e \in P_k(e), \quad \forall\, e \in \mathcal{T}_h\}, \tag{5.1}$$

where $P_k$ is the space of polynomial of degree up to $k$. To get the error estimate, we need some regularity conditions on the triangulation similar to those in chapter 3 of [10]:

1 There exists a constant $\theta_0 \geq 0$, such that all angles in the triangles are larger than $\theta_0$.

2 There exists a constant C, such that: ($h_e$ denotes the diameter of triangle $e$)

$$\max_{e\in\mathcal{T}_h} h_e < C \min_{e\in\mathcal{T}_h} h_e$$

For the corresponding variable $u$ we denote its numerical solution $u_h$, which belongs to the finite element space $V_h^k$. Note that functions in $V_h^k$ are allowed to have discontinuities across element interfaces. In the line integral over the boundary of a cell, we denote $u_h^{(in)}$ as the value of $u_h$ taken from inside of that cell, and $u_h^{(out)}$ from the neighboring cell sharing that boundary. We denote by $||\cdot||$ the $L^2$ norm over the domain $\Omega$.

## 5.2 The semi-discrete DG method

The semi-discrete DG method for (4.7)-(4.12) can be formulated as follows: Find

$$E_{xh}, E_{yh}, H_{zh}, J_{xh}, J_{yh}, K_{zh} \in C^1([0,T]; V_h^k)$$

such that

$$\epsilon_0 \int_e \frac{\partial E_{xh}}{\partial t}\phi_x + \int_e H_{zh}\frac{\partial \phi_x}{\partial y} - \int_{\partial e} \hat{H}_{zh}\phi_x^{(in)} n_y^{(in)} + \int_e J_{xh}\phi_x = 0, \tag{5.2}$$

$$\epsilon_0 \int_e \frac{\partial E_{yh}}{\partial t}\phi_y - \int_e H_{zh}\frac{\partial \phi_y}{\partial x} + \int_{\partial e} \hat{H}_{zh}\phi_y^{(in)} n_x^{(in)} + \int_e J_{yh}\phi_y = 0, \tag{5.3}$$

$$\mu_0 \int_e \frac{\partial H_{zh}}{\partial t}\psi - \int_e E_{yh}\frac{\partial \psi}{\partial x} + \int_e E_{xh}\frac{\partial \psi}{\partial y} + \int_{\partial e} (\hat{E}_{yh} n_x^{(in)} - \hat{E}_{xh} n_y^{(in)})\psi^{(in)} + \int_e K_{zh}\psi = 0, \tag{5.4}$$

$$\frac{1}{\epsilon_0\omega_{pe}^2}\int_e \frac{\partial J_{xh}}{\partial t}u_1 + \frac{\Gamma_e}{\epsilon_0\omega_{pe}^2}\int_e J_{xh}u_1 - \int_e E_{xh}u_1 = 0, \tag{5.5}$$

$$\frac{1}{\epsilon_0\omega_{pe}^2}\int_e \frac{\partial J_{yh}}{\partial t}u_2 + \frac{\Gamma_e}{\epsilon_0\omega_{pe}^2}\int_e J_{yh}u_2 - \int_e E_{yh}u_2 = 0, \tag{5.6}$$

$$\frac{1}{\mu_0\omega_{pm}^2}\int_e \frac{\partial K_{zh}}{\partial t}v + \frac{\Gamma_m}{\mu_0\omega_{pm}^2}\int_e K_{zh}v - \int_e H_{zh}v = 0, \tag{5.7}$$

for all test functions $\phi_x, \phi_y, \psi, u_1, u_2, v \in V_h^k$ and all triangle cells $e \in \mathcal{T}_h$. $\hat{H}_{zh}, \hat{E}_{yh}, \hat{E}_{xh}$ are the cell boundary terms obtained from integration by parts, and they are the so-called numerical fluxes.

We choose the alternating flux as in the previous chapter. To define alternating flux in a triangulation, we need to first choose a fix direction $\boldsymbol{\beta}$ that is not parallel with any triangle boundary edge. On each edge, we can define the "right" and "left" side with respect to $\boldsymbol{\beta}$. On each side there is an outward normal direction, $\boldsymbol{n}$, orthogonal to the edge. We define a side is the "right" side if $\boldsymbol{n} \cdot \boldsymbol{\beta} < 0$. The alternating flux is defined as always choosing $E_{xh}$ and $E_{yh}$ on the "right" side and $H_{zh}$ on the "left" side:

$$\hat{E}_{xh} = E_{xh}^{R}, \tag{5.8}$$

$$\hat{E}_{yh} = E_{yh}^{R}, \tag{5.9}$$

$$\hat{H}_{zh} = H_{zh}^{L}. \tag{5.10}$$

A more detailed explanation of alternating flux for triangulation can be found in [50]. It is easy to check that the definition of the alternating flux on the rectangular meshes (4.21)-(4.28) is a special case of the one here with $\boldsymbol{\beta} = (1, 1)$. If we adopt a periodic boundary condition, the above definition of alternating flux is enough. However, to satisfy the PEC boundary condition in (4.14), we take

$$\hat{E}_{xh} = 0, \text{ on } y = c, d, \tag{5.11}$$

$$\hat{E}_{yh} = 0, \text{ on } x = a, b, \tag{5.12}$$

$$\hat{H}_{zh} = H_{zh}^{(in)}, \text{ on } \partial\Omega. \tag{5.13}$$

### 5.2.1 The stability analysis

In this section, we show the stability of our scheme on triangular meshes, which is similar to that on rectangular meshes in Section 4.3.1.

**Theorem 5.2.1.** *The semi-discrete DG method (5.2)-(5.7) with alternating fluxes (5.8)-(5.13) satisfies the following energy identity: For any* $t \geq 0$*:*

$$\begin{aligned}
&\left[\epsilon_0(||E_{xh}||^2 + ||E_{yh}||^2) + \mu_0||H_{zh}||^2 + \frac{1}{\epsilon_0\omega_{pe}^2}(||J_{xh}||^2 + ||J_{yh}||^2) + \frac{1}{\mu_0\omega_{pm}^2}||K_{zh}||^2\right](t) \\
&+ \int_0^t \left[\frac{2\Gamma_e}{\epsilon_0\omega_{pe}^2}(||J_{xh}||^2 + ||J_{yh}||^2) + \frac{2\Gamma_m}{\mu_0\omega_{pm}^2}||K_{zh}||^2\right](s)ds \\
&= \left[\epsilon_0(||E_{xh}||^2 + ||E_{yh}||^2) + \mu_0||H_{zh}||^2 + \frac{1}{\epsilon_0\omega_{pe}^2}(||J_{xh}||^2 + ||J_{yh}||^2) + \frac{1}{\mu_0\omega_{pm}^2}||K_{zh}||^2\right](0).
\end{aligned} \tag{5.14}$$

*Proof.* Taking $\phi_x = E_{xh}, \phi_y = E_{yh}, \psi = H_{zh}, u_1 = J_{xh}, u_2 = J_{yh}, v = K_{zh}$ in (5.2)-(5.7), respectively, adding the resultants together over all cells, we have

$$\begin{aligned}
&\frac{1}{2}\frac{d}{dt}\int_\Omega \left[\epsilon_0(|E_{xh}|^2 + |E_{yh}|^2) + \mu_0|H_{zh}|^2 + \frac{1}{\epsilon_0\omega_{pe}^2}(|J_{xh}|^2 + |J_{yh}|^2) + \frac{1}{\mu_0\omega_{pm}^2}|K_{zh}|^2\right] \\
&+ \int_\Omega \left[\frac{\Gamma_e}{\epsilon_0\omega_{pe}^2}(|J_{xh}|^2 + |J_{yh}|^2) + \frac{\Gamma_m}{\mu_0\omega_{pm}^2}|K_{zh}|^2\right] \\
&+ \sum_{e\in\mathcal{T}_h}\int_{\partial e}\left(-\hat{H}_{zh}E_{xh}^{(in)}n_y^{(in)} + \hat{H}_{zh}E_{yh}^{(in)}n_x^{(in)} + H_{zh}^{(in)}\hat{E}_{yh}n_x^{(in)} - H_{zh}^{(in)}\hat{E}_{xh}n_y^{(in)}\right) \\
&+ \sum_{e\in\mathcal{T}_h}\int_e\left(H_{zh}\frac{\partial E_{xh}}{\partial y} - H_{zh}\frac{\partial E_{yh}}{\partial x} - E_{yh}\frac{\partial H_{zh}}{\partial x} + E_{xh}\frac{\partial H_{zh}}{\partial y}\right) = 0.
\end{aligned} \tag{5.15}$$

Using integration by parts, the terms in the last two lines of (5.15) become $F_x - F_y$, where

$$F_x = \sum_{e\in\mathcal{T}_h}\int_{\partial e}\left(H_{zh}^{(in)}E_{xh}^{(in)}n_y^{(in)} - \hat{H}_{zh}E_{xh}^{(in)}n_y^{(in)} - H_{zh}^{(in)}\hat{E}_{xh}n_y^{(in)}\right), \tag{5.16}$$

$$F_y = \sum_{e\in\mathcal{T}_h}\int_{\partial e}\left(H_{zh}^{(in)}E_{yh}^{(in)}n_x^{(in)} - \hat{H}_{zh}E_{yh}^{(in)}n_x^{(in)} - H_{zh}^{(in)}\hat{E}_{yh}n_x^{(in)}\right). \tag{5.17}$$

By grouping terms by sides of triangles instead of triangles, we have:

$$\begin{aligned} F_x = &\sum_{s\in\mathcal{S}_I} n_y^R \int_s \left(H_{zh}^R E_{xh}^R - H_{zh}^L E_{xh}^L - H_{zh}^L E_{xh}^R + H_{zh}^L E_{xh}^L - H_{zh}^R E_{xh}^R + H_{zh}^L E_{xh}^R\right) \\ &+ \sum_{s\in\mathcal{S}_L} n_y^R \int_s \left(H_{zh}^R E_{xh}^R - H_{zh}^R E_{xh}^R\right) + \sum_{s\in\mathcal{S}_R} n_y^L \int_s \left(H_{zh}^L E_{xh}^L - H_{zh}^L E_{xh}^L\right) = 0, \end{aligned} \tag{5.18}$$

where $\mathcal{S}_I$ denotes the set of all non-boundary sides, $\mathcal{S}_L$ represents the set of sides on $x = a$, and $\mathcal{S}_R$ on $x = b$. We can similarly deduce $F_y = 0$. We conclude the proof by integrate (5.15) over $[0, t]$. □

### 5.2.2 The error analysis

We denote the errors between the exact solutions $(E_x, E_y, H_z, J_x, J_y, K_z)$ of (4.7)-(4.12) and the corresponding numerical solutions $(E_{xh}, E_{yh}, H_{zh}, J_{xh}, J_{yh}, K_{zh})$ of the semi-discrete scheme (5.2)-(5.7) by

$$\mathcal{E}_x = E_x - E_{xh}, \mathcal{E}_y = E_y - E_{yh}, \mathcal{H}_z = H_z - H_{zh}, \mathcal{J}_x = J_x - J_{xh}, \mathcal{J}_y = J_y - J_{yh}, \mathcal{K}_z = K_z - K_{zh}. \tag{5.19}$$

Subtracting (5.2)-(5.7) from the weak formulation of (4.7)-(4.12) and assuming that the exact solutions are continuous in the domain $\Omega$, we can obtain the error equations:

$$\epsilon_0 \int_e \frac{\partial \mathcal{E}_x}{\partial t}\phi_x + \int_e \mathcal{H}_z \frac{\partial \phi_x}{\partial y} - \int_{\partial e} \hat{\mathcal{H}}_z \phi_x^{(in)} n_y^{(in)} + \int_e \mathcal{J}_x \phi_x = 0, \tag{5.20}$$

$$\epsilon_0 \int_e \frac{\partial \mathcal{E}_y}{\partial t}\phi_y - \int_e \mathcal{H}_z \frac{\partial \phi_y}{\partial x} + \int_{\partial e} \hat{\mathcal{H}}_z \phi_y^{(in)} n_x^{(in)} + \int_e \mathcal{J}_y \phi_y = 0, \tag{5.21}$$

$$\mu_0 \int_e \frac{\partial \mathcal{H}_z}{\partial t}\psi - \int_e \mathcal{E}_y \frac{\partial \psi}{\partial x} + \int_e \mathcal{E}_x \frac{\partial \psi}{\partial y} + \int_{\partial e} (\hat{\mathcal{E}}_y n_x^{(in)} - \hat{\mathcal{E}}_x n_y^{(in)})\psi^{(in)} + \int_e \mathcal{K}_z \psi = 0, \tag{5.22}$$

$$\frac{1}{\epsilon_0 \omega_{pe}^2} \int_e \frac{\partial \mathcal{J}_x}{\partial t} u_1 + \frac{\Gamma_e}{\epsilon_0 \omega_{pe}^2} \int_e \mathcal{J}_x u_1 - \int_e \mathcal{E}_x u_1 = 0, \tag{5.23}$$

$$\frac{1}{\epsilon_0\omega_{pe}^2}\int_e \frac{\partial \mathcal{J}_y}{\partial t}u_2 + \frac{\Gamma_e}{\epsilon_0\omega_{pe}^2}\int_e \mathcal{J}_y u_2 - \int_e \mathcal{E}_y u_2 = 0, \tag{5.24}$$

$$\frac{1}{\mu_0\omega_{pm}^2}\int_e \frac{\partial \mathcal{K}_z}{\partial t}v + \frac{\Gamma_m}{\mu_0\omega_{pm}^2}\int_e \mathcal{K}_z v - \int_e \mathcal{H}_z v = 0. \tag{5.25}$$

**Theorem 5.2.2.** *Let $(E_x, E_y, H_z, J_x, J_y, K_z)$ and $(E_{xh}, E_{yh}, H_{zh}, J_{xh}, J_{yh}, K_{zh})$ be the solutions of (4.7)-(4.12) and (5.2)-(5.7), respectively. The following error estimate holds true:*

$$\begin{aligned}
& \max_{0\le t\le T}\Big[\epsilon_0(||E_x - E_{xh}||^2 + ||E_y - E_{yh}||^2) + \mu_0||H_z - H_{zh}||^2 \\
& + \frac{1}{\epsilon_0\omega_{pe}^2}(||J_x - J_{xh}||^2 + ||J_y - J_{yh}||^2) + \frac{1}{\mu_0\omega_{pm}^2}||K_z - K_{zh}||^2\Big](t) \\
\le\ & CTh^{2k} + C\left(\epsilon_0(||E_x - E_{xh}||^2 + ||E_y - E_{yh}||^2) + \mu_0||H_z - H_{zh}||^2\right)(0) \\
& + C\left(\frac{1}{\epsilon_0\omega_{pe}^2}(||J_x - J_{xh}||^2 + ||J_y - J_{yh}||^2) + \frac{1}{\mu_0\omega_{pm}^2}||K_z - K_{zh}||^2\right)(0),
\end{aligned}$$

*where the constant $C > 0$ is independent of $h$, and $k \ge 1$ is the order of the basis function in $V_h^k$.*

*Proof.* Using the defined projections, we can decompose the errors given in (5.19) as follows:

$$\begin{aligned}
\mathcal{E}_x &= E_x - E_{xh} = (\Pi E_x - E_{xh}) - (\Pi E_x - E_x) := E_{x\xi} - E_{x\eta}, \\
\mathcal{E}_y &= E_y - E_{yh} = (\Pi E_y - E_{yh}) - (\Pi E_y - E_y) := E_{y\xi} - E_{y\eta}, \\
\mathcal{H}_z &= H_z - H_{zh} = (\Pi H_z - H_{zh}) - (\Pi H_z - H_z) := H_{z\xi} - H_{z\eta}, \\
\mathcal{J}_x &= J_x - J_{xh} = (\Pi J_x - J_{xh}) - (\Pi J_x - J_x) := J_{x\xi} - J_{x\eta}, \\
\mathcal{J}_y &= J_y - J_{yh} = (\Pi J_y - J_{yh}) - (\Pi J_y - J_y) := J_{y\xi} - J_{y\eta}, \\
\mathcal{K}_z &= K_z - K_{zh} = (\Pi K_z - K_{zh}) - (\Pi K_z - K_z) := K_{z\xi} - K_{z\eta}
\end{aligned}$$

where $\Pi$ is the usual $L^2$ projection onto $V_h^k$.

We denote the summation of (5.20) − (5.25) as:

$$B(\mathcal{E}_x, \mathcal{E}_y, \mathcal{H}_z, \mathcal{J}_x, \mathcal{J}_y, \mathcal{K}_z; \phi, \psi, \chi, u_1, u_2, v) = 0. \tag{5.26}$$

Substituting the error decomposition into (5.26), and choosing the test functions $\phi_x = E_{x\xi}, \phi_y = E_{y\xi}, \psi = H_{z\xi},\ u_1 = J_{x\xi}, u_2 = J_{y\xi}, v = K_{z\xi}$, we obtain:

$$\begin{aligned} &B(E_{x\xi}, E_{y\xi}, H_{z\xi}, J_{x\xi}, J_{y\xi}, K_{z\xi}; E_{x\xi}, E_{y\xi}, H_{z\xi}, J_{x\xi}, J_{y\xi}, K_{z\xi}) \\ =&B(E_{x\eta}, E_{y\eta}, H_{z\eta}, J_{x\eta}, J_{y\eta}, K_{z\eta}; E_{x\xi}, E_{y\xi}, H_{z\xi}, J_{x\xi}, J_{y\xi}, K_{z\xi}). \end{aligned} \tag{5.27}$$

If we sum (5.27) over all triangles and look at the left hand side (LHS), we could observe that it is exactly the same thing as in the stability proof. Hence we have:

$$\begin{aligned} \text{LHS} =&\frac{1}{2}\frac{d}{dt}\left(\epsilon_0(||E_{x\xi}||^2 + ||E_{y\xi}||^2) + \mu_0||H_{z\xi}||^2 + \frac{1}{\epsilon_0\omega_{pe}^2}(||J_{x\xi}||^2 + ||J_{y\xi}||^2) + \frac{1}{\mu_0\omega_{pm}^2}||K_{z\xi}||^2\right) \\ &+ \frac{2\Gamma_e}{\epsilon_0\omega_{pe}^2}(||J_{x\xi}||^2 + ||J_{y\xi}||^2) + \frac{2\Gamma_m}{\mu_0\omega_{pm}^2}||K_{z\xi}||^2. \end{aligned} \tag{5.28}$$

Now consider the terms on the right hand side (RHS). By the property of the projection $\Pi u_t = (\Pi u)_t$, and the fact that $E_{x\xi}, E_{y\xi}, H_{z\xi}, J_{x\xi}, J_{y\xi}, K_{z\xi}|_e \in P_k(e)$, we can have

$$\text{RHS} = \sum_{e\in\mathcal{T}_h} \int_{\partial e} \left( -\hat{H}_{z\eta} E_{x\xi}^{(in)} n_y^{(in)} + \hat{H}_{z\eta} E_{y\xi}^{(in)} n_x^{(in)} + \hat{E}_{y\eta} H_{z\xi}^{(in)} n_x^{(in)} - \hat{E}_{x\eta} H_{z\xi}^{(in)} n_y^{(in)} \right). \tag{5.29}$$

Let us focus on the first term:

$$\begin{aligned} \sum_{e\in\mathcal{T}_h} \int_{\partial e} \hat{H}_{z\eta} E_{x\xi}^{(in)} n_y^{(in)} \leq & \sum_{e\in\mathcal{T}_h} \frac{1}{\delta h} \int_{\partial e} \left| \hat{H}_{z\eta} \right|^2 + \delta h \int_{\partial e} \left| E_{x\xi}^{(in)} \right|^2 \\ \leq & C \sum_{e\in\mathcal{T}_h} \left( \frac{1}{\delta} \|H_{z\eta}\|_{L^\infty(e)}^2 + \delta h^2 \|E_{x\xi}\|_{L^\infty(e)}^2 \right) \\ \leq & \frac{C}{\delta}\, h^{2k} \|H_z\|_{H^{k+1}(\Omega)}^2 + C\delta\, \|E_{x\xi}\|_{L^2(\Omega)}^2, \end{aligned} \tag{5.30}$$

where the estimation of the first term is due to the approximating property of polynomial preserving operators (see Theorem 3.1.4 in [10]), and that of the second term can be justified by the standard inverse inequality [10]. Note that the constants are not necessarily the same, but are all written as $C$ for brevity. The constants are all of course independent of the mesh sizes.

Treating the remaining terms in (5.29) similarly, we can get the following inequality:

$$\begin{aligned} & \frac{1}{2}\frac{d}{dt} \left( \epsilon_0 (||E_{x\xi}||^2 + ||E_{y\xi}||^2) + \mu_0 ||H_{z\xi}||^2 + \frac{1}{\epsilon_0 \omega_{pe}^2} (||J_{x\xi}||^2 + ||J_{y\xi}||^2) + \frac{1}{\mu_0 \omega_{pm}^2} ||K_{z\xi}||^2 \right) \\ \leq & \frac{C}{\delta}\, h^{2k} \left( \|E_x\|_{H^{k+1}(\Omega)}^2 + \|E_y\|_{H^{k+1}(\Omega)}^2 + \|H_z\|_{H^{k+1}(\Omega)}^2 \right) + C\delta \left( \|E_{x\xi}\|^2 + \|E_{y\xi}\|^2 + \|H_{z\xi}\|^2 \right). \end{aligned} \tag{5.31}$$

Integrating (5.31) from $t = 0$ to any $t \leq T$, we have

$$
\begin{aligned}
&\left(\epsilon_0(||E_{x\xi}||^2 + ||E_{y\xi}||^2) + \mu_0||H_{z\xi}||^2 + \frac{1}{\epsilon_0\omega_{pe}^2}(||J_{x\xi}||^2 + ||J_{y\xi}||^2) + \frac{1}{\mu_0\omega_{pm}^2}||K_{z\xi}||^2\right)(t) \\
&- \left(\epsilon_0(||E_{x\xi}||^2 + ||E_{y\xi}||^2) + \mu_0||H_{z\xi}||^2 + \frac{1}{\epsilon_0\omega_{pe}^2}(||J_{x\xi}||^2 + ||J_{y\xi}||^2) + \frac{1}{\mu_0\omega_{pm}^2}||K_{z\xi}||^2\right)(0) \\
\leq &\frac{C}{\delta}\, h^{2k} \int_0^t \left(\|E_x\|^2_{H^{k+1}(\Omega)} + \|E_y\|^2_{H^{k+1}(\Omega)} + \|H_z\|^2_{H^{k+1}(\Omega)}\right)(s)\, ds \\
&+ CT\delta \max_{0\leq t\leq T}\left(\|E_{x\xi}\|^2 + \|E_{y\xi}\|^2 + \|H_{z\xi}\|^2\right)(t).
\end{aligned}
\tag{5.32}
$$

Taking maximum of (5.32) with respect to time $t$, choosing $\delta = o(\frac{1}{T})$ small enough so that the last term on the right hand side can be controlled by the LHS, and using the triangle inequality and the error estimate of $L^2$ projections, we conclude the proof. $\square$

**Remark 5.2.1.** *The sub-optimal $k$-th order convergence rate in Theorem 5.2.2 is confirmed by the numerical results given in Table 5.1 below. We showed in Theorem 4.3.2 that DG schemes with alternating flux and solution space $Q_k$ in rectangular meshes have optimal $(k+1)$-th order rate convergence. Note that $Q_k = \left\{x^i y^j,\ i,j \in [0,k]\right\}$ and $P_k = \left\{x^i y^j,\ i+j \in [0,k]\right\}$ and $Q_k$ has almost twice as many degrees of freedom as $P_k$ for large $k$. We implemented DG schemes with alternating flux and solution space $P_k$ in rectangular meshes and they show suboptimal convergence rate too. The proof of optimal convergence rate in Theorem 4.3.2 heavily relies on the structure of $Q_k$ and our numerical results show that it is indeed critical for optimality.*

## 5.3 The fully-discrete DG method

We consider the following leap-frog LDG scheme: For any $n \geq 0$, find

$$E_{xh}^{n+1}, E_{yh}^{n+1}, H_{zh}^{n+\frac{3}{2}}, J_{xh}^{n+\frac{3}{2}}, J_{yh}^{n+\frac{3}{2}}, K_{zh}^{n+2} \in V_h^k$$

such that

$$\epsilon_0 \int_e \frac{E_{xh}^{n+1} - E_{xh}^n}{\tau}\phi_x - \int_{\partial e} \hat{H}_{zh}^{n+\frac{1}{2}} \phi_x^{(in)} n_y^{(in)} + \int_e H_{zh}^{n+\frac{1}{2}} \frac{\partial \phi_x}{\partial y} + \int_e J_{xh}^{n+\frac{1}{2}} \phi_x = 0, \tag{5.33}$$

$$\epsilon_0 \int_e \frac{E_{yh}^{n+1} - E_{yh}^n}{\tau}\phi_y + \int_{\partial e} \hat{H}_{zh}^{n+\frac{1}{2}} \phi_y^{(in)} n_x^{(in)} - \int_e H_{zh}^{n+\frac{1}{2}} \frac{\partial \phi_y}{\partial x} + \int_e J_{yh}^{n+\frac{1}{2}} \phi_y = 0, \tag{5.34}$$

$$\begin{aligned} &\mu_0 \int_e \frac{H_{zh}^{n+\frac{3}{2}} - H_{zh}^{n+\frac{1}{2}}}{\tau}\psi + \int_{\partial} \hat{E}_{yh}^{n+1} \psi^{(in)} n_x^{(in)} - \int_e E_{yh}^{n+1} \frac{\partial \psi}{\partial x} \\ &\quad - \int_{I_i} \hat{E}_{xh}^{n+1} \psi^{(in)} n_y^{(in)} + \int_e E_{xh}^{n+1} \frac{\partial \psi}{\partial y} + \int_e K_{zh}^{n+1}\psi = 0, \end{aligned} \tag{5.35}$$

$$\frac{1}{\epsilon_0 \omega_{pe}^2} \int_e \frac{J_{xh}^{n+\frac{3}{2}} - J_{xh}^{n+\frac{1}{2}}}{\tau} u_1 + \frac{\Gamma_e}{\epsilon_0 \omega_{pe}^2} \int_e \frac{J_{xh}^{n+\frac{3}{2}} + J_{xh}^{n+\frac{1}{2}}}{2} u_1 - \int_e E_{xh}^{n+1} u_1 = 0, \tag{5.36}$$

$$\frac{1}{\epsilon_0 \omega_{pe}^2} \int_e \frac{J_{yh}^{n+\frac{3}{2}} - J_{yh}^{n+\frac{1}{2}}}{\tau} u_2 + \frac{\Gamma_e}{\epsilon_0 \omega_{pe}^2} \int_e \frac{J_{yh}^{n+\frac{3}{2}} + J_{yh}^{n+\frac{1}{2}}}{2} u_2 - \int_e E_{yh}^{n+1} u_2 = 0, \tag{5.37}$$

$$\frac{1}{\mu_0 \omega_{pm}^2} \int_e \frac{K_{zh}^{n+2} - K_{zh}^{n+1}}{\tau} v + \frac{\Gamma_m}{\mu_0 \omega_{pm}^2} \int_e \frac{K_{zh}^{n+2} + K_{zh}^{n+1}}{2} v - \int_e H_{zh}^{n+\frac{3}{2}} v = 0, \tag{5.38}$$

for all test functions $\phi, \psi, \chi, u_1, u_2, v \in V_h^k$, with the following fluxes consistent with (5.8)-(5.13):

$$\hat{E}_{xh}^n = E_{xh}^{n,R} \tag{5.39}$$

$$\hat{E}_{yh}^n = E_{yh}^{n,R} \tag{5.40}$$

$$\hat{H}_{zh}^{n+\frac{1}{2}} = H_{zh}^{n+\frac{1}{2},L} \tag{5.41}$$

$$\hat{E}^n_{xh} = 0, \text{ on } y = c, d \tag{5.42}$$

$$\hat{E}^n_{yh} = 0, \text{ on } x = a, b \tag{5.43}$$

$$\hat{H}^{n+\frac{1}{2}}_{zh} = H^{n+\frac{1}{2},(in)}_{zh}, \text{ on } \partial\Omega. \tag{5.44}$$

With the above preparation, we can now prove the following stability. To shorten the notation, we introduce the vector $L^2$ norm $||\boldsymbol{E}_h||^2 = ||E_{xh}||^2 + ||E_{yh}||^2$ for vector $\boldsymbol{E}_h = (E_{xh}, E_{yh})$. Similar notation will be used for $||\boldsymbol{J}_h||^2$ and $\boldsymbol{J}_h$. Any variable in the integration over the boundary of elements are by default the value taken from inside of the elements if not specified otherwise.

**Theorem 5.3.1.** *Denote $C_v = \frac{1}{\sqrt{\epsilon_0\mu_0}}$ for the speed of light, and $C_{inv}$ for the positive constant in the standard inverse estimate $||\frac{\partial u_h}{\partial i}|| \le C_{inv}h^{-1}||u_h||$ for any $u_h \in V_h^k$ and $i = x, y$. Under the assumption*

$$\tau \le \min\left(\frac{1}{2\omega_{pe}}, \frac{1}{2\omega_{pm}}, \frac{h}{2C_{inv}C_v}\right), \tag{5.45}$$

*for any $m \ge 1$ we have*

$$\begin{aligned}
&\epsilon_0||\boldsymbol{E}_h^{m+1}||^2 + \mu_0||H_{zh}^{m+\frac{3}{2}}||^2 + \frac{1}{\epsilon_0\omega_{pe}^2}||\boldsymbol{J}_h^{m+\frac{3}{2}}||^2 + \frac{1}{\mu_0\omega_{pm}^2}||K_{zh}^{m+2}||^2 \\
\le\ & C\left(\epsilon_0||\boldsymbol{E}_h^0||^2 + \mu_0||H_{zh}^{\frac{1}{2}}||^2 + \frac{1}{\epsilon_0\omega_{pe}^2}||\boldsymbol{J}_h^{\frac{1}{2}}||^2 + \frac{1}{\mu_0\omega_{pm}^2}||K_{zh}^1||^2\right),
\end{aligned} \tag{5.46}$$

*where the constant $C > 1$ is independent of the mesh size $h$ and the time step size $\tau$.*

*Proof.* Choosing $\phi = \tau(E_{xh}^{n+1} + E_{xh}^n), \psi = \tau(E_{yh}^{n+1} + E_{yh}^n), \chi = \tau(H_{zh}^{n+\frac{3}{2}} + H_{zh}^{n+\frac{1}{2}})$, $u_1 = \tau(J_{xh}^{n+\frac{3}{2}} + J_{xh}^{n+\frac{1}{2}}), u_2 = \tau(J_{yh}^{n+\frac{3}{2}} + J_{yh}^{n+\frac{1}{2}}), v = \tau(K_{zh}^{n+2} + K_{zh}^{n+1})$ in (5.33)-(5.38), summing them up over elements $e \in \mathcal{T}_h$, and time levels $0 \leq n \leq m$ for any $m \geq 1$ we have:

$$\begin{aligned} &\epsilon_0(||\boldsymbol{E}_h^{m+1}||^2 - ||\boldsymbol{E}_h^0||^2) + \mu_0(||H_{zh}^{m+\frac{3}{2}}||^2 - ||H_{zh}^{\frac{1}{2}}||^2) \\ &+ \frac{1}{\epsilon_0\omega_{pe}^2}(||\boldsymbol{J}_h^{m+\frac{3}{2}}||^2 - ||\boldsymbol{J}_{zh}^{\frac{1}{2}}||^2) + \frac{1}{\mu_0\omega_{pm}^2}(||K_{zh}^{m+2}||^2 - ||K_{zh}^1||^2) \\ \leq &\tau \int_\Omega \left( \boldsymbol{E}_h^{m+1} \cdot \boldsymbol{J}_h^{m+\frac{3}{2}} - \boldsymbol{E}_h^0 \cdot \boldsymbol{J}_h^{\frac{1}{2}} - H^{m+\frac{3}{2}} K_{zh}^{m+2} + H^{\frac{1}{2}} K^1 \right) \\ &+ F_1 + F_m + F_{x1} + F_{x2} - F_{y1} - F_{y2}, \end{aligned} \tag{5.47}$$

where the terms on the right hand side are:

$$\begin{aligned} F_m &= \tau \sum_{e \in \mathcal{T}_h} \int_e \left( -E_{xh}^{m+1} \frac{\partial H_{zh}^{m+\frac{3}{2}}}{\partial y} + E_{yh}^{m+1} \frac{\partial H_{zh}^{m+\frac{3}{2}}}{\partial x} \right) + \int_{\partial e} \left( \hat{E}_{xh}^{m+1} H_{zh}^{m+\frac{3}{2}} n_y - \hat{E}_{yh}^{m+1} \hat{H}_{zh}^{m+\frac{3}{2}} n_x \right), \\ F_0 &= \tau \sum_{e \in \mathcal{T}_h} \int_e \left( -H_{zh}^{\frac{1}{2}} \frac{\partial E_{xh}^0}{\partial y} + H_{zh}^{\frac{1}{2}} \frac{\partial E_{yh}^0}{\partial x} \right) + \int_{\partial e} \left( \hat{H}_{zh}^{\frac{1}{2}} E_{xh}^0 n_y - \hat{H}_{zh}^{\frac{1}{2}} E_{yh}^0 n_x \right), \\ F_{x1} &= \tau \sum_{n=0}^{m} \sum_{e \in \mathcal{T}_h} \int_{\partial e} \left( \hat{H}_{zh}^{n+\frac{1}{2}} E_{xh}^{n+1} n_y + \hat{E}_{xh}^{n+1} H_{zh}^{n+\frac{1}{2}} n_y \right) + \int_e \left( -H_{zh}^{n+\frac{1}{2}} \frac{\partial E_{xh}^{n+1}}{\partial y} - E_{xh}^{n+1} \frac{\partial H_{zh}^{n+\frac{1}{2}}}{\partial y} \right), \\ F_{x2} &= \tau \sum_{n=1}^{m} \sum_{e \in \mathcal{T}_h} \int_{\partial e} \left( \hat{H}_{zh}^{n+\frac{1}{2}} E_{xh}^{n} n_y + \hat{E}_{xh}^{n} H_{zh}^{n+\frac{1}{2}} n_y \right) + \int_e \left( -H_{zh}^{n+\frac{1}{2}} \frac{\partial E_{xh}^{n}}{\partial y} - E_{xh}^{n} \frac{\partial H_{zh}^{n+\frac{1}{2}}}{\partial y} \right), \\ F_{y1} &= \tau \sum_{n=0}^{m} \sum_{e \in \mathcal{T}_h} \int_{\partial e} \left( \hat{H}_{zh}^{n+\frac{1}{2}} E_{yh}^{n+1} n_x + \hat{E}_{yh}^{n+1} H_{zh}^{n+\frac{1}{2}} n_x \right) + \int_e \left( -H_{zh}^{n+\frac{1}{2}} \frac{\partial E_{yh}^{n+1}}{\partial x} - E_{yh}^{n+1} \frac{\partial H_{zh}^{n+\frac{1}{2}}}{\partial x} \right), \\ F_{y2} &= \tau \sum_{n=1}^{m} \sum_{e \in \mathcal{T}_h} \int_{\partial e} \left( \hat{H}_{zh}^{n+\frac{1}{2}} E_{yh}^{n} n_x + \hat{E}_{yh}^{n} H_{zh}^{n+\frac{1}{2}} n_x \right) + \int_e \left( -H_{zh}^{n+\frac{1}{2}} \frac{\partial E_{yh}^{n}}{\partial x} - E_{yh}^{n} \frac{\partial H_{zh}^{n+\frac{1}{2}}}{\partial x} \right). \end{aligned}$$

We cancel the flux terms similarly to (5.18) in the proof of Theorem 5.2.1 and get:

$$F_{x1} = 0, F_{x2} = 0, F_{y1} = 0, F_{y2} = 0. \tag{5.48}$$

By using the Cauchy-Schwartz inequality, we have:

$$
\begin{aligned}
&\tau \int_{\Omega} \left( \boldsymbol{E}_h^{m+1} \cdot \boldsymbol{J}_h^{m+\frac{3}{2}} - \boldsymbol{E}_h^0 \cdot \boldsymbol{J}_h^{\frac{1}{2}} - H^{m+\frac{3}{2}} K_{zh}^{m+2} + H^{\frac{1}{2}} K^1 \right) \\
\leq &\frac{\tau\omega_{pe}}{2} \left( \frac{1}{\epsilon_0 \omega_{pe}^2} ||\boldsymbol{J}_h^{\frac{1}{2}}||^2 + \epsilon_0 ||\boldsymbol{E}_h^0||^2 \right) + \frac{\tau\omega_{pe}}{2} \left( \frac{1}{\epsilon_0 \omega_{pe}^2} ||\boldsymbol{J}_h^{m+\frac{3}{2}}||^2 + \epsilon_0 ||\boldsymbol{E}_h^{m+1}||^2 \right) \\
&+ \frac{\tau\omega_{pm}}{2} \left( \frac{1}{\mu_0 \omega_{pm}^2} ||K_{zh}^1||^2 + \mu_0 ||H_{zh}^{\frac{1}{2}}||^2 \right) + \frac{\tau\omega_{pm}}{2} \left( \frac{1}{\mu_0 \omega_{pm}^2} ||K_{zh}^{m+2}||^2 + \mu_0 ||H_{zh}^{m+\frac{3}{2}}||^2 \right).
\end{aligned}
\tag{5.49}
$$

We utilize the inverse inequality along with Cauchy-Schwarz inequality to estimate $F_m + F_0$: (similar to the proof of Theorem 3.2.6 in [10])

$$
\begin{aligned}
F_0 + F_m \leq &\tau \cdot \frac{C_{inv} C_v}{2h} \left( \epsilon_0 ||E_{xh}^{m+1}||^2 + \mu_0 ||H_{zh}^{m+\frac{3}{2}}||^2 + \epsilon_0 ||E_{xh}^0||^2 + \mu_0 ||H_{zh}^{\frac{1}{2}}||^2 \right) \\
&+ \tau \cdot \frac{C_{inv} C_v}{2h} \left( \epsilon_0 ||E_{yh}^{m+1}||^2 + \mu_0 ||H_{zh}^{m+\frac{3}{2}}||^2 + \epsilon_0 ||E_{yh}^0||^2 + \mu_0 ||H_{zh}^{\frac{1}{2}}||^2 \right).
\end{aligned}
\tag{5.50}
$$

The proof is concluded by substituting (5.48)–(5.50) into (5.47) and applying assumption (5.45) in the above inequality. □

**Remark 5.3.1.** *Under the same assumption as Theorem 5.3.1 coupled with the assumptions on the initial value:*

$$
\epsilon_0 ||\boldsymbol{E}^0 - \boldsymbol{E}_h^0||^2 + \mu_0 ||H_z^{\frac{1}{2}} - H_{zh}^{\frac{1}{2}}||^2 + \frac{1}{\epsilon_0 \omega_{pe}^2} ||\boldsymbol{J}^{\frac{1}{2}} - \boldsymbol{J}_h^{\frac{1}{2}}||^2 + \frac{1}{\mu_0 \omega_{pm}^2} ||K_z^1 - K_{zh}^1||^2 \leq C h^{2k},
$$

*we can prove the following error estimate: for any $m \geq 1$*

$$
\begin{aligned}
&\epsilon_0 ||\boldsymbol{E}^{m+1} - \boldsymbol{E}_h^{m+1}||^2 + \mu_0 ||H_z^{m+\frac{3}{2}} - H_{zh}^{m+\frac{3}{2}}||^2 \\
&+ \frac{1}{\epsilon_0 \omega_{pe}^2} ||\boldsymbol{J}^{m+\frac{3}{2}} - \boldsymbol{J}_h^{m+\frac{3}{2}}||^2 + \frac{1}{\mu_0 \omega_{pm}^2} ||K_z^{m+2} - K_{zh}^{m+2}||^2 \leq C \left( h^k + \tau^2 \right)^2.
\end{aligned}
$$

*The proof can be carried out by following the similar idea to the proofs of Theorems 5.2.2 and 5.3.1 coupled with time discretization estimates (cf. [36, Ch.3]).*

## 5.4 Numerical results

In this section we present the error tables demonstrating the convergence rates, and two interesting simulations showing the backward wave propagation across the interface of vacuum and metamaterial. For the error tables, we use the same equations and exact solutions as in Section 4.5.

### 5.4.1 Error table with leap-frog time stepping

We implement the leap-frog scheme (5.33)-(5.38) with alternating flux (5.39)–(5.44) and polynomial space of degree 2. The $L^2$ error and error rate for each variable is shown in Table 5.1. The error is evaluated at $T = 0.1$. For the purpose of showing the sub-optimal convergence rate, we choose $\Delta t = 0.05h^{\frac{3}{2}}$ so that the error from time stepping would be $O(h^3)$. In Table 5.1, we can see that the space error of $\boldsymbol{E}$ and $\boldsymbol{J}$ is of second order and dominates the time error. To compare our results with existing work using the central flux [35]:

$$\hat{E}_{xh} = \frac{1}{2}\left(E_{xh}^R + E_{xh}^L\right), \hat{E}_{yh} = \frac{1}{2}\left(E_{yh}^R + E_{yh}^L\right), \hat{H}_{zh} = \frac{1}{2}\left(H_{zh}^R + H_{zh}^L\right)$$

instead of our alternating flux (5.8)–(5.10), we implement the same scheme with the flux replaced by the central flux and get similar results shown in Table 5.2.

As discussed in Remark 5.2.1, the alternating flux is optimal for DG schemes with $Q_k$ solution spaces on rectangular meshes while the central flux is suboptimal. It appears that, for DG schemes on triangular meshes with $P_k$ solution spaces, these two fluxes are rather similar in terms of convergence rates.

Table 5.1: Leap-frog, alternating flux, $P_2$ basis function, $T = 0.1$, $\Delta t = 0.05h^{\frac{3}{2}}$

| Level of Refinement | Error of $E_x$ $L^2$ Error | Order | Error of $E_y$ $L^2$ Error | Order | Error of $H_z$ $L^2$ Error | Order |
|---|---|---|---|---|---|---|
| 1 | 8.42e-03 | -inf | 9.91e-03 | -inf | 6.37e-03 | -inf |
| 2 | 1.68e-03 | 2.33 | 2.45e-03 | 2.01 | 8.72e-04 | 2.87 |
| 3 | 3.65e-04 | 2.20 | 5.93e-04 | 2.05 | 1.01e-04 | 3.10 |
| 4 | 8.57e-05 | 2.09 | 1.46e-04 | 2.02 | 1.36e-05 | 2.90 |
| 5 | 2.08e-05 | 2.04 | 3.65e-05 | 2.00 | 1.85e-06 | 2.88 |
| Level of Refinement | Error of $J_x$ $L^2$ Error | Order | Error of $J_y$ $L^2$ Error | Order | Error of $K_z$ $L^2$ Error | Order |
| 1 | 1.92e-02 | -inf | 2.09e-02 | -inf | 1.63e-02 | -inf |
| 2 | 3.00e-03 | 2.68 | 4.09e-03 | 2.35 | 2.31e-03 | 2.82 |
| 3 | 5.90e-04 | 2.35 | 9.19e-04 | 2.15 | 2.79e-04 | 3.05 |
| 4 | 1.32e-04 | 2.16 | 2.22e-04 | 2.05 | 3.49e-05 | 3.00 |
| 5 | 3.15e-05 | 2.06 | 5.49e-05 | 2.02 | 4.38e-06 | 2.99 |

Table 5.2: Leap-frog, central flux, $P_2$ basis function, $T = 0.1$, $\Delta t = 0.05h^{\frac{3}{2}}$

| Level of Refinement | Error of $E_x$ $L^2$ Error | Order | Error of $E_y$ $L^2$ Error | Order | Error of $H_z$ $L^2$ Error | Order |
|---|---|---|---|---|---|---|
| 1 | 8.36e-03 | -inf | 8.36e-03 | -inf | 7.84e-03 | -inf |
| 2 | 1.44e-03 | 2.54 | 1.44e-03 | 2.54 | 7.63e-04 | 3.36 |
| 3 | 3.01e-04 | 2.26 | 3.01e-04 | 2.26 | 9.61e-05 | 2.99 |
| 4 | 7.17e-05 | 2.07 | 7.17e-05 | 2.07 | 1.05e-05 | 3.19 |
| 5 | 1.76e-05 | 2.02 | 1.76e-05 | 2.02 | 1.27e-06 | 3.04 |
| Level of Refinement | Error of $J_x$ $L^2$ Error | Order | Error of $J_y$ $L^2$ Error | Order | Error of $K_z$ $L^2$ Error | Order |
| 1 | 2.05e-02 | -inf | 2.05e-02 | -inf | 1.73e-02 | -inf |
| 2 | 2.83e-03 | 2.86 | 2.83e-03 | 2.86 | 2.06e-03 | 3.07 |
| 3 | 5.10e-04 | 2.47 | 5.10e-04 | 2.47 | 2.61e-04 | 2.98 |
| 4 | 1.11e-04 | 2.20 | 1.11e-04 | 2.20 | 3.23e-05 | 3.01 |
| 5 | 2.67e-05 | 2.06 | 2.67e-05 | 2.06 | 4.03e-06 | 3.00 |

Table 5.3: Runge-Kutta, upwind flux, $P_2$ basis function, $T = 0.1$, $\Delta t = 0.05h$

| Level of | Error of $E_x$ | | Error of $E_y$ | | Error of $H_z$ | |
|---|---|---|---|---|---|---|
| Refinement | $L^2$ Error | Order | $L^2$ Error | Order | $L^2$ Error | Order |
| 1 | 4.83e-03 | – | 4.83e-03 | – | 3.67e-03 | – |
| 2 | 5.03e-04 | 3.27 | 5.03e-04 | 3.27 | 4.33e-04 | 3.08 |
| 3 | 5.85e-05 | 3.10 | 5.85e-05 | 3.10 | 5.14e-05 | 3.07 |
| 4 | 7.07e-06 | 3.05 | 7.07e-06 | 3.05 | 6.28e-06 | 3.03 |
| 5 | 8.69e-07 | 3.02 | 8.69e-07 | 3.02 | 7.80e-07 | 3.01 |
| Level of | Error of $J_x$ | | Error of $J_y$ | | Error of $K_z$ | |
| Refinement | $L^2$ Error | Order | $L^2$ Error | Order | $L^2$ Error | Order |
| 1 | 1.71e-02 | – | 1.71e-02 | – | 1.63e-02 | – |
| 2 | 2.11e-03 | 3.02 | 2.11e-03 | 3.02 | 2.01e-03 | 3.02 |
| 3 | 2.65e-04 | 2.99 | 2.65e-04 | 2.99 | 2.50e-04 | 3.00 |
| 4 | 3.30e-05 | 3.01 | 3.30e-05 | 3.01 | 3.11e-05 | 3.01 |
| 5 | 4.11e-06 | 3.00 | 4.11e-06 | 3.00 | 3.87e-06 | 3.00 |

### 5.4.2 Error table with Runge-Kutta time stepping

In this section we implement one more flux, the upwind flux, and further compare the convergence rate between fluxes. For the ease of implementation, we used the Runge-Kutta time stepping, see e.g. [17]. As shown in Table 5.3, the upwind flux produces optimal convergence rate. DG schemes with alternating and central fluxes still show suboptimal convergence rates in Tables 5.4 and 5.5.

### 5.4.3 Wave propagation in a rectangular metamaterial slab

One of the advantage of triangular meshes over the rectangular meshes is the flexibility in the shape of physical domains they can model. In this section we consider a rectangular region with a triangular metamaterial slab located inside a vacuum as in [35]. To absorb the outgoing waves, we wrap the whole region by a perfectly matched layer (PML).

Table 5.4: Runge-Kutta, alternating flux, $P_2$ basis function, $T = 0.1$, $\Delta t = 0.05h$

| Level of Refinement | Error of $E_x$ $L^2$ Error | Order | Error of $E_y$ $L^2$ Error | Order | Error of $H_z$ $L^2$ Error | Order |
|---|---|---|---|---|---|---|
| 1 | 8.17e-03 | – | 9.85e-03 | – | 5.76e-03 | – |
| 2 | 1.65e-03 | 2.31 | 2.43e-03 | 2.02 | 7.95e-04 | 2.86 |
| 3 | 3.61e-04 | 2.19 | 5.92e-04 | 2.04 | 9.19e-05 | 3.11 |
| 4 | 8.58e-05 | 2.08 | 1.46e-04 | 2.02 | 1.14e-05 | 3.01 |
| 5 | 2.08e-05 | 2.04 | 3.65e-05 | 2.00 | 1.48e-06 | 2.94 |
| Level of Refinement | Error of $J_x$ $L^2$ Error | Order | Error of $J_y$ $L^2$ Error | Order | Error of $K_z$ $L^2$ Error | Order |
| 1 | 1.93e-02 | – | 2.08e-02 | – | 1.66e-02 | – |
| 2 | 2.99e-03 | 2.69 | 4.05e-03 | 2.36 | 2.32e-03 | 2.84 |
| 3 | 5.87e-04 | 2.35 | 9.15e-04 | 2.15 | 2.80e-04 | 3.05 |
| 4 | 1.31e-04 | 2.16 | 2.22e-04 | 2.05 | 3.50e-05 | 3.00 |
| 5 | 3.15e-05 | 2.06 | 5.49e-05 | 2.01 | 4.38e-06 | 3.00 |

Table 5.5: Runge-Kutta, central flux, $P_2$ basis function, $T = 0.1$, $\Delta t = 0.05h$

| Level of Refinement | Error of $E_x$ $L^2$ Error | Order | Error of $E_y$ $L^2$ Error | Order | Error of $H_z$ $L^2$ Error | Order |
|---|---|---|---|---|---|---|
| 1 | 8.20e-03 | – | 8.20e-03 | – | 7.85e-03 | – |
| 2 | 1.44e-03 | 2.51 | 1.44e-03 | 2.51 | 7.50e-04 | 3.39 |
| 3 | 3.00e-04 | 2.26 | 3.00e-04 | 2.26 | 9.14e-05 | 3.04 |
| 4 | 7.15e-05 | 2.07 | 7.15e-05 | 2.07 | 9.55e-06 | 3.26 |
| 5 | 1.76e-05 | 2.02 | 1.76e-05 | 2.02 | 1.08e-06 | 3.15 |
| Level of Refinement | Error of $J_x$ $L^2$ Error | Order | Error of $J_y$ $L^2$ Error | Order | Error of $K_z$ $L^2$ Error | Order |
| 1 | 2.06e-02 | – | 2.06e-02 | – | 1.75e-02 | – |
| 2 | 2.82e-03 | 2.87 | 2.82e-03 | 2.87 | 2.08e-03 | 3.07 |
| 3 | 5.08e-04 | 2.47 | 5.08e-04 | 2.47 | 2.61e-04 | 2.99 |
| 4 | 1.11e-04 | 2.19 | 1.11e-04 | 2.19 | 3.23e-05 | 3.02 |
| 5 | 2.67e-05 | 2.06 | 2.67e-05 | 2.06 | 4.03e-06 | 3.00 |

In the mesh visualization (Figure 5.1) the blue triangle, with vertices (0.024,0.002), (0.054,0.002), and (0.024,0.062), consists of the metamaterial. The red area, a rectangle $[0, 0.07] \times [0, 0.064]$, represents the vacuum. The green band with thickness $dd = 2.4 \times 10^{-3}$ on the boundary is the PML.

The equation in the metamaterial is the Drude model (4.7)–(4.12), with $\Gamma_e = \Gamma_m = 1 \times 10^8, \mu_0 = 4\pi \times 10^{-7}, c_v = 3 \times 10^8, \epsilon_0 = 1/(c_v^2\mu_0), w_{pe} = w_{pm} = 2\sqrt{2}\pi$. Those in the vacuum are the usual Maxwell's equations. The PML equations we used are the following [35]:

$$\epsilon_0 \frac{\partial E_x}{\partial t} = \epsilon_0(\sigma_x - \sigma_y)E_x + \frac{\partial H_z}{\partial y} - J_x, \tag{5.51}$$
$$\epsilon_0 \frac{\partial E_y}{\partial t} = \epsilon_0(\sigma_y - \sigma_x)E_y - \frac{\partial H_z}{\partial x} - J_y, \tag{5.52}$$
$$\mu_0 \frac{\partial H_z}{\partial t} = -\mu_0(\sigma_x + \sigma_y)H_z + \frac{\partial E_x}{\partial y} - \frac{\partial E_y}{\partial x} - K_z, \tag{5.53}$$
$$\frac{\partial J_x}{\partial t} = -\sigma_x J_x + \epsilon_0(\sigma_x - \sigma_y)\sigma_x E_x, \tag{5.54}$$
$$\frac{\partial J_y}{\partial t} = -\sigma_y J_y + \epsilon_0(\sigma_y - \sigma_x)\sigma_y E_y, \tag{5.55}$$
$$\frac{\partial K_z}{\partial t} = \mu_0 \sigma_x \sigma_y H_z, \tag{5.56}$$

where

$$\sigma_x(x, y) = \begin{cases} \sigma_m \left(\frac{x-0.07}{dd}\right)^4, & x \geq 0.07, \\ \sigma_m (x/dd)^4, & x \leq 0, \\ 0, & \text{otherwise}, \end{cases} \tag{5.57}$$

with $\sigma_m = -log(err) * 5 * 0.07 * c_v/(2 * dd)$ and $err = 10^{-7}$. $\sigma_y$ has the same form with $x$ replaced by y. The initial condition is zero in the whole region, and the wave is incited by a source wave

$$e^{-10000(y-0.03)^2} f(t)$$

imposed on the line of $x = 0.004$ and $y \in [0.025, 0.035]$. Here $f$ is defined as

$$\alpha(x) = \begin{cases} 0, & t < 0 \\ g_1(t)\sin(\omega_0 t), & 0 < t < mT_p \\ \sin(\omega_0 t), & mT_p < t < (m+k)T_p \\ g_2(t)\sin(\omega_0 t), & (m+k)Tp < t < (2m+k)Tp \\ 0, & t > (2m+k)T_p, \end{cases}$$

where $T_p = 1/f_0, f_0 = 3 \times 10^8, m = 2, k = 100$, and

$$g_1(t) = 10x_1^3 - 15x_1^4 + 6x_1^5, \text{ with } x_1 = t/mT_p,$$

$$g_2(t) = 1 - 10x_2^3 - 15x_2^4 + 6x_2^5, \text{ with } x_2 = t - (m+k)T_p/mT_p.$$

We use a time step $\tau = 0.1$ ps and plot the $H_z$ field at 1000, 2000, 3000, 4000, and 5000 time steps in Figures 5.2–5.6, showing results consistent with the simulation in [35].

### 5.4.4 Wave propagation in a rectangular metamaterial slab

We replace the triangular stab of metamaterial in the previous section by a rectangular one $[0.024, 0.054] \times [0.002, 0.062]$, and obtain snapshots of $H_z$ shown in Figures 5.7–5.12. Again, our results are consistent with the simulation obtained in [35].

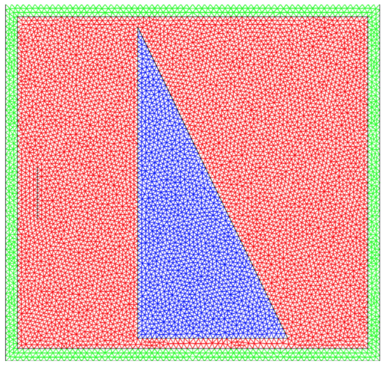

Figure 5.1: Mesh of triangular slab in vacuum

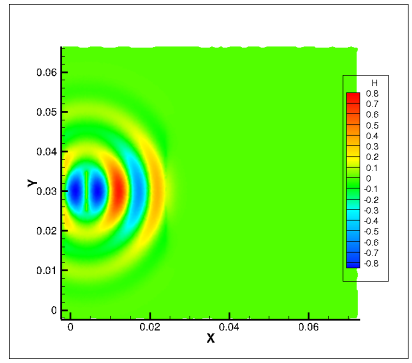


Figure 5.2: $H_z$ value at 1000 time step

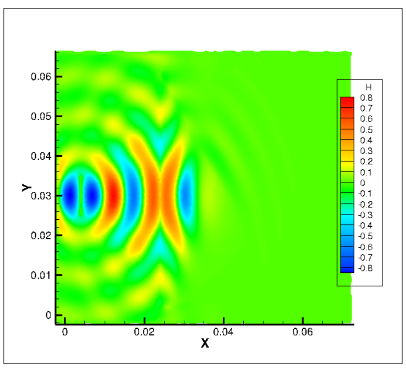


Figure 5.3: $H_z$ value at 2000 time step

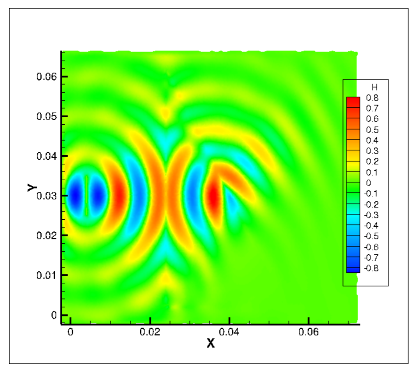


Figure 5.4: $H_z$ value at 3000 time step

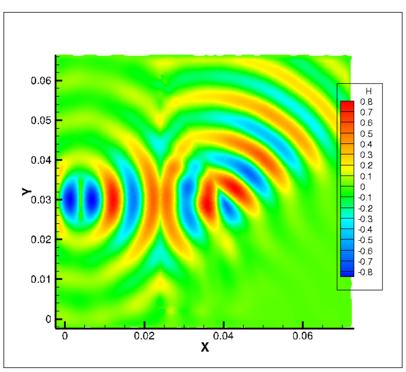


Figure 5.5: $H_z$ value at 4000 time step

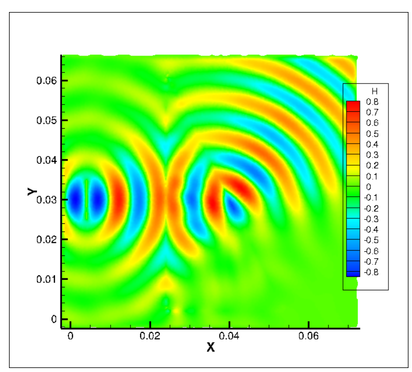


Figure 5.6: $H_z$ value at 5000 time step

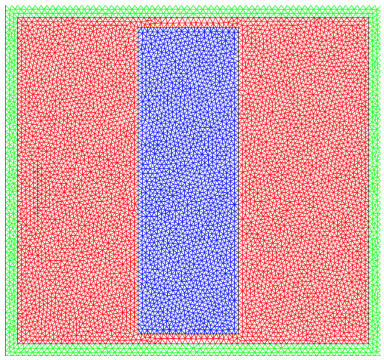

Figure 5.7: Mesh of triangular slab in vacuum

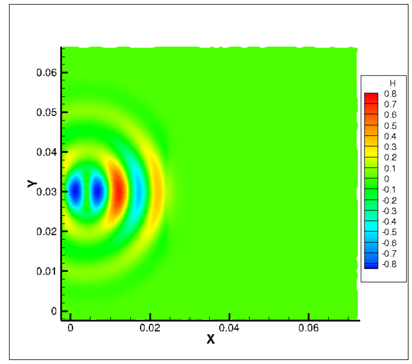


Figure 5.8: $H_z$ value at 1000 time step

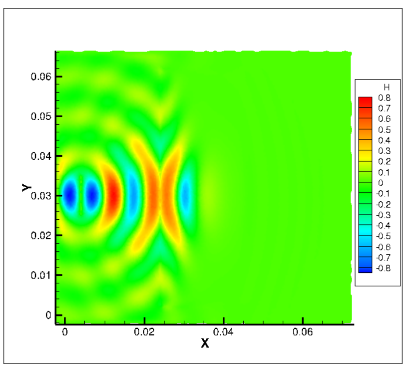


Figure 5.9: $H_z$ value at 2000 time step

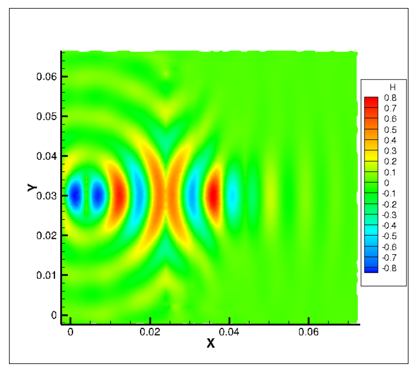


Figure 5.10: $H_z$ value at 3000 time step

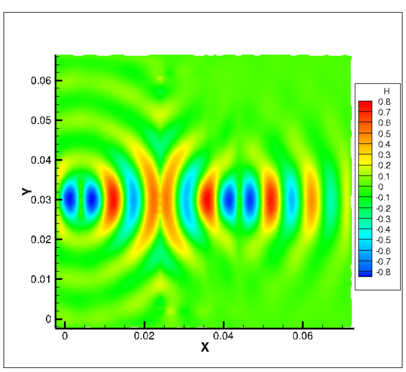


Figure 5.11: $H_z$ value at 4000 time step

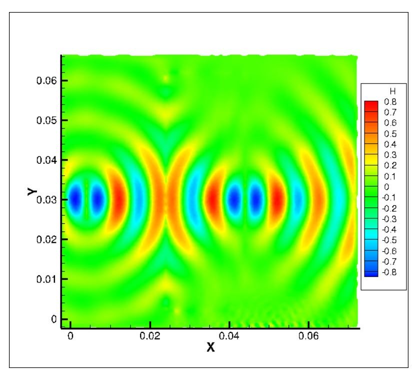


Figure 5.12: $H_z$ value at 5000 time step

# Chapter Six

# Conclusion

This dissertation presents two topics on numerical solutions solving hyperbolic equations from both theoretical and practical points of view.

In the first part, we have given a rigorous definition of the local conservation property for numerical methods solving hyperbolic equations in both one and two space dimensions. Lax-Wendroff type theorems are stated and proved for locally conservative numerical schemes thus defined. Our definition serves as a general framework for the discussion of local conservation property. We have shown that the CG methods among others are considered locally conservative in our framework. Hence, their solutions would converge to a weak solution of the underlying conservation law if they do converge.

In the second part, we have developed and analyzed non-dissipative DG methods for solving the time domain Maxwell's equations when metamaterials are involved. Optimal error estimates are proved for the scheme in rectangular meshes, while the DG methods with on triangular meshes only have sub-optimal convergence rates. We postulate that the sub-optimality is inherent in the $P_k$ solution space. We present convergence rate tables which are consistent with our theoretical error estimates for DG methods on both the rectangular and triangular meshes. The simulations of backward wave propagation Drude metamaterials demonstrate the flexibility of triangular meshes, even though the DG methods on them are not optimally convergent.

# Bibliography


[1] R. Abgrall, *On a class of high order schemes for hyperbolic problems*, Proceedings of the International Congress of Mathematicians, Seoul, (2014), pp. 699–725.

[2] R. Abgrall, K. Mer, and B. Nkonga, *A Lax-Wendroff type theorem for residual schemes*, in Innovative Methods for Numerical Solution of Partial Differential Equations, M. M. Hafez and J.-J. Chattot, eds., World Scientific, 2011, pp. 243–266.

[3] A. Buffa, P. Houston, and I. Perugia, *Discontinuous Galerkin computation of the Maxwell eigenvalues on simplicial meshes*, Journal of Computational and Applied Mathematics, 204 (2007), pp. 317 – 333.

[4] L. Bush and V. Ginting, *On the application of the continuous Galerkin finite element method for conservation problems*, SIAM Journal on Scientific Computing, 35 (2013), pp. A2953–A2975.

[5] C.-S. Chou, C.-W. Shu, and Y. Xing, *Optimal energy conserving local discontinuous Galerkin methods for second-order wave equation in heterogeneous media*, Journal of Computational Physics, 272 (2014), pp. 88–107.

[6] E. T. Chung and P. Ciarlet, *A staggered discontinuous Galerkin method for wave propagation in media with dielectrics and meta-materials*, Journal of Computational and Applied Mathematics, 239 (2013), pp. 189–207.

[7] E. T. Chung, P. Ciarlet, and T. F. Yu, *Convergence and superconvergence of staggered discontinuous Galerkin methods for the three-dimensional Maxwells equations on Cartesian grids*, Journal of Computational Physics, 235 (2013), pp. 14 – 31.

[8] E. T. Chung and B. Engquist, *Optimal discontinuous Galerkin methods for wave propagation*, SIAM Journal on Numerical Analysis, 44 (2006), pp. 2131–2158.

[9] E. T. Chung and B. Engquist, *Optimal discontinuous Galerkin methods for the acoustic wave equation in higher dimensions*, SIAM Journal on Numerical Analysis, 47 (2009), pp. 3820–3848.

[10] P. Ciarlet, *The Finite Element Method for Elliptic Problems*, Society for Industrial and Applied Mathematics, 2002.

[11] B. Cockburn, S. Hou, and C.-W. Shu, *The Runge–Kutta local projection discontinuous Galerkin finite element method for conservation laws. IV. the multidimensional case*, Mathematics of Computation, 54 (1990), pp. 545–581.

[12] B. Cockburn, G. Kanschat, I. Perugia, and D. Schötzau, *Superconvergence of the local discontinuous Galerkin method for elliptic problems on Cartesian grids*, SIAM Journal on Numerical Analysis, 39 (2001), pp. 264–285.

[13] B. Cockburn, F. Li, and C.-W. Shu, *Locally divergence-free discontinuous Galerkin methods for the Maxwell equations*, Journal of Computational Physics, 194 (2004), pp. 588–610.

[14] B. Cockburn and C.-W. Shu, *TVB Runge-Kutta local projection discontinuous Galerkin finite element method for conservation laws II: General framework*, Mathematics of Computation, 52 (1989), pp. 411–435.

[15] B. Cockburn and C.-W. Shu, *Nonlinearly stable compact schemes for shock calculations*, SIAM Journal on Numerical Analysis, 31 (1994), pp. 607–627.

[16] B. Cockburn and C.-W. Shu, *The local discontinuous Galerkin method for time-dependent convection-diffusion systems*, SIAM Journal on Numerical Analysis, 35 (1998), pp. 2440–2463.

[17] B. Cockburn and C.-W. Shu, *The Runge-Kutta discontinuous Galerkin method for conservation laws V: Multidimensional systems*, Journal of Computational Physics, 141 (1998), pp. 199 – 224.

[18] B. Cockburn and C.-W. Shu, *Runge–Kutta discontinuous Galerkin methods for convection-dominated problems*, Journal of Scientific Computing, 16 (2001), pp. 173–261.

[19] C. M. Dafermos, *Hyperbolic Systems of Balance Laws*, Springer Berlin Heidelberg, 2010, pp. 53–74.

[20] L. Demkowicz, J. Kurtz, D. Pardo, M. Paszynski, W. Rachowicz, and A. Zdunek, *Computing with Hp-Adaptive Finite Elements, Vol. 2: Frontiers Three Dimensional Elliptic and Maxwell Problems with Applications*, Chapman & Hall/CRC, 2007.

[21] B. Dong and C.-W. Shu, *Analysis of a local discontinuous Galerkin method for linear time-dependent fourth-order problems*, SIAM Journal on Numerical Analysis, 47 (2009), pp. 3240–3268.

[22] L. Fezoui, S. Lanteri, S. Lohrengel, and S. Piperno, *Convergence and stability of a discontinuous Galerkin time-domain method for the 3d heterogeneous Maxwell equations on unstructured meshes*, Mathematical Modelling and Numerical Analysis, 39 (2005), pp. 1149–1176.

[23] V. Ginting and R. Johnson, *Locally conservative B–spline finite element methods for two-point boundary value problems*, Procedia Computer Science, 80 (2016), pp. 1279–1290.

[24] M. J. Grote, A. Schneebeli, and D. Schtzau, *Interior penalty discontinuous Galerkin method for Maxwell's equations: optimal $L^2$–norm error estimates*, IMA Journal of Numerical Analysis, 28 (2008), pp. 440–468.

[25] Y. Hao and R. Mittra, *FDTD modeling of metamaterials: Theory and applications*, Artech house, 2008.

[26] J. S. Hesthaven and T. Warburton, *Nodal discontinuous Galerkin methods: algorithms, analysis, and applications*, Springer Science & Business Media, 2007.

[27] K. Höllig, *Finite Element Methods with B–Splines*, Society for Industrial and Applied Mathematics, 2003.

[28] T. J. Hughes, G. Engel, L. Mazzei, and M. G. Larson, *The continuous Galerkin method is locally conservative*, Journal of Computational Physics, 163 (2000), pp. 467–488.

[29] D. Kröner and M. Rokyta, *Convergence of upwind finite volume schemes for scalar conservation laws in two dimensions*, SIAM Journal on Numerical Analysis, 31 (1994), pp. 324–343.

[30] D. Kröner, M. Rokyta, and M. Wierse, *A Lax–Wendroff type theorem for upwind finite volume schemes in 2-d*, East-West Journal of Numerical Mathematics, 4 (1996), pp. 279–292.

[31] S. Lanteri and C. Scheid, *Convergence of a discontinuous Galerkin scheme for the mixed time-domain Maxwell's equations in dispersive media*, IMA Journal of Numerical Analysis, 33 (2012), pp. 432–459.

[32] P. Lax and B. Wendroff, *Systems of conservation laws*, Communications on Pure and Applied Mathematics, 13 (1960), pp. 217–237.

[33] R. J. LeVeque, *Numerical Methods for Conservation Laws*, Birkhäuser, 2005.

[34] J. Li, *Development of discontinuous Galerkin methods for Maxwell's equations in metamaterials and perfectly matched layers*, Journal of Computational and Applied Mathematics, 236 (2011), pp. 950–961.

[35] J. Li and J. S. Hesthaven, *Analysis and application of the nodal discontinuous Galerkin method for wave propagation in metamaterials*, Journal of Computational Physics, 258 (2014), pp. 915–930.

[36] J. Li and Y. Huang, *Time-domain finite element methods for Maxwell's equations in metamaterials*, vol. 43, Springer Science & Business Media, 2012.

[37] J. Li, J. W. Waters, and E. A. Machorro, *An implicit leap-frog discontinuous Galerkin method for the time-domain Maxwells equations in metamaterials*, Computer Methods in Applied Mechanics and Engineering, 223 (2012), pp. 43–54.

[38] J. Li and A. Wood, *Finite element analysis for wave propagation in double negative metamaterials*, Journal of Scientific Computing, 32 (2007), pp. 263–286.

[39] Y. Liu and C.-W. Shu, *Analysis of the local discontinuous Galerkin method for the drift-diffusion model of semiconductor devices*, Science China Mathematics, 59 (2016), pp. 115–140.

[40] T. Lu, P. Zhang, and W. Cai, *Discontinuous Galerkin methods for dispersive and lossy Maxwell's equations and PML boundary conditions*, Journal of Computational Physics, 200 (2004), pp. 549–580.

[41] A. Macchi, G. Moruzzi, and F. Pegoraro, *Chapter 8 Maxwell Equations and Conservation Laws*, Springer International Publishing, Cham, 2017, pp. 65–71.

[42] X. Meng, C.-W. Shu, and B. Wu, *Optimal error estimates for discontinuous Galerkin methods based on upwind-biased fluxes for linear hyperbolic equations*, Mathematics of Computation, 85 (2016), pp. 1225–1261.

[43] P. Monk, *Finite element methods for Maxwell's equations*, Oxford University Press, 2003.

[44] L. Mu, J. Wang, X. Ye, and S. Zhang, *A weak Galerkin finite element method for the Maxwell equations*, Journal of Scientific Computing, 65 (2015), pp. 363–386.

[45] J. B. Perot, *Discrete conservation properties of unstructured mesh schemes*, Annual Review of Fluid Mechanics, 43 (2011), pp. 299–318.

[46] I. Perugia, D. Schötzau, and P. Monk, *Stabilized interior penalty methods for the time-harmonic Maxwell equations*, Computer Methods in Applied Mechanics and Engineering, 191 (2002), pp. 4675–4697.

[47] W. H. Reed and T. Hill, *Triangular mesh methods for the neutron transport equation*, tech. rep., Los Alamos Scientific Lab., N. Mex.(USA), 1973.

[48] B. Wang, Z. Xie, and Z. Zhang, *Error analysis of a discontinuous Galerkin method for Maxwell equations in dispersive media*, Journal of Computational Physics, 229 (2010), pp. 8552–8563.

[49] Y. Xing, C.-S. Chou, and C.-W. Shu, *Energy conserving local discontinuous Galerkin methods for wave propagation problems.*, Inverse Problems & Imaging, 7 (2013), pp. 967–986.

[50] Y. Xu and C.-W. Shu, *Local discontinuous Galerkin methods for high-order time–dependent partial differential equations*, Communications in Computational Physics, 7 (2010), pp. 1–46.

[51] Q. Zhang and C.-W. Shu, *Stability analysis and a priori error estimates of the third order explicit Runge–Kutta discontinuous galerkin method for scalar conservation laws*, SIAM Journal on Numerical Analysis, 48 (2010), pp. 1038–1063.

[52] X. Zhang, Y. Liu, and C.-W. Shu, *Maximum-principle-satisfying high order finite volume weighted essentially nonoscillatory schemes for convection-diffusion equations*, SIAM Journal on Scientific Computing, 34 (2012), pp. A627–A658.